# Fish mortality to be expected from prototype scale turbine

**D2.6**

| | |
|---|---|
| **Grant Agreement No.** | 883553 |
| **Start date of Project** | 1 April 2020 |
| **Duration of the Project** | 48 months |
| **Deliverable Number** | D2.6 |
| **Deliverable Leader** | University of Tuscia |
| **Dissemination Level** | Public |
| **Version** | V1.0 |
| **Submission Date** | 29-03-2022 |
| **Author(s)** | Miccoli, Andrea*; De Luca, Antonio; Marcelli, Marco; Scapigliati, Giuseppe<br>University of Tuscia (Italy)<br>*andrea.miccoli@unitus.it |
| **Co-author(s)** | Peviani, Máximo<br>External Expert in hydropower and marine energy |
| **Co-author(s)** | Joseph, Melvin; Zangeneh, Mehrdad<br>Advanced Design Technology Ltd (United Kingdom) |


*This project has received funding from the European Union's Horizon 2020 research and innovation programme under grant agreement No 883553.*

**Modification Control**

| Version # | Description | Author | Organisation | Date |
|---|---|---|---|---|
| 1 | | Miccoli, A., et al. | UNITUS, ADT | 28-03-2022 |

**Release Approval**

| Name | Role | Date |
|---|---|---|
| Jeremy, Bricker | Project coordinator | 24-03-2022 |
| Pål-Tore, Selbo Storli | WP2 leader | 28-03-2022 |
| Roelof Moll | Executive project coordinator | 29-03-2022 |

**History of Changes**

| Section, page number | Change made | Date |
|---|---|---|
| | | |

# Table of contents

# List of figures

# List of tables

## Executive Summary

As with all anthropogenic structures, hydropower projects impose severe stressors to the biotic and abiotic components of marine and freshwater ecosystems. The construction of a plant can block or delay the migration of fish, thus contributing to the decline of stocks that strongly depend on habitat connectivity during certain life stages, and the mortality or extent of injury caused by hydropower turbines during downstream passage may be elevated. Environment-wise, habitat loss or alteration, hydrodynamics modifications, changes in water quality and temperature, altered morphology of the river stream or coastal areas were all demonstrated impacts.

The present deliverable particularly addresses the hazards put in place by hydropower. Hydropower-induced degradation of habitat quality is introduced in the first section and its assessment is suggested to be conducted by applying the provisions of Directive 2008/56/EC "Marine Strategy Framework Directive". The MSFD descriptors suitable for informing about the impacts of hydropower projects throughout their installation, operation, and decommissioning phases are mentioned. Among them, particularly relevant is Descriptor 3 - Commercial Fish and shellfish, rooted in the identification of safe biological limits and health status of marine stocks.

The reader is then provided with an in-depth systematic analysis of all hydropower stressors suffered by fish: the mechanisms affecting injury and mortality of fish during downstream passage through hydropower plants are dissected and the factors on which their extent and severity depend are identified; the most efficient mitigation measures, broadly classifiable as low-impact turbine design and protective structures, are specified together with the parameters that must be considered for achieving the most environment- and fish-friendly technology.

The two target species on which this deliverable and future ALPHEUS field studies has and will be focused, namely the European eel *Anguilla anguilla* and Atlantic salmon *Salmo salar*, are described both from a biological and a physiological perspective to enable a sound understanding of all subsequent chapters, which represent the core of the deliverable. A literature review narrating the knowledge generated on fish susceptibility to individual hydropower mechanisms under controlled conditions follows: data acquired on surrogate species (i.e. American eel *Anguilla rostrata* and various Salmonidae species) was also included to provide the reader with the most informative scenario in case the testing on target species was not extensive.

The following two chapters, i.e. "FPHI - Fish Population Hazard Index" and "BioPA - Biological Performance Assessment" are built upon two tools that have gained increasing popularity within the hydropower sector in recent years. FPHI was one of the research products delivered by the FIThydro "Fishfriendly Innovative Technologies for Hydropower" project, funded by the H2020 research and innovation programme under grant agreement # 727830; its usefulness in coarsely classifying hydropower plants on the basis of few constructive, operational and technical features is presented. BioPA is instead a tool developed by the Pacific Northwest National Laboratory (PNNL) within the framework of Hydropassage

(www.hydropassage.org) that is being employed by various stakeholders for comparatively evaluating the biological performance of various turbine designs: the general description, technical specifications and relevant biological response models developed for predicting the likelihood of several endpoints on target or surrogate species are reported.

Previous project deliverables already provided detailed description of the design process for the Shaft-Driven and Rim-Driven variable-speed Contra-Rotating propeller reversible Pump Turbines (SDCRRPT and RDCRRPT) along with the performance data of the initial designs and the optimized model scale designs. The last chapter of this deliverable presents the fish friendliness study of such turbine designs implemented by the collaborative effort of University of Tuscia and ADT using the BioPA tool. Passage Quality Indices were calculated for both *A. anguilla* and *S. salar* assuming body lengths of 300 and 150 mm, respectively, considering literature data on average size at downstream migration and the experimental design of the field test scheduled within ALPHEUS' WP4.

# 1 The impacts of hydropower on habitat quality

Climate change effects, including rising temperatures, ocean acidification and sea level rise, together with the EU policy concerning the decarbonization of the electric system, have led to the development of a growing interest in the use of marine renewable energy devices. This interest supported the development of studies concerning the impacts that this type of devices has on the biotic and abiotic components of marine ecosystems. As far as low head pumped hydro is concerned, these marine energy storage plants are currently highly experimental, therefore, no information is available on how these marine energy systems affect the abiotic and biotic parts of marine environments (ICES, 2019b). In general, the production of energy from marine renewable sources is governed by meteorological conditions which vary regardless of the demand for electricity. In this context, the use of so-called energy storage systems is of particular importance, among which the Pumped Hydro System (PHS) represents a promising technology.

With regard to the potential impacts of such a technology on the coastal marine ecosystem, it is possible to refer to what is currently present in the European legislation. In this sense Directive 2008/56/EC Marine Strategy Framework Directive (MSFD) is particularly relevant. The MSFD establishes a framework within which Member States must take action to achieve or maintain Good Environmental Status (GES) for the marine environment.

The MSFD identifies 11 qualitative descriptors of the marine environment that can be of great help in identifying the environmental compartments potentially affected by the impacts of marine renewable devices, including the PHS technology. By considering these 11 descriptors, it is possible to pre-assess which environmental components are potentially affected by the installation, operation and decommissioning of seawater pumped hydro devices, as shown in Table 1.

MSFD descriptors that are likely to interact with low head PHS technology, and be impacted by it, can be used to identify which environmental compartments and habitats are involved in the installation, operation, and decommissioning phases. These include (EC, 2008):

- **Descriptor 1** - Biodiversity: “The quality and occurrence of habitats and the distribution and abundance of species are in line with prevailing physiographic, geographic and climatic conditions.”
- **Descriptor 3** - Commercial Fish and shellfish: “Populations of all commercially exploited fish and shellfish are within safe biological limits, exhibiting a population age and size distribution that is indicative of a healthy stock”
- **Descriptor 6** - Sea-floor Integrity: “Sea-floor integrity is at a level that ensures that the structure and functions of the ecosystems are safeguarded and benthic ecosystems, in particular, are not adversely affected”
- **Descriptor 7** - Hydrographical Conditions: “Permanent alteration of hydrographical conditions does not adversely affect marine ecosystems”

- **Descriptor 8** - Contaminants: "Contaminants are at a level not giving rise to pollution effects."
- **Descriptor 11** - Energy incl. Underwater Noise: “Introduction of energy, including underwater noise, is at levels that do not adversely affect the marine environment”

It is possible to classify the MSFD descriptors into status descriptors and pressure descriptors (Patrício et al., 2014). For the identified descriptors mainly involved in the case of installation and operation of low head pumped hydro devices, the only status descriptor is D.1 Biodiversity. Descriptors D.2. Non-indigenous Species, D.5. Eutrophication, D.9. Contaminants in seafood, D.10. Marine Litter are not taken into consideration for assessing PHS impacts on the environment or biota, as they and their related impacts and pressures, presented in Table 2 of Annex III of the MSFD Directive, can be considered negligible in the case of PHS technology.

*Table 1 MSFD descriptors and low head PHS potential interactions*

| Qualitative Descriptors | Drivers subject to MSFD |
|---|---|
| **D.1. Biological Diversity** | Environmental protection, renewable energy generation (wind, wave, and tidal energy), cables and pipelines, oil and gas exploitation, sand and gravel extraction, benthic trawling, anchoring, other infrastructure |
| **D.3. Commercial Fish and shellfish** | Environmental protection, fisheries (especially gear types and discarding), offshore wind farms, oil and gas, aquaculture |
| **D.6. Sea-floor Integrity** | Benthic trawling, maintenance of shipping lanes, land reclamation, cables and pipelines, oil and gas exploitation, renewable energy generation, sand and gravel extraction, anchoring, other infrastructure |
| **D.7. Hydrographical Conditions** | Maintenance of shipping lanes, land reclamation, renewable energy generation, other infrastructure |
| **D.8. Contaminants** | Legacy sites from past disposal of wastes and dredge spoil, shipping lanes and oil platforms |
| **D.11. Energy incl. Underwater Noise** | Shipping and offshore wind farms, but potentially a large variety of sources |

Descriptors of MSFD include both biotic and abiotic receptors. Following methodologies proposed in the literature for the preliminary schematization of the environmental compounds affected by potential impacts of marine and PHS renewable energy production technologies (ICES, 2019b; Scanu et al., 2015), the following main environmental compounds have been identified, and their habitat impacts related to GES descriptors are included in Table 2:

- Hydrodynamics
- Seabed and sediment transport

- Benthos
- Fish
- Marine Mammals
- Birds

Hydrodynamics, seabed, and sediment transport, although closely related to the biotic compartment (benthos, fish, marine mammals, and birds), can be considered abiotic factors. PHS impact on hydrodynamics can affect waves and tidal flows. Changes in hydrodynamic conditions can also affect water column mixing dynamics (Shields et al., 2011). The hydrodynamic regime also influences the sedimentary dynamics of the marine coastal environment. Changes in hydrodynamic flows can lead to local or regional variation in the sedimentary balance with erosion and accumulation phenomena that pose a serious threat to benthic biocenoses. In freshwater environments, where most of the knowledge related to hydropower was generated, the technology was demonstrated to causing environmental damages such as (Cutler et al., 2020; Poff and Schmidt, 2016):

- change in morphology (e.g. erosion/aggradation process, bottom embeddedness, reduction in habitat complexity, fragmentation of river network);
- hydrology (e.g. flooding of free-flowing rivers, hydropeaking, reduction of instream flow, distortion of natural sedimentation patterns);
- ecosystem functioning (e.g. reduction of water quality, increase in water temperature, reduction of dissolved oxygen, shift in fish communities, modification in productivity).

*Table 2 Identification of environmental compounds and habitat impacts related to GES descriptors of MSFD for low head PHS technology*

| Qualitative Descriptors | Hydrodynamics | Seabed and sediment transport | Benthos | Fish | Marine Mammals | Birds |
|---|---|---|---|---|---|---|
| **D.1. Biological Diversity** | Disturbance in water mixing. Direct effect on wave and currents | Direct impact on substrates. Burial effects and siltation processes | Direct impact on substrates. Burial effects and siltation processes | Fish aggregation. Impediments to migrations. Fish strike | Displacement. Attraction for fish aggregation | Displacement. Impediments to migrations |
| **D.3. Commercial Fish and shellfish** | | | | Fish aggregation. Impediments to migrations. Fish strike | | |
| **D.6. Sea-floor Integrity** | | Direct impact on substrates. Burial effects and siltation processes | Direct impact on substrates. Burial effects and siltation processes | | | |
| **D.7. Hydrographical Conditions** | Disturbance in water mixing. Direct effect on wave and currents | Coastal sediment transport modification. Littoral drift modification. River solid transport modification | Burial effects and siltation processes | | | |
| **D.8. Contaminants** | | | Bioaccumulation and biomagnification processes | Bioaccumulation and biomagnification processes | Bioaccumulation and biomagnification processes | Bioaccumulation and biomagnification processes |
| **D.11. Energy incl. Underwater Noise** | | | Electro Magnetic Fields | Electro Magnetic Fields. Noise | Electro Magnetic Fields. Noise | Electro Magnetic Fields. Noise |

Using the Table 2 of Annex III of MSFD, it is possible to identify the pressures and impacts that are more strictly related to the chosen descriptors, hence particularly involved in the case of installation and operation of PHS devices in the marine environment (Table 3).

*Table 3 Pressure and Impacts from Annex III related to PHS and subsequent impact on habitats*

| Pressure | Impacts | Impact on habitat |
|---|---|---|
| **Physical loss** | Smothering, sealing | Mainly benthos |
| **Physical damage** | Siltation, abrasion, selective extraction | Mainly benthos |
| **Other physical disturbance** | Underwater noise | Fish, marine mammals, birds |
| **Interference with hydrological processes** | Significant changes in salinity regime | Benthos, fish, marine mammals, birds |
| **Contamination by hazardous substances** | Introduction of synthetic substances, introduction of non synthetic substances | Benthos, fish, marine mammals, birds |
| **Biological Disturbance** | Selective extraction of species | Mainly fish |

PHS devices are particularly impactful on fish. Fish fall under the umbrella of descriptors D.1 and D.3, with particular reference to the biological disturbance pressure of Annex III of MSFD.

# 2 Hydropower as source of damages on fish

Hydropower plants pose a series of hazards to downstream passing fish that can be classified as direct or indirect. Fish passing through operating hydropower turbines may be subject to lethal injuries resulting in *direct* immediate mortality. Non-lethal injuries and elevated stress levels may instead lead to delayed mortality, which is anyway regarded as a direct turbine effect. *Indirect* impacts are, on the other hand, potentially negative effects that fish are more likely to experience downstream turbine passage: they consist in higher susceptibility to diseases, increased predation and adversely affected behavior (e.g. disorientation).

Both direct and indirect effects ultimately result in serious ecologically-significant consequences to fish populations, especially in case of long-distance migrators (e.g. salmon, eel), as they are disrupted in their migrating patterns for feeding or reproductive purposes, or short-distance migrators, because they are prevented from reaching habitat for flood shelter or wintering.

Indirect impacts are generally more difficult to assess than direct ones and, historically, turbine fish friendliness was assessed by short-lasting experiments in which injuries and mortality rates were monitored for up to 120 hours post-passage. Estimates on indirect impacts are therefore only theoretical.

In the next paragraph, an overview of the most significant parameters imposed by the operating conditions and the mechanical design of hydropower turbines that affect fish survival following passage are reported.

## 2.1 Mechanisms affecting mortality of fish during turbine passage

The main mechanisms leading to injury and mortality in fish following downstream passage through hydropower turbines are water pressure change (also known as rapid decompression), cavitation, fluid shear stress (also known as velocity change rate), turbulence and collision (also referred to as strike or crush). The location within the turbine where the above mentioned mechanisms are more likely to occur, in relation to turbine components, is graphically represented in Fig. 1 and Fig. 2.

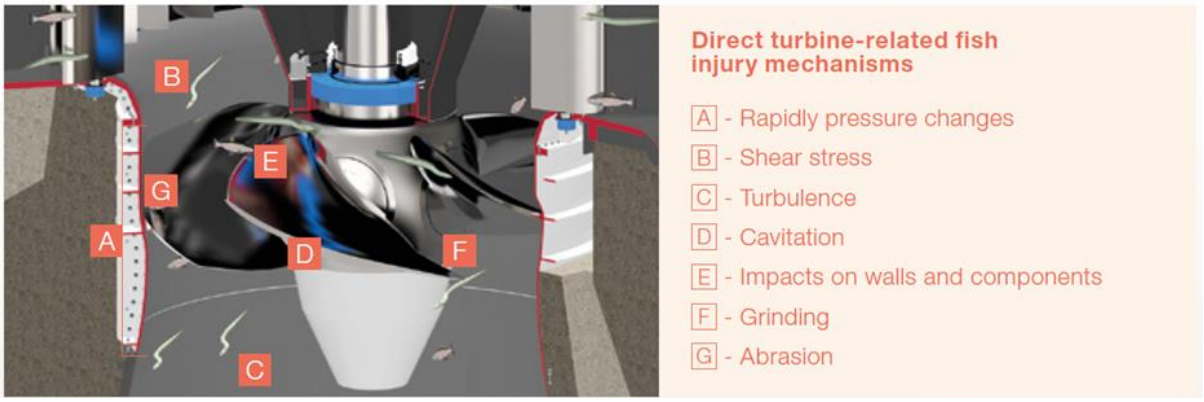


*Fig. 1 Direct fish injury mechanisms in relation to turbine components (Rammler, 2017)*

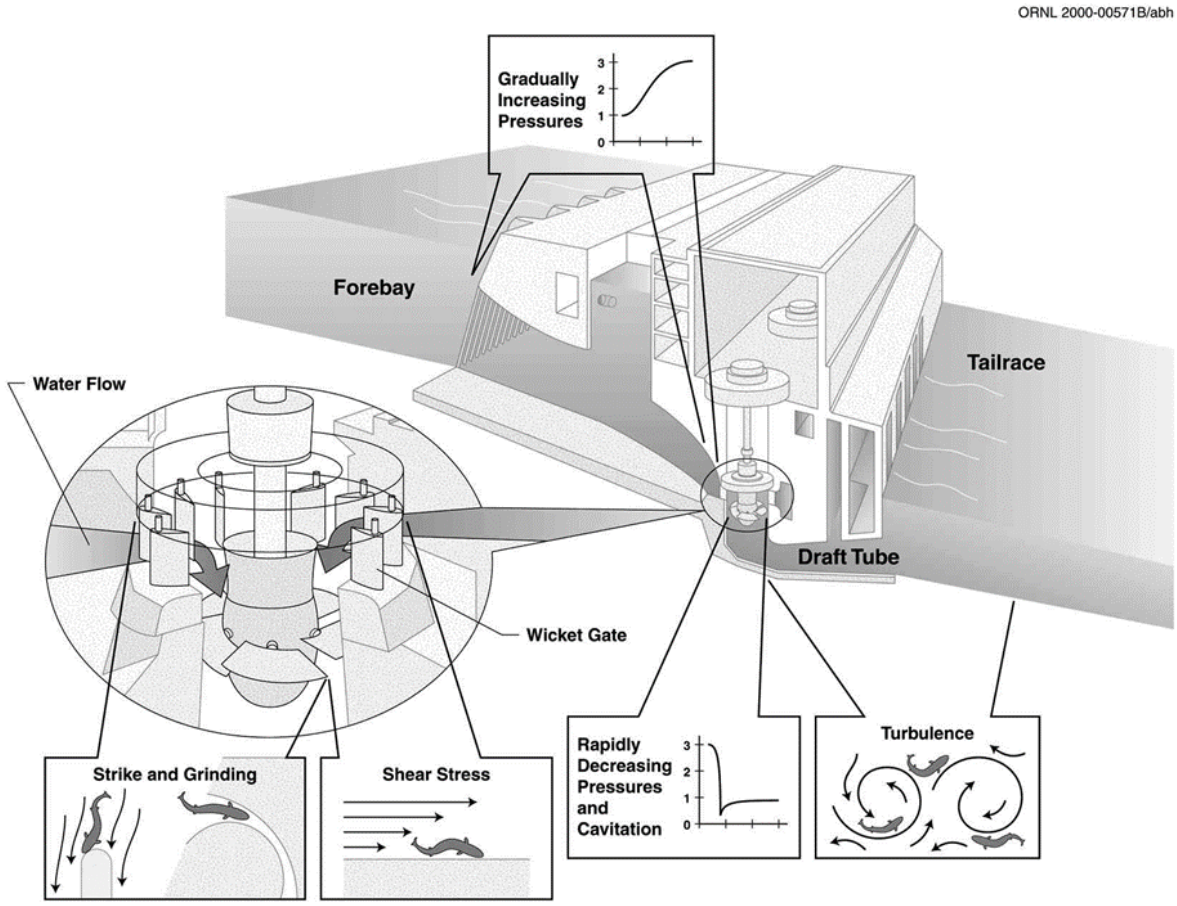


*Fig. 2 Locations within a hydroelectric turbine at which particular injury mechanisms to downstream passing fish tend to be most severe (Čada, 2001)*

### 2.1.1 Rapid decompression

Rapid decompression, or changes in ambient pressure, causes barotrauma to fish that are not able to adjust to the sudden decrease in pressure prior to returning to near surface pressure in the downstream channel.

When entering hydropower plants, fish promptly relocate from deep to shallow waters and experience sub-atmospheric pressure conditions especially during turbine passage. Pressures associated with conventional hydro turbines range between 460-2 kPa (EPRI, 2011) and the extent of decompression depends on several features of the turbine such as the runner design, the operating conditions, the elevation of the turbine runner relative to the downstream water surface elevation, the head of the plant and the flow path (Carlson et al., 2008; Pflugrath et al., 2021).

Overall, the potential of pressure-related damages depends on the magnitude and rapidity of pressure reduction, on fish acclimation time to changing pressure conditions, and the acclimation pressure of fish when entering the turbine intake (Jacobson et al., 2012). It was demonstrated that fish may be unharmed by the change in water pressure if they are given a sufficiently long time to acclimatize to such a condition. However, in hydropower settings, various changes in pressures occur instantaneously (Abernethy et al., 2001) (Fig. 3):

- Following the entrainment into a turbine intake, fish are subjected to an increase in pressure upstream of the runner that may last from seconds to minutes depending on how strongly the specimens can resist the flow via their swimming activity.
- When passing through the turbine, fish experience a rapid decrease in pressure below atmospheric levels often in less than 1 s (Neitzel et al., 2000; Pflugrath et al., 2021).
- After the turbine runner, fish return to depth-equivalent ambient pressures in the draft tube or are exposed to near atmospheric pressure as they surface in the tailrace.

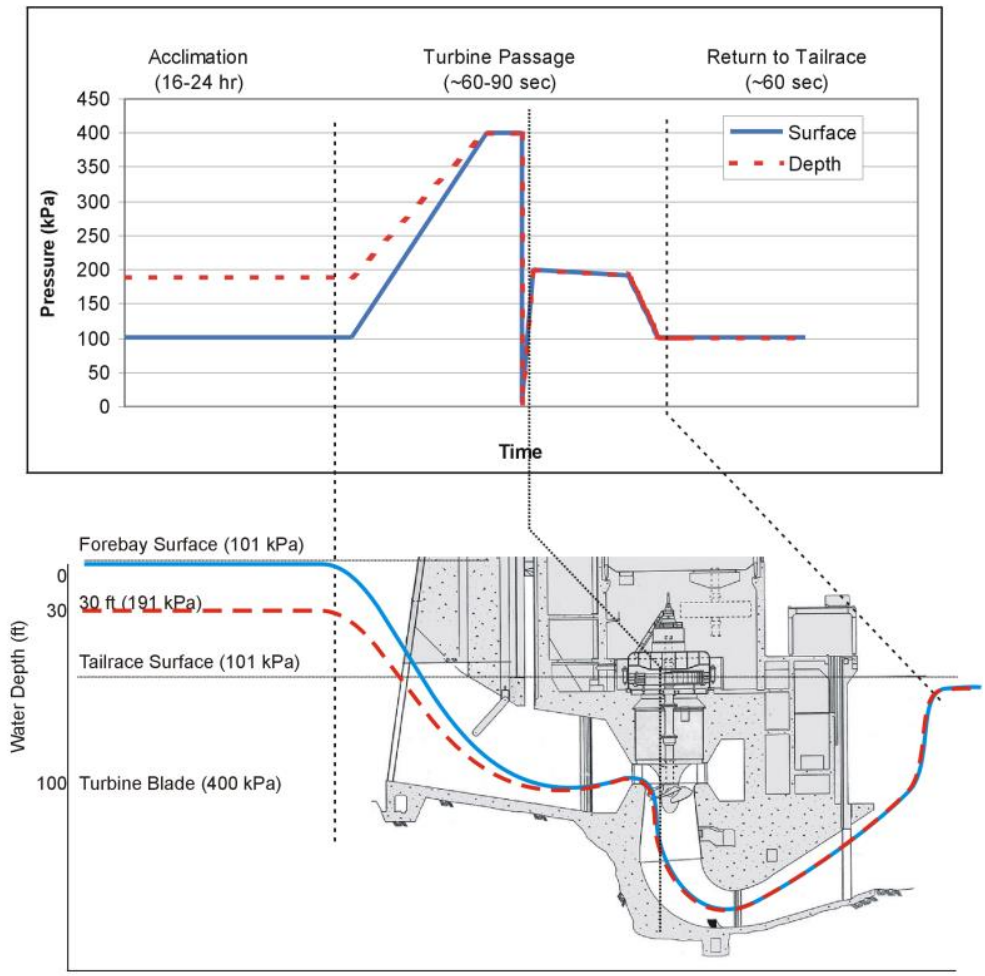


*Fig. 3 Pressure exposure simulation of turbine passage for fish acclimated to surface (blue continuous line) and depth (red dotted line), with an indication of duration and location in the various turbine components (Abernethy et al., 2001)*

The decrease in pressure causes an expansion in volume of the gas contained in the swim bladder, ultimately leading to its rupture (Brown, 2012). Other barotrauma injuries typically include exophthalmia, eversion of stomach and intestine, emphysema (or formation of bubbles, in accordance with Henry's law, which states that the amount of dissolved gas in a liquid is proportional to its partial pressure above the liquid) and both internal and external hemorrhaging in the fins, musculature and organs (Odeh, 1999; Abernethy et al., 2002; Jacobson et al., 2012; Brown et al., 2014). Rapid decompression is regarded as the most serious hydropower mechanism of damage to fish biodiversity, as most migratory fish are lethally impacted by sudden swim bladder rupture (Quaranta et al., 2021).

The swim bladder is an organ filled either with air or oxygen that plays a key role in maintaining neutral buoyancy and lowering energy costs for fish to remain at any certain depth (Helfman et al., 2009). Three categories of fish can be described on the basis of the presence, structure and the evolutionary pattern of the swim bladder:

- **Physoclistous**: fishes in which the connection between the swim bladder and the gastrointestinal tract is lost in the adult phase. This results in slower adjustments to bladder volume via gas diffusion through the swim bladder wall. Examples of physoclistous fish are Siluriformes in general. Despite being anatomically classified as physostomes, some fish species such as Anguilliformes are functionally physoclists.
- **Physostomes**: fishes in which the swim bladder is connected to the digestive system by means of a pneumatic duct. This allows rapid intake and venting of gas, preventing the rupture of the swim bladder in case of rapid ascension to shallow waters. Typical examples of physostome fishes are carps and Salmonidae (e.g. trout and salmon) (Fig. 4).
- **Fish with no swim bladder**: Myxiniformes (hagfishes) and Petromyzontiformes (lampreys) are typical examples of fish species in which the swim bladder is absent. Because of this, they usually show low susceptibility to barotrauma (Colotelo et al., 2012).

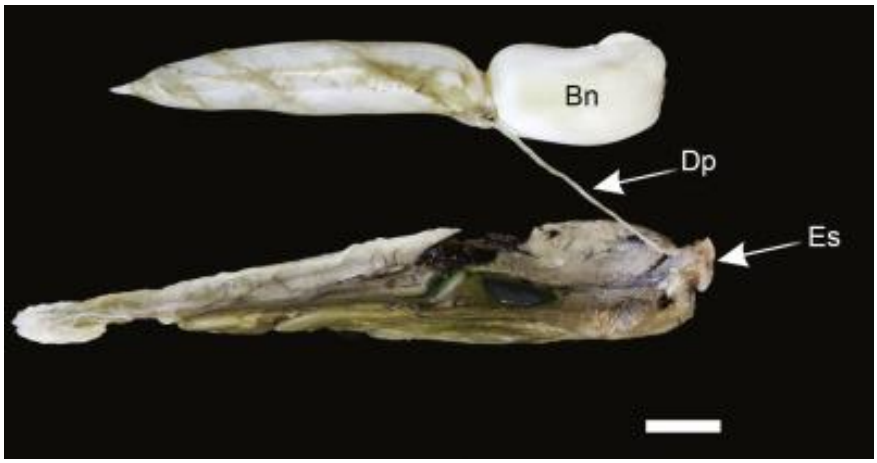


*Fig. 4 Digestive system and swim bladder of the physostomous grass carp Ctenopharyngodon idella. The attention is called on the presence of the pneumatic duct (Dp) connecting the swim bladder (Bn) to the esophagus (Es). Scale bar: 2 cm (Sado et al., 2020)*

Because physoclistous fish possess a limited ability to compensate for the rapid pressure changes that typically occur during turbine passage compared to physostomous fish, they are more susceptible to pressure-induced damages. Hence, swim bladder morphology is a paramount trait to consider for best defining the actual susceptibility of a given species to rapid decompression and barotrauma (Becker et al., 2003). Additional parameters to consider are:

- **Behavior**: behavioral features such as buoyancy or acclimation depth prior to exposure to nadir pressures may contribute in determining susceptibility to barotrauma. A higher incidence of immediate mortality, emboli in the gills, swim bladder rupture and internal hemorrhage was found in neutrally buoyant than

negatively buoyant fish, with buoyancy state being identified as one of the statistically significant endpoint predictors (Stephenson et al., 2010). This may be explained by the fact that negatively buoyant fish have a lower amount of gas in the swim bladder, with less severe consequences with regard to volume expansion in decompression situations (Abernethy et al., 2003).

- **Life stage / fish size**: oocytes and embryonated eggs are usually not susceptible to barotrauma because no gas is contained within the zona pellucida or developing tissues (Brown et al., 2013). However, fertilized eggs may be induced triploidy, i.e. a 3n chromosomal state achieved via the retention of the oocyte polar body caused by several conditions, including hydrostatic pressures. Worthy of note, triploid fish are viable but usually sterile due to a lack of gonadal development, particularly in females. Larval stages are usually susceptible to rapid decompression upon swim bladder inflation. The trend appears reversed in other life stages: Meng et al. (2019) demonstrated that smaller Crucian carps have higher survival rate than larger ones during the same simulated turbine passage tests. Boys et al. (2014) suggested that exposure pressure should not fall below 40% and 60% of acclimation pressure for larvae and juveniles, respectively. Sensor Fish measurements taken at Kaplan turbines have shown a typical nadir of ~87 kPa and lowest nadir of 7 kPa. Assuming swim at surface, 5 m or 10 m depth, fish would be exposed to RPCs of 0.9, 0.6 or 0.4, and 0.07, 0.05 or 0.03, respectively.
- **Swimming activity**: susceptibility to barotrauma may be increased or decreased depending on the species, likely due to differences in physiological traits such as nitric oxide production, by swimming activity prior to exposure to rapid decompression (Pflugrath, 2017).

Table 4, extracted from Brown et al. (2014), provides a thorough outlook on additional traits that influence the susceptibility of fish to barotrauma, along with species examples.

*Table 4 Fish traits influencing the susceptibility to barotrauma (Brown et al., 2014)*

| Physiological, behavioral, or life history trait affecting susceptibility to barotrauma | Presence or absence | Susceptibility to barotrauma | Example species or project | References |
|---|---|---|---|---|
| **The amount of free (undissolved) gas in the body** | | | | |
| Presence of a swim bladder | Yes | High | Chinook Salmon | Colotelo et al. (2012) |
| | No | Low | Pacific Lamprey | |
| Type of swim bladder | Open (physostomous) | Low | Chinook Salmon | Abernethy et al. (2001) |
| | Closed (physoclistous) | High | Bluegill | |
| Ability to expel gas out of the swim bladder through pneumatic duct | Better | Low | Large Rainbow Trout | Shrimpton et al. (1990) |
| | Poorer | High | Small Rainbow Trout | |
| Ability to fill the swim bladder with vasculature (rete) | Better | High | Bluegill | Harvey (1963); Fange (1983) |
| | Poorer | Low | Chinook Salmon | |
| Acclimation depth ability | Better | High | Burbot, Rainbow Trout | Fange (1983) |
| | Poorer | Low | Chinook Salmon | |
| **Pressure exposure** | | | | |
| Acclimation depth | Deeper | High | Burbot | Stephenson et al. (2010); Fange (1983) |
| | Shallower | Low | Chinook Salmon | |
| Exposure pressure | Higher | Low | Irrigation weirs/spillways | Brown et al. (2012b) |
| | Lower | High | High-head dams | |
| Ratio of pressure change (acclimation pressure/ exposure pressure) | Higher | High | Hydroturbine | Brown et al. (2012a) |
| | Lower | Low | Bypass system | |
| Rate of ratio pressure change | Higher | High | Hydroturbine | Brown et al. (2012e) |
| | Lower | Low | Angling | |
| **Life history** | | | | |
| Migrational patterns | More migratory | High | Murray Cod, Salmonids | |
| | More sedentary | Low | Trout Perch (*Percopsis omiscomaycus*) | |
| Larval or juvenile drift stage | Yes | High | Sturgeon, Murray Cod | Brown et al. (2013); Baumgartner et al. (2009) |
| | No | Low | Salmonids | |
| **Structural integrity** | | | | |
| | High | Low | Adult fish | Baumgartner et al. (2009); Tsvetkov et al. (1972) |
| | Low | High | Larval or juvenile fish or eggs | |

According to Boyle's law, the volume of a gas is inversely proportional to the absolute pressure acting on the volume if the temperature is fixed within a closed system (Van Heuvelen, 1982). The corresponding equation is:

$$\frac{P1}{P2} = \frac{V2}{V1}$$

where P1 and V1 are the initial pressure and volume, and P2 and V2 are the resultant pressure and volume. In all experiments evaluating the effects of rapid decompression on fish by means of baro-chambers, it is common practice to represent the ratio of gas volume change within the fish (V2/V1) as P1/P2, the so-called Ratio of Pressure Change. Here, P1 is the acclimation pressure, i.e. the pressure at which the fish achieves neutral buoyancy prior to being exposed to decompression, and P2 is the nadir pressure, i.e. the lowest pressure to which the fish is exposed during decompression. In other words, a fish acclimated to the bottom of the river is more likely to suffer from barotrauma than one swimming close to the surface. For facilitating the calculation, representation and comparison among different experimental settings, RPC is transformed using the natural log, yielding the so-called Log Ratio Pressure Change (LRP). LRP is often used as the independent variable for statistical analysis, as it has been found to be predictive of the likelihood of mortality and injury for fish exposed to simulated turbine passage (Brown et al., 2012b).

### 2.1.2 Cavitation

Cavitation is the rapid vaporization and condensation process of a liquid. Turnpenny (1992) defines cavitation as the process of formation and collapse of gas bubbles in a liquid that is caused by a localized reduction in pressure up to vapor pressure. Such conditions occur wherever pressure is low, flow velocities are high, direction of flow changes abruptly or if the surface is irregular or rough. The bubbles grow within the vapor pressure region and, as they move to areas with higher pressures, become unstable and collapse violently, creating shock waves that cause injury to fish in the surrounding area (Weitkamp et al., 2003).

Reproducing cavitation under controlled conditions is difficult, and therefore a thorough description of such a mechanism is not available. However, it was suggested that cavitation is strongly related to the mechanisms of rapid decompression and fluid shear. For instance, while interpreting the causes of injuries (i.e. decapitation, torn operculum, eye damage, and broken vertebral columns) recorded in juvenile rainbow trout (body length of 76-305 mm), Chinook salmon (BL of 76 to 229 mm) and Coho salmon (BL of 76-229 mm) exposed to 24 and 28 m $s^{-1}$ jet velocities (equivalent to strain rates of 1333.3 and 1555.5 $s^{-1}$), the author concluded that cavitation and fluid shear may have occurred simultaneously, and that the former may have contributed to the injuries and mortality observed, making it hard to discern the biological consequences of each mechanism (Johnson, 1972).

Importantly, turbine designs that minimize pressure reductions to no greater than 60% of ambient will not cavitate and cavitation-related fish injury will not occur (EPRI, 2011).

### 2.1.3 Shear

Shear is a mechanism generated when two masses of water moving in different directions or distinct velocities intersect, or where moving water slows near a solid structure. In both cases, shear results in friction forces acting on the fish body (Čada et al., 2006). Shear is a naturally-occurring stress mechanism, and fish have evolved several adaptations to counteract it (Vogel, 1994). They suffer minor, if any, injuries from shear in the wild, where it was estimated to account for 100 N $m^{-2}$ during normal flows (Costa 1987; Statzner and Müller 1989). At hydropower plants, instead, shear can range from 500 to 5000 N $m^{-2}$ (McEwen and Scobie, 1992). Shear forces are expected to be greatest along solid boundaries (i.e. spillway, draft tube, stay vane, wicket gate) or at the leading edge of turbine blades (Čada et al., 1997). Extreme shear stress conditions occur near the periphery of the blade (blade tip vortex) and near the hub (hub leakage vortex). However, it must be noted that fish are exposed to the highest end of the above shear spectrum only for a very limited amount of time: Turnpenny et al. (1998), by applying CFD simulations to identify the risk of injury from shear effects in small low-head (< 30 m) Francis and Kaplan turbines, revealed that shear was of minor importance in both turbine types based on the low occurrence probabilities. Also, under typical operating conditions, computational models estimated that the areas where potentially damaging shear levels occur comprised less than 2% of the flow path through the modeled turbine (Čada et al., 2006). In fact, the overall water volume interested by shear stress did not correlate well with observed fish mortalities in field studies (Čada et al., 2006).

Neitzel et al. (2000) referred to the index of the physical force that fish experience when subjected to a shear environment as strain rate. This is defined by the following equation:

$$S = \frac{\Delta \bar{v}}{\Delta y}$$

where $\Delta \bar{v}$ is the change of mean water velocity and $\Delta y$ is the distance, perpendicular to the force, over which such velocity change occurs. Strain rate is expressed as cm $s^{-1}$ $cm^{-1}$, and hereon simplified as $s^{-1}$. It is worth specifying that the above Δy term is key in defining the actual extent of strain rate: a given change in mean water velocity produces different strain rates depending on the distance over which it occurs. In the work of Neitzel et al. (2000), Δy was set equal to 1.8 cm because this was the minimum size of the tested salmonids. A positive correlation exists between strain rates and jet velocities, as shown in Fig. 5.

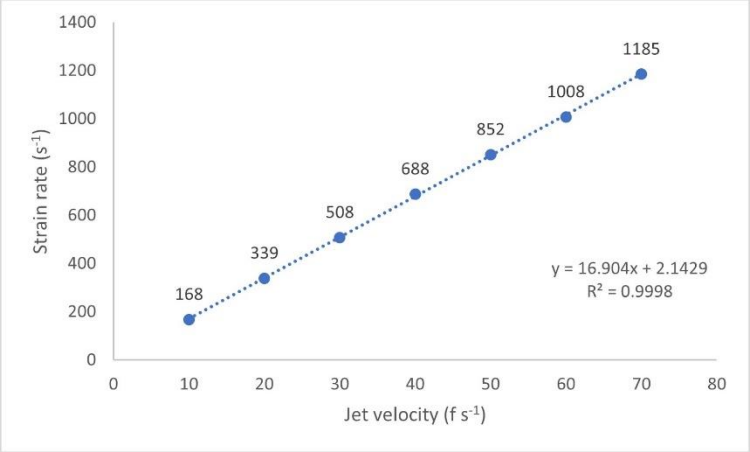


*Fig. 5 Correspondence between jet exit velocities (feet $s^{-1}$) and estimated strain rates ($s^{-1}$), described as Δy of 1.8 cm) applied to four fish species. Recreated from data published by Neitzel et al. (2000).*

Due to the difficulty in truthfully recreating shear under controlled conditions, its actual effects on downstream passing fish are not well understood. From field studies, it was suggested that shear can cause the loss of mucous layer, descaling, tearing or bruising of tissues and, in most severe cases, decapitation (e.g. Normandeau Associates, 1996). From studies conducted under controlled conditions employing water jets, injuries such as scale losses, hemorrhaging, and eye, skin and skeletal damages, as well as mortality were reported as consequence of shear; also, some species that survived shear were found more susceptible to predation following passage, therefore being subject to so-called indirect or latent mortality (Neitzel et al., 2000).

Based on the knowledge acquired on shear stress by means of field and laboratory studies, the five key drivers demonstrated to influence the severity of shear stress consequences to fish fauna are body length (i.e. a proxy of the developmental stage), body morphology, inherent species sensitivity, turbine type across which they pass and hydraulic conditions of operating turbines. In particular:

- Shear, together with turbulence, was deemed a relevant source of mortality for fish during early life stages (Pracheil et al., 2016);
- Juvenile salmon of 85 mm BL did not suffer any minor and major injuries at strain rates of 517 and 688 $s^{-1}$, respectively, while American shad was already susceptible at rates of 341 $s^{-1}$. The latter set of data, though, was not supported by statistical significance compared to untreated controls (Neitzel et al., 2000).
- Strain rates less than 500 $s^{-1}$ are usually considered safe and cause no major injury to juveniles, while egg mortality occurs at rates as low as 150 $s^{-1}$.
- Damages following passage through Francis turbine are more severe and more often life-threatening than those occurring downstream of Kaplan turbines (Franke et al., 1997).

Shear was correlated to hydraulic conditions measured by sensor fish and categorized in its magnitude as slight, for accelerations ranging between 245 and 490 m $s^{-2}$, moderate, for

acceleration ranging between 490 and 932 m $s^{-2}$ and severe, for acceleration greater than 932 m $s^{-2}$ (Deng et al., 2005).

### 2.1.4 Turbulence

Turbulence occurs when fluid masses in a flowing water body make tiny but strong changes in directions other than the bulk flow direction (Vogel, 1981), and it may also be caused by the breakdown of shear zones (Turnpenny et al., 1992). Turbulent motions and eddies within the flow can cause localized injuries or disorientation to an extent dependent on their intensity and scale. Turbulence is supposedly constrained to areas of the hydropower plant past the hub and near the draft tube piers, where the water spreads out and slows down as it is discharged to the tailwaters (Cada, 2006), and in fact it was estimated to occur only in 2% of the flow in conventional turbines (Cook et al., 2003; Lin et al., 2004). Small-scale turbulence can be found throughout a conventional turbine passageway, particularly in the wake of the runner blades (Turnpenny et al., 1998), whereas large-scale turbulence tends to be highest within the turbine draft tube (Cada et al., 1997). The former has been found to result in body rotation, compression and distortion in fish, leading to injury and mortality (Morgan et al., 1976); the latter often creates vortices which spin fish and cause disorientation. Among other problems, disorientation can make the fish easier targets for predators. Hydrokinetic turbines lacking structures leading to and from the rotors or blades (e.g. stay vanes, wicket gates, draft tubes) and operating in conditions of low velocity and little change in flow direction would have lower likelihood of occurrence of turbulence-related injury (EPRI, 2011).

Turbulence has been usually related to shear stress because shear forces are present in turbulent flow, and it is therefore difficult to discern the individual effects or to acquire focused information on the biological effects of such a stressor under controlled conditions (EPRI, 2011). Although it is the least understood mechanism of injury (Stoltz and Geiger, 2019), it is assumed that only eddies as large as the size of fish be actually hazardous to fish, causing disorientation (Cada, 2006) that can subsequently lead to indirect impacts such as adversely affected behavior and increased predation downstream of hydropower plants, while smaller ones are converted to thermal energy without disturbing the fish.

Turbulence was not identified as a relevant source of damages for downstream passing fish (DOE, 2009).

### 2.1.5 Blade strike

Collisions with physical structures of the hydropower plant, either fixed (e.g. stay or guide vanes) or moveable (e.g. turbine blades), are the predominant source of injury and death in fish (Pracheil et al., 2016) and result in abrasion, grinding and striking of organisms. Abrasion is the result of the rubbing action of a fish against a turbine system component or objects in the flow field. Grinding occurs when a fish is drawn into small clearances (gaps of sizes similar to that of the fish) within the turbine system, potentially causing localized bruises, deep cuts, and even decapitation. Striking refers to the collision of a fish against a turbine system component. Due to the many factors involved and the fact that similar biological endpoints (e.g. scale and mucous loss or exophthalmia), can be provoked by multiple types of collision, only blade striking will be discussed hereon.

Fish are subject to several injury types following the impact with runner blades: contusions, lacerations, rib and vertebral fractures, fin amputation, decapitation, eye damage, scale and mucous loss, internal hemorrhaging, blood clotting, damages to internal organs such as liver, heart, swim bladder and kidney or to the musculature (EPRI, 2008; Turnpenny et al., 1992, 1998; Saylor et al., 2019, 2020; Bevelhimer et al., 2019), with fractures of the vertebral column being the most lethal injury type.

The risk and severity of injury from blade strike is associated to several factors:

- **Turbine types**: Francis and Kaplan turbine types are the most common in hydropower plants globally (Uria-Martinez et al., 2018). Francis turbines are being installed less frequently at new hydropower projects as they usually cause more severe rates of injuries and mortality due to blade thickness of 10-25 mm, blade velocities up to 23 m $s^{-1}$ and a higher number of blades (Fu et al., 2016; Martinez et al., 2019; Pflugrath et al., 2021). Kaplan turbines have up to eight blades and blade leading edge thickness as well as velocity may differ along the hub-tip length: blades at hub are thicker and slower, in fact allowing for a decreased probability of damage to fish passing closer to such a location. Indeed, Kaplan turbines cause lower fish mortality rates (5-15% on average) than Francis turbines (5-50% on average) (Eicher et al., 1987; EPRI, 1992; Franke et al., 1997). In contrast, other turbine types such as the Archimedes screw appear as the most fish friendly due to low rotational and tip speeds and number of blades of typically 3 or fewer. Minimal injury or mortality was demonstrated on a variety of fish species and size classes (Spah, 2001; Bracken and Lucas, 2013). The impact of a given turbine type in terms of mortality and injury rates may differ also depending on the rotational speed and head, as demonstrated on *A. anguilla* specimens of 682-720 mm BL exposed to a straflo and a bulb turbine (two variant of the Kaplan type) operating at slightly different rotational speeds and heads (Ammar et al., 2020).
- **Blade characteristics**: Velocity, shape and leading edge thickness of the blades are among the most critical factors affecting the probability of injury and mortality from strike impact. All tested species but American eel, for instance, experienced 100% mortality when struck at a 90° angle at the center of the fish (mid-body) by 26–76 mm

thick blades at velocities above 10 m $s^{-1}$. As a general rule, thinner and faster blades cause more severe damage rates than thicker and slower ones: fish struck by narrow blade profiles at higher speeds suffer from severe damages such as mucous loss, bruising, eye damage, internal bleeding and broken spines because strike energy is transferred to a much confined surface of fish; on the other hand, strikes from wider (thicker) blade leading edges at slower speeds caused little damage and no mortality (Turnpenny et al., 1992). In general, impact velocities above 10 m $s^{-1}$ are likely lethal. Studies performed with the Lucid Spherical Turbine (Darrieus type cross flow) and Welka UPG (horizontal-axis propeller turbine) have reported that strike velocities up to 5 m $s^{-1}$ cause little to no mortality in trout, sturgeon and bass (Amaral et al., 2011). In particular, Welka UPG provoked 0% mortality at 1.5 and 2.1 m $s^{-1}$ approach velocities. On the other hand, strike velocity equal or greater than 5 m $s^{-1}$ can cause fatal injuries to fish of lengths greater than the thickness of the leading edge (L/t > 1, see bullet below). Strike velocities lower than 4.8 m $s^{-1}$ and lower ratio of fish length to blade thickness is suggested to result in less injury (Jacobson et al., 2012). With regard to optimal blade geometry, results from CFD modeling and laboratory testing highlighted that a semi-circular-shaped blade creates the highest differential forces (i.e. leading edge pressures) and thus have the greatest potential to deflect a fish prior to impact (EPRI, 2008, 2011b).

- **Blade strike impact**: The damages provoked by blade strikes change according to three variables, namely body location of impact (i.e. head, mid-body and tail), body orientation (i.e. dorsal, ventral and lateral) and angle of impact (i.e. typically 45, 90 and 135°, even though 30° and 75° have also been tested). Extensive research was conducted to establish where the greatest severity of strike occurs. With regards to body location, the collision is most severe when fish are struck mid-body or at the head region, because vital organs and vertebral column are found in those locations (Amaral et al., 2020; Turnpenny et al., 1992), and least severe if it occurs at the tail region, as found by the limited rate of mortality recorded following strikes up to 12 m $s^{-1}$. The morphological features of fish species play a key role in determining the relationship between body orientation and strike. Depending on fish shape (see bullet "Morphological features of fish" below), the extension of the lateral rather than the dorsal surfaces is different. In elongated and laterally compressed species, the probability of strike on the side is higher, as are the rates of severe injury and mortality sustained even below the above-mentioned critical velocity of 10 m $s^{-1}$ (Bevelhimer et al., 2019). At last, the location of strike along the body strongly affects strike survival. Above the safe threshold of 7 m $s^{-1}$, for which 100% survival can be recorded regardless of the slant angles evaluated, survival declines steeply from 30° to 90° (Amaral et al., 2020). A mid-bod strike at a 90° angle is regarded as the most lethal to all fish species. Head strikes at 45° and mid-body strikes at 135° are also hazardous to fish because energy is transferred towards the musculoskeletal system and operculum/gills, respectively (Pflugrath et al., 2021).
- **Fish-blade interaction**: The severity of damages is proportional to the ratio between the fish length (L) and blade thickness (t), i.e. the blade ratio, and the relative velocity

of the fish to the strike object (Amaral, 2008). The blade ratio metric is useful for standardizing the results obtained from collision experiments performed with different species (Jacobson et al., 2012). An increase in blade thickness, particularly a blade ratio equal to or less than 2, corresponds to a less damaging strike event, with higher survival rates (EPRI 2008, 2011; Bevelhimer et al., 2017, 2019) (Fig. 6). Survival rates above 90% following strike at velocities up to 12.1 m $s^{-1}$ were reported for Salmoniformes species when the blade ratio was equal to or less than 1 (i.e. when fish length equalled or was greater than the leading edge blade thickness). Below the strike velocity of about 5 m $s^{-1}$ mortality is unlikely to occur, as demonstrated by the survival rates of approximately 100% when testing such a threshold with L/t ratios up to 25, regardless of fish length and blade thickness. Dramatic decrease in survival rates occurred at blade ratio of 4 or greater when strike velocity increased to 7.3 m $s^{-1}$ (EPRI, 2011b). Importantly, such a trend seems to hold true for morphologically diverse fish species.

- **Biological and behavioral features of fish**: body length, movement and orientation of the passing fish contribute to determining the location and angle of blade strike and must be also taken into account when predicting strike-related damages. For instance, the highest rates of injury and mortality were reported when fish were struck mid-body and from the side (Pflugrath et al., 2021). With regard to body lengths, no clear trends between injury or mortality rates and fish size that can be applied to all tested species exist, suggesting that, except where surrogacy can be clearly or has been historically established, blade strike studies under controlled conditions must be performed for multiple species.

- **Morphological features of fish**: although no experiment has ever been conducted to clarify the relationship between fish shape and susceptibility of species to blade strike, it is reasonable to assume that the two variables are linked. A large morphological diversity exists in fish, and the swimming activity and performance are influenced by traits like body elongation, width and number of fins. Five main types of fish body shapes can be identified: streamlining, laterally compressed, vertically compressed (i.e. dorso-ventrally elongated, flattened from side to side), elongated and unusual. Biological surveys at locations that are selected for hosting hydropower projects are therefore strongly recommended to account for the diversity of local fish populations. Typical freshwater species include species with laterally-compressed bodies to a variable extent, which display less musculature along the flanks. Such a trait would translate to a much higher energy being transferred from turbine blades to internal organs and vertebrae, resulting in higher probability of hemorrhaging and fractures.

- **Species sensitivity**: some species inherently exhibit a higher susceptibility to blade strike compared to others. For instance, following the exposure to equivalent blade ratios, lower survival rates were found for rainbow trout than white sturgeon or American eel. These two species were also reported to have higher survival rates when exposed to L/t ratios and strike speeds greater than those tested with rainbow trout. (EPRI, 2008).

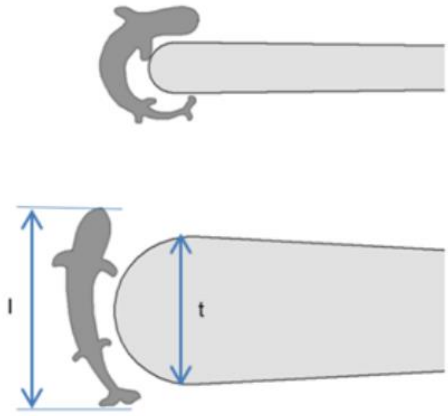


*Fig. 6 ratio between the fish length (L) and blade thickness (t) (Amaral, 2008)*

Several authors attempted the modeling of strike and mortality probability by considering several parameters related to turbine geometry, site features and biological information and few assumptions (Fig. 7). The general theory behind the models is that fish can avoid being stroke by turbine blades if they pass through the plane of the leading edges of the blades in a turbine runner after the sweep of one blade and before the sweep of the next (Deng et al., 2007).

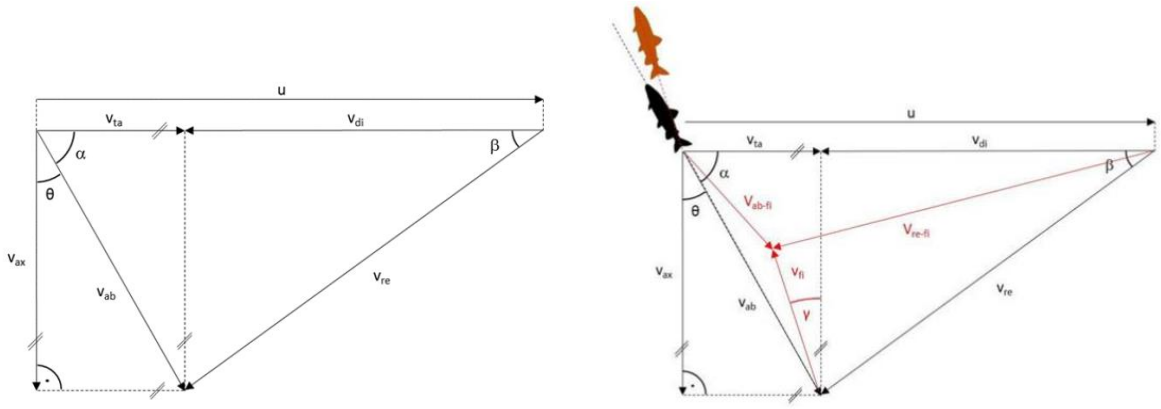


*Fig. 7 Schematic representation of the hydraulic parameters at runner entrance needed for basic (left) and generalized (right) strike modeling (Stoltz and Geiger, 2019)*

- **Von Raben, 1958**: by assuming that fish are oriented with their body length parallel to the ambient current, which is considered typical behavior when fish are moving in fast currents, the probability of strike is given by the following equation:

$$P(s) = \left(\frac{n}{60}\right) * z * L * \frac{\cos(\theta)}{Vax}$$

where n is revolution in RPM per minute, z is the number of blades, L is the fish length in m, θ is the angle between absolute velocity (Vab) and axial velocity (Vax). Any fish longer than the so-called "water length" (i.e. the chance of passage between two successive blades) would be struck by a blade. The concept of water length was defined by Turnpenny et al. (2000).

- **Monten, 1985**: the underlying assumption is that fish are oriented perpendicular perpendicular to the relative velocity. The general form of the equation is:

$$P(s) = n * z * L * \frac{Vrel}{u * Vax}$$

where Vrel (relative velocity) is the ratio between Vax and the angle between u and Vrel, and u is the circumferential velocity.

- **Geiger, 2018**: the assumption of defined fish orientation is lacking, and strike probability is given by the following equation:

$$P(s) = n * z * L * \frac{Vd}{u} * (\frac{\cos(\gamma)}{Vax} + \frac{\sin(\gamma)}{Vdi}$$

where Vdi is the velocity difference between u and the tangential velocity, and γ is the orientation of the fish (Fig. 7 right).

- **Hecker and Allen, 2005**: using the same assumption of Von Raben, 1958, the probability of strike is a function of the distance that blade leading edges move, compared to the total distance between two consecutive leading edges, in the time it takes a fish to be carried or swim past the arc of leading edge motion (Jacobson et al., 2012). The general form of the equation is:

$$P(s) = n * (L * \sin(\alpha)) * \frac{z}{60 * Vr}$$

where α is the angle between the absolute inflow velocity and a tangent line to the runner circumference, and Vr is the radial component of inflow velocity.

This equation was developed for a real world application aimed at understanding how fish length and the relative velocity of turbine inflow to blade speed (strike velocity) influence strike injury and mortality rates. The authors then used the equation to compare the friendliness of a prototype Alden turbine to a Kaplan Minimum Gap Runner (MGR) (see section 3.1 - Environment-friendly turbines) employing 100 mm long fish in a site with turbine discharge of 1,500 cfs and head of 92 ft (28 m). The mortality rates recorded with the prototype turbine was 5-fold lower than that caused by the MGR Kaplan, likely due to:

  - lower inflow-to-blade velocity (i.e. strike velocity);
  - lower rotational speed;
  - more tangential absolute flow velocity;
  - lower number of blades (3 vs. 6 in the MGR Kaplan)

Similar conclusions were drawn by Turnpenny et al. (2000), who applied the basic modeling of Von Raben. The authors found that rates of strike injury were highly dependent on fish size, turbine type, the runner diameter and rotational rate (rpm), the number of blades, and operating load, and that the strike-mortality relationship was in function of fish length.

For these reason, the probability of strike may be lowered by altering:

- the number and length of blades;
- the area per blade channel;
- the thickness and bluntness of blade leading edges;
- the blade tilt.

# 3 Mitigation measures

## 3.1 Environment-friendly turbines

As specified in the first two chapters, traditional hydropower poses severe risks to the environment and the biota, with habitat quality and fish being extensively investigated. Several well-known companies working in the development of hydropower projects have evaluated technical solutions to mitigate the damage to fishes during downstream turbine passage. This resulted in the development of several so called environmentally-enhanced (Quaranta et al., 2021) or fish-friendly turbine designs for low-head sites (i.e. with less than 10 m of head). These aimed at improving the environmental performance of hydropower structures at existing projects or promoting environmentally sustainable development at existing non-powered dams or other new projects.

According to Rammler (2017), Andritz Hydro recommendations for improving fish friendliness are:

- **Variable turbine speed**: Bulb turbines with additional speed variation have very high efficiencies across a wide operating range whereas conventional double regulated turbines show high efficiency over a narrower operating range.
- **Optimization of operating scheme**: This parameter is applicable to sites where migratory fishes are identified. The implementation of this strategy requires the acknowledgment of the size of migratory fish in order to allow plant operators to adapt the operating scheme of the turbines with the ultimate aim of increasing fish survival rates.
- **Reduced gap runner**: Reducing the gap between rotating and stationary components can boost survival rates by diminishing the risk of fish being trapped and reducing turbulence.
- **Least turbulence and cavitation**: Smaller gaps at the runner diminish the turbulence level in the draft tube. In general, turbulence in hydraulic passages can be classified on the basis of the small and large-scale effects they produce, which affect fish differently. Turbulence at small scales (i.e. scales smaller than the fish length) is present in the same locations as high shear, and lead to similar injuries such as compression, stretching, and bending: small-scale turbulence injuries can usually be lumped together with shear stress injuries. Large scale turbulence (i.e. scales greater than fish length) causes disorientation, hence increased stress on the fish. Such effects taken individually do not harm the fish but increase the incidence of indirect mortality.
- **Blunt leading edge**: this factor results in relevant increases in survival rates, particularly for small-sized fish species with regards to the L/t ratio. The optimal choice of the leading edge thickness can be achieved by CFD modeling, from which information on performance and cavitation characteristic of the resulting blade is obtained.

- **Alignment of stay and guide vanes**: this reduces the probability that a fish will hit the wicket gate.

The U.S. Department of Energy (DOE), Electric Power Research Institute (EPRI), and the Hydropower Research Foundation launched the Advanced Hydropower Turbine System Program (AHTS) in 1993 with the aim of developing environmentally friendly hydropower turbines. Two proposals originally submitted by Voith Hydro, Inc. and Alden Research Laboratory, Inc. together with Northern Research and Engineering Corporation (ARL/NREC team, DOE contract No. DE-AC07-95ID13383), were selected for funding in 1995 (Sale et al., 2001).

Voith Hydro's approach consisted in optimizing a Kaplan turbine to a Minimum Gap Runner (MGR) design (Fig. 8). The gaps between the runner blades and hub and the outer discharge ring were reduced to eliminate the added probability of fish injury and enhance the turbine efficiency. The severity of other stress mechanisms (strike, pressure changes) was also reduced in the design of the MGR. In a 1999 field test in Oregon, the overall mortality of juvenile Chinook salmon was 1.5%. Further data on this technology were gathered in 2005 when Grant County Public Utility District No. 2 replaced one of the 10 Kaplan turbines at its 1,038 MW Wanapum Dam on the Columbia River in Washington State with an MGR turbine: although salmon survival rates were found to be similar for both turbine designs (i.e. Kaplan and MGR), the MGR provided about a 10% increase in power production over the existing units. The MGR design allows greater hydraulic performances over most operating conditions compared to the standard Kaplan turbine while achieving a fish survival rate of up to 97% (Quaranta et al., 2021).

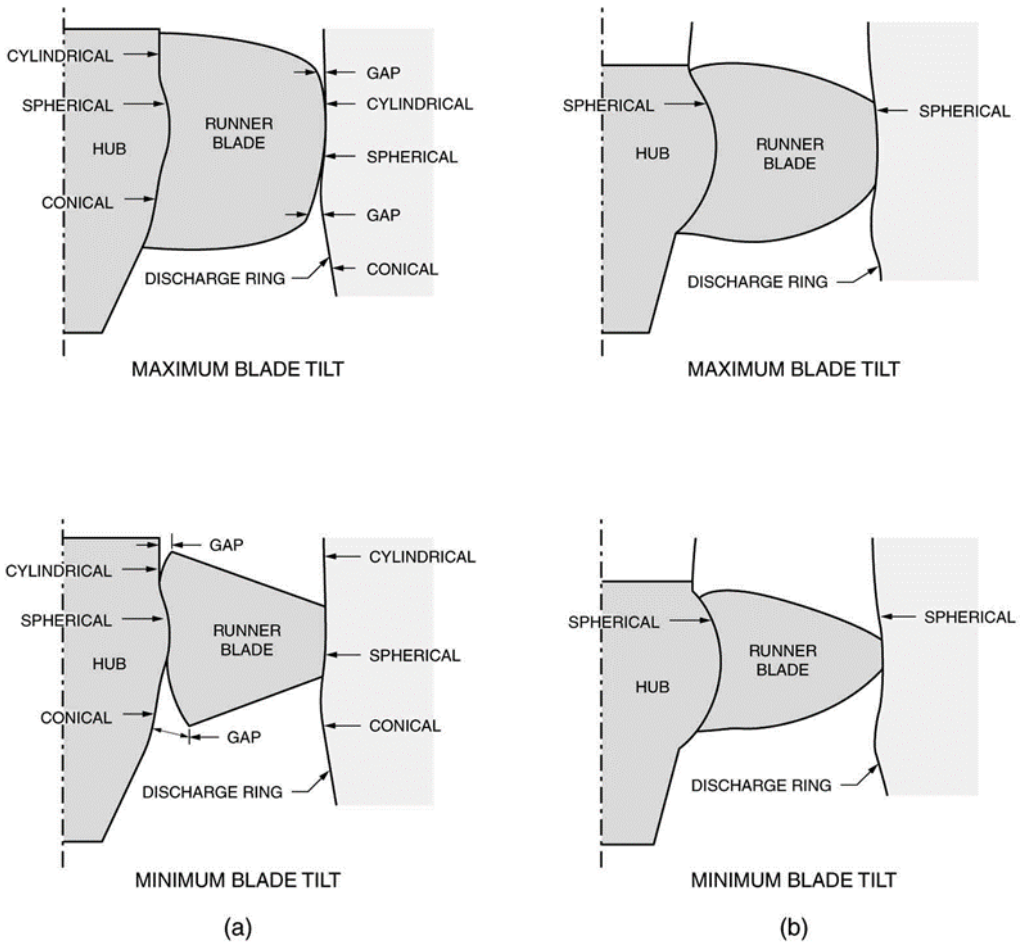


*Fig. 8 Comparison of (a) a conventional Kaplan turbine runner and (b) a Minimum Gap Runner (MGR) at two tilt angles*

Alden's approach, on the other hand, consisted in an entirely new turbine concept (Fig. 9), based on a commercially available pump that is used to pump fish and vegetables with minimum damage. The prototype was designed to operate at a flow of 28 $m^3$ $sec^{-1}$ and at a head range of 23-30 m.

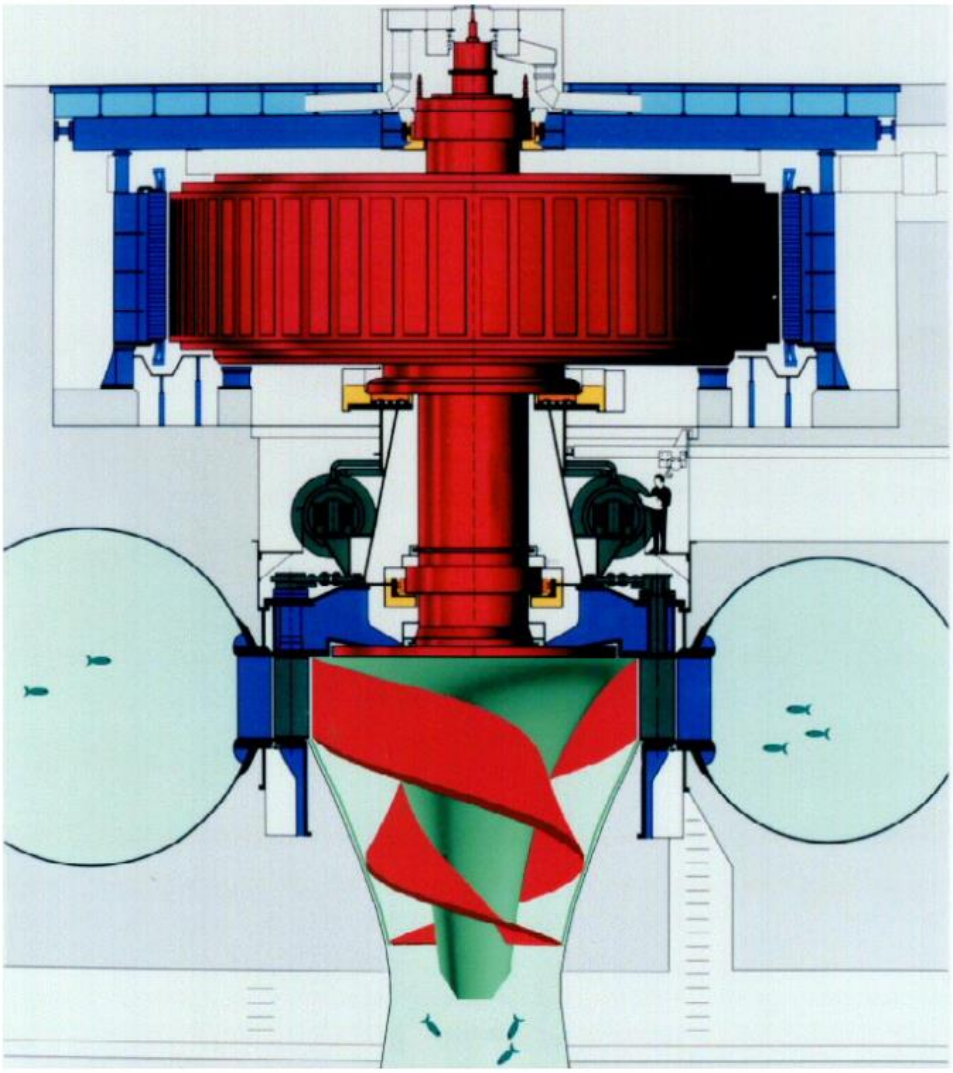

*Fig. 9 Conceptual installation of the Alden turbine runner at a hydroelectric plant*

The criteria for design and evaluation of the novel design are reported as follow (Odeh, 1999):

- Peripheral runner tip velocity less than 40 ft $s^{-1}$ (~12 m $s^{-1}$) and preferably 20 ft $s^{-1}$ (~ 6 m $s^{-1}$).
- Minimum pressure 10 PSI absolute (psia), equivalent to 68.8 kPa: this was based on the assumption of fish acclimation depth of ~10 m (30 psia, 206 kPa) and typical occurrence of mortality caused by a rapid decompression larger than 30% of acclimation pressure.
- Pressure gradient less than 80 psi $s^{-1}$ (equivalent to 550.3 kPa $s^{-1}$): assuming that fish injury occurs at a pressure rate of 160 psia/sec in Kaplan turbines, there was the need to limit negative pressure change rates.
- Velocity gradient / shear stress less than 15 ft/sec/inch (equivalent to 180 m/s/m): this was based on experimental data obtained on a susceptible fish species belonging to the family of Clupeidae, namely *Alosa pseudoharengus*, which was not harmed by the above-mentioned shear stress value.

- Clearance between runner and fixed turbine housing components less than 2 mm: small clearances reduce the possibility of entrainment and subsequent mechanical injury.
- Minimization of the number of blades and length of leading edges: fewer blades and shorter leading edges reduce probability of strike.
- Limitation of the relative velocity of the inflow to the blades.
- Maximization of the distance between the runner inlet and wicket gates trailing edges and minimization of clearances between other components. Fig. 10 illustrates the layout of the fixed and moving components as the fish pass through the turbine.

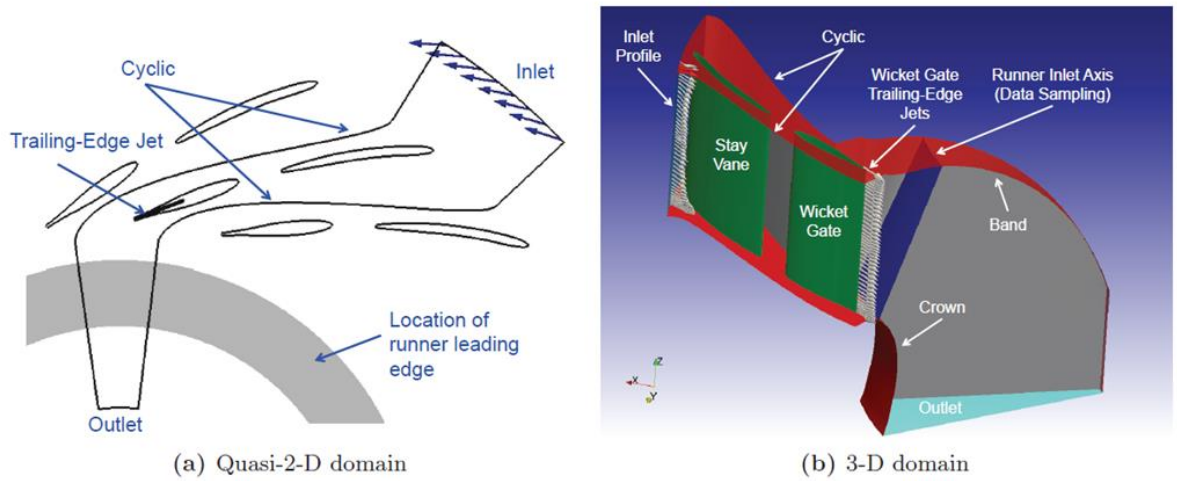


*Fig. 10 Scheme of the fixed and moving components, in case of quasi-2-D (left) and 3-D (right) numerical modeling*

The end-result was a 2-bladed runner design attached to a rotating shroud, eliminating the low-pressure vortices that typically occur near the blade tips and thus the chance of fish being caught between the blades and outer discharge ring. The runner blades were 4 inches thick with the trailing edge rounded, had nearly 180 degrees of wrap around the hub and were longer in the flow direction than conventional blades.

Biological testing was conducted on a number of fish species and several body lengths for each, including rainbow trout (38 mm, 85 mm and 175 mm), American eel (249 mm and 431 mm), the susceptible *Alosa pseudoharengus* (87 mm) and coho salmon (102 mm). Results of tests indicated that fish survival through a full-scale turbine (with increased leading edge blade thickness) at a 28-m head site would exceed 98% for fish up to 200 mm in length, ensuring a maximum hydraulic efficiency of 93.6% (Cada and Amaral, 2011). The costs of the electro-mechanical equipment of the Alden turbine are 39% and 35% higher than a Francis turbine and a MGR Kaplan-Bulb unit, respectively (Dixon and Hogan, 2015). However, in an overall cost-benefit analysis, the operations related to an Alden turbine are recommended due to cheaper civil works and the unnecessary fishways or fish bypass systems (Nielson et al., 2015).

The hydrokinetic turbine produced by HGE (Hydro Green Energy) (Fig. 11) was the industry's first surface-suspended, asymmetrically-ducted, horizontal axis turbine to be installed in the U.S.A. in the Mississippi Lock and Dam No. 2 Hydroelectric Project in December 2008. The rotational spin was 21 RPM, making the device the slowest spinning hydrokinetic turbine in the industry, and the capacity is 100 kW at 3.5 m $s^{-1}$. Minor impacts were found on fish populations as demonstrated by mark and recapture of five species and two size classes (i.e. 115-235 mm and 388-710 mm) of fish (Normandeau Associates, 2009).

*Fig. 11 Model of the HGE's hydrokinetic turbine installed at the City of Hastings Hydro Project, Mississippi Lock and Dam No. 2 (https://www.hydro.org/wp-content/uploads/2017/08/Hydrokinetic-Power-Development-for-HGE-Stover.pdf)*

Following are the major findings of the field test on fish friendliness:

- The average recapture rate was 98%.
- The average 1 h direct relative survival estimates for both fish sizes was 99%. The 48 h calculated relative survival estimate for each small-sized species was 100% after adjusting for control mortalities. The 48 h calculated relative survival estimate for large-sized species ranged between 98 and 100% after adjusting for control survival, depending on the species.
- None of the 196 small-sized and 201 large-sized treatment specimens examined had any sign of blade-strike related damages.

- Predation due to disorientation was not evident or observed for any of the five species tested during the investigation.

The reasons for such a negligible impact on resident fish species are likely a result of:

- The measured water velocities around the HGE unit (i.e. ranging from 5.67 to 9.68 ft $s^{-1}$, equivalent to 1.72-2.95 m $s^{-1}$): these values are well below the critical values of 20 or 58 ft $s^{-1}$ (6 or 17.6 m $s^{-1}$) identified by laboratory studies, at which fish start to suffer lethal injuries (Bell et al., 1972) or mortality (Neitzel et al., 2000).
- The low number of runner blades (i.e. 3) and the relatively large diameter of the runner (i.e. 12 ft, 3.6 m): injuries associated with common hydropower turbines are primarily a function of the number of runner blades and fish size relative to turbine runner diameter size (Franke et al., 1997). In hydrokinetic turbines, the typical mechanisms of damage (see section 2 - Hydropower as source of damages on fish) do not occur.
- The potential of entrainment at the turbine hub or tip is null.

A couple of turbine designs intended for low head and very low head sites (20 m or 66 ft and less and 3 m or 10 ft and less, respectively) were recently produced and described as being extremely fish friendly thanks to their operational parameters (Hogan et al., 2014). These are reported as Very Low Head (VLH) turbine and Archimedes screw turbine and their friendliness was reported recently (e.g. Bozhinova et al., 2013; Piper et al., 2018).

The VLH turbine incorporated a Kaplan runner with 8 blades and was designed for sites with a head of 1.4-4.5 m and flow rates of 10 to 30 $m^3$ $s^{-1}$. Thanks to the large diameter of the runner (i.e. 4.5 m) with large spaces between blades, low runner speed (i.e. approximately 40 RPM), water velocity inside the runner less than 2 m $s^{-1}$, small pressure variations and minimization of gaps, very low injury and mortality rates were expected. On-site tests were performed in France using five fish species including Atlantic salmon *Salmo salar* smolts (147-240 mm) and European eel *Anguilla anguilla* (0.7-1.2 m), the two target species of this deliverable.

- Immediate turbine passage survival for salmon varied depending on the site of release (i.e. periphery, mid-blade, hub), with lowest rates of 96.9% for periphery and 99% for hub. Delayed survival after 3-4 days post-passage accounted for 98.6%. Compared to control, which exhibited an extended survival rate of 97.9%, the consequences of passage were regarded as negligible.
- Cumulative survival for eel was 95%. In this case as well, the site of release was a key factor in determining susceptibility: specimens injected at the hub had a survival rate of 100%, those released near the blade tips had a survival rate of 84%.
- The overall survival rate of the three additional species ranged from 95.6% and 100% across all tested sizes.

Archimedes screw turbines are appropriate for sites with a head of 10 m. They are considered to be fish-friendly because of very low rotational and tip speeds (about 30 RPM and 3.8 m $s^{-1}$, respectively), lack of significant pressure changes or damaging shear forces, minimal number of blades (typically 3 or less), the existence of only one significant point of contact (i.e. the leading edge of the screw) and large diameters (1.5 to 3.5 m) (Fishtek Consulting, 2007). Injury and mortality data was produced for a variety of fish species, namely post-spawn Atlantic salmon, European eels, adult sea-run brown and lamprey, and different size classes. In all cases, minimal (1.5% at most) mortality was recorded. No damage was caused by passage through the turbine across the full range of operating speeds of up to 31 RPM. For Atlantic salmon smolts, limited and recoverable scale loss occurred in 1.4% of the fish (Fishtek Consulting, 2007). For downstream-migrating kelt (or post-spawn Atlantic salmon), safe passage was recorded in 100% of cases (Fishtek Consulting, 2008). For European eel, following the modifications to the leading edge of the helical screw overhanging the trough, the turbine was found to be extremely safe, as only 0.64% of specimens suffered minor and recoverable damage to the tail (Fishtek Consulting, 2008).

At last, the most recent entry on the hydropower industry is Natel Energy's RHT (Restoration Hydro Turbine) (Fig. 12), available with runner diameters from 0.5 m to over 2.5 m. The radial and axial turbine configurations are optimized for low-head sites (2-20 m), and the fish-safe runner presents curved blades and slanted tips that deflect fish and enable a glancing contact, rather than direct collision, in the region of the blade where relative velocities are highest, therefore reducing the severity of strike, respectively. This patented design lacks the typical features of conventional low head small hydropower turbine such as high rotational speeds, high strike velocities (i.e. relative velocity of fish to approaching blade), and thin leading edges, which overall contribute to high strike probabilities and low survival rates (Amaral et al., 2018).


*Fig. 12 Natel's D190 RHT prior to installation at the Monroe hydropower project in Madras, Oregon (USA). This turbine features the uniquely thick, fish-safe runner detailed in the diagrams and photograph on the right (Adapted from https://www.natelenergy.com/turbines)*

Laboratory testing and CFD-based strike model development led to a series of live fish passage tests. The two size classes of rainbow trout (110-163 mm and 182-236 mm) corresponded to average L/t ratios of roughly 1.4 and 2 for the tested blades. External injury types and severity, along with percent scale loss, 1-hour and 48-hour survival rates were recorded. As expected, the lower L/t ratio led to higher strike survival. At the velocity of 7 m $s^{-1}$, survival rates were at least 98% for both size classes, while at higher velocities survival was high only at more acute slant angles, testifying to the importance of steeply slanted blunt blades in ensuring fish friendliness. A survival of 98% was achieved also with a L/t ratio of 2 at a velocity of 10 m $s^{-1}$ when the slant angle was 30°. With regards to injury, the majority of external damages following strike were haemorrhaging and bruising, and only a minority of specimens experienced eye damage, fin tears or lacerations (Amaral et al., 2020).

As general recommendations and based on the features and outcome of above-mentioned studies, it was demonstrated that hydropower turbines can achieve an elevated degree of fish friendliness if they:

- Maximize open space between blades and other structures.
- Include blunt and not sharp leading edges.
- Have low rotational speed.
- Direct fish toward the hub and away from the periphery.

It must be remembered that the above environmentally-enhanced turbines have demonstrated their efficiency only at low-head sites. However, fish friendliness has not reached 100% so far, warranting the continued reliance of dedicated passages for a safe downstream migration of fish.

## 3.2 Fish screens

Fish protection and habitat connectivity are considered fundamental in the design, construction and operation of hydro power plants (HPPs). The displacement of artificial structures (eg. dams) in rivers can constitute a barrier for fish populations (Jonsson et al., 1999); in particular, the fragmentation of riverine habitats caused by HPPs strongly influences migratory fish (Larinier, 2001).

Fish mortality caused by hydropower plants turbines during the downstream migration of fish is considered of significant importance in Europe, in particular, the decline of salmon (*Salmo salar*), sea trout (*Salmo trutta*) and European eel (*Anguilla anguilla*) at the silver stage is a cause for concern (Travade and Larinier 2006, Travade et al., 2010). The populations of Atlantic salmon and the European eel have declined strongly in Europe due the hydropower dams (Hindar, 2004; ICES, 2001).

Migrating fish usually swim within the main current, so in the absence of protection at the water intake or alternative passages, they will consequently pass through the turbines (Williams et al., 2012). Mortality and injuries are however dependent on many factors, such as the type of turbine installed, total head, operating conditions of the HPP or fish size and morphology (Cada, 2001).

The installation of fish-friendly turbines is one of the options available to increase the survival of migratory fish, but unfortunately they are efficient for limited head and discharge ranges, and therefore they cannot be used widely (Albayrak et al., 2018).

It is common to apply trash racks at the HPP water intake to collect and divert floating debris and sediment. These tracks are installed perpendicular to the flow and with a bar clearance ranging from 20 mm to 500 mm (Meusburger, 2002).

There are different systems in HPPs to prevent fish from entering water intakes, broadly classifiable as they can be physical or behavioral barriers. The former physically exclude fish from the turbine intakes; they are usually trash racks with horizontal or vertical bars that are angled to the flow direction or inclined to the bottom (Larinier et al., 1999) (Fig. 13). Behavioral barriers induce fish to swim away from the intakes by attracting or repelling them in response to natural stimuli. Visual, auditory, hydrodynamic and electrical stimuli have all been tested in many experimental barriers (Larinier and Travade, 2002).

Some studies show that trash racks can delay migration or provoke injuries to migrating fish, depending on the size and type of the HPP and its intake structures (Bruijs and Durif, 2009).

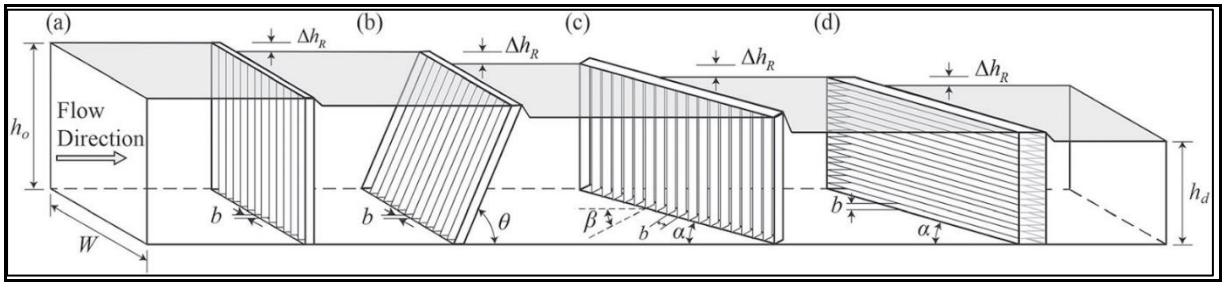


*Fig. 13 Detailed geometries of (a) conventional trash rack, (b) vertically inclined trash rack, (c) louvre, angled bar rack and modified angled bar rack (MBR), and (d) horizontal bar rack (HBR) (Albayrak et al., 2018).*

The presence of dedicated fish bypasses however does not guarantee the success of the migration without delays in the up- and downstream passages. Upstream migrating salmonids can fail to pass (Gowans et al., 2003; Thorstad et al., 2008), and in the case of downstream migratory fish, there may also be an increase in mortality due to the effects of spill, bypass or turbine passage (Ferguson, 2005; Ferguson et al., 2006).

Fish mortality related to intakes and turbines can be high based on the different fish morphology in relation to the width of the bars in the trash racks, so fish size must be taken into consideration in the planning phase of hydro power structures. Fish smaller than the width of the bars could reach the turbines with the risk of being hit by the blades, larger fish may get stuck in the bars when the approach flow exceeds their swimming capability (Adam and Bruijs, 2006).

Some HPPs attempted to solve this issue by adopting trash racks with a different design that avoids impingement and guides the fish towards a bypass (Calles et al., 2013).

It is possible to increase the fish friendliness of trash racks in order to avoid the passage of fish through the bars, impeding them to pass through operating turbines. Bar clearance must be chosen adequately to prevent fish from passing through based on the features of the populations upstream of project such as size classes and sex ratio. The equation to estimate the maximum length (Lmax) of fish that can pass a screen of a given bar clearance (c) considering the empirically estimated fish width/length ratio of 0.11 (b) (Ebel et al., 2013) is:

$$Lmax = \frac{c}{b}$$

For instance, given a fine bar clearance of 25 mm, fish up to 227 mm might be able to pass the screen.

The majority of Atlantic salmon juveniles smolt are 1 year old and have a body length of 12-17 cm, even though few specimens reach 3 years of life and a size of 22 cm before undergoing the downstream migration (Heland and Dumas, 1994). The size of downstream migrating European eels, on the other hand, is sex-dependent, and account for 30-50 cm for males and 40-90 cm for females (Acou, 1999). Based on this knowledge, the ideal bar clearance was suggested to be less than 25 mm for Atlantic salmon smolts, even though the use of smaller

clearances up to 15 mm constituting a physical barrier could be justified to obtain maximum efficiency from the device, and between 15–20 mm for European eels, a size that should induce a repulsive behavior in smaller eels (Courret and Larinier, 2008). The bars should also be inclined or angled to direct fish towards the bypasses located at the downstream end of the rack (Courret and Larinier, 2008). Experiments conducted at a small scale prototype using fish screen with a bar clearance less than or equal to 20 mm and flow velocities ranging from 0.3 to 0.5 m $s^{-1}$ demonstrated an efficiency of 100% for fish specimens more than ten times larger the bar clearance due to the physical barrier of the trash rack, except for European eel (Ball et al., 2020).

Over the years, several fish friendly trash rack designs have been devised (Amaral et al., 2002; Boubee and Williams, 2006; Larinier, 2008), with different approaches:

- Reduction of the space between the bars to prevent juvenile fish from passing through the bars (Bruijs and Durif, 2009).
- Inclination of the trash-racks from the bottom (inclined trash racks) or setting an orientation angle to side (angled trash-racks) (DWA, 2005).
- Changing of the bar position (Albayrak et al., 2017; Tsikata et al., 2014).

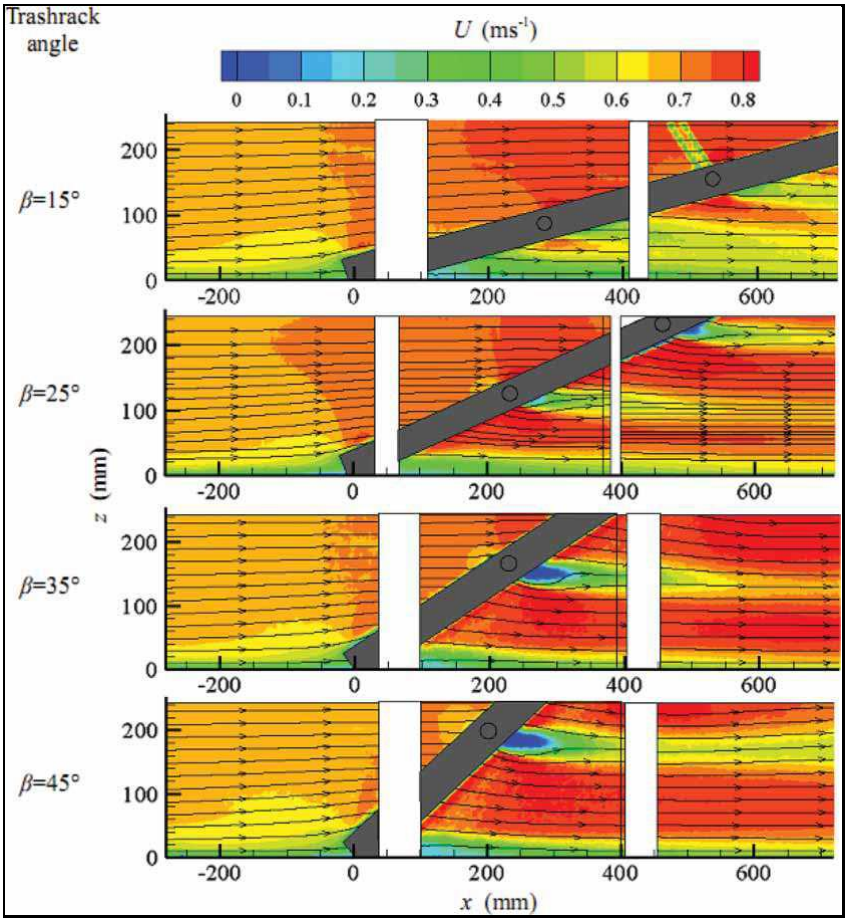


*Fig. 14 Upstream and downstream velocity map of a trash rack inclined at different angles (β = 15, 25, 35 and 45°) (Raynal et al., 2013)*

For smaller HPPs, Boes et al. (2016) showed that trash racks with horizontal bars (HBRs) (small bar spacing 10 – 30mm) connected to a bypass are to be preferred for fish protection, while trash-racks with vertical bars (VBR), with large bar spacing functioning as behavioral barriers, can be adopted for larger HPPs.

Regarding large HPP facilities, Albayrak et al. (2017) tested louvres, angled and modified angled bar racks (spacing of 50 - 230 mm) with a 10 mm bar thickness for optimal protection of a certain fish size.

French HPPs provided with a surface bypass showed that the fish guidance efficiency (FGE) of the racks for juvenile salmonids varied from 10–20% to 55–85% depending on the hydraulic conditions (Larinier & Travade, 2002).

In addition to the ecological aspects, it is important to underline that the optimal solution must also take into consideration economic parameters, such as head-losses and maintenance.

In order to make the intakes more fish friendly, Raynal et al. (2013) proposes the use of trash racks with low inclination and narrow spaces between bars (Fig. 14). This configuration, considering the head loss, would be optimal because the reduced space between the bars is compensated by the inclination of the bars and the relative widening of the screen area. However, flow velocity at the screen should not exceed 0.5 m $s^{-1}$ (Wolter et al., 2020).

# 4 Description of target species

## 4.1 *Anguilla anguilla* (Linnaeus, 1758)

The European eel *Anguilla anguilla* (Linnaeus, 1758), also commonly known as Common eel, River eel, Glass eel, Silver eel and Weed eel, is a teleost species belonging to the Order of Anguilliformes.

It is natively distributed along the coasts of the Eastern Atlantic Ocean (from Scandinavia to Morocco) and Europe (from the Black Sea to the White Sea), and inhabits the rivers of the North Atlantic, Baltic and Mediterranean regions. Spawning area is located in the western Atlantic offshore Bermuda Islands (Fig. 15).

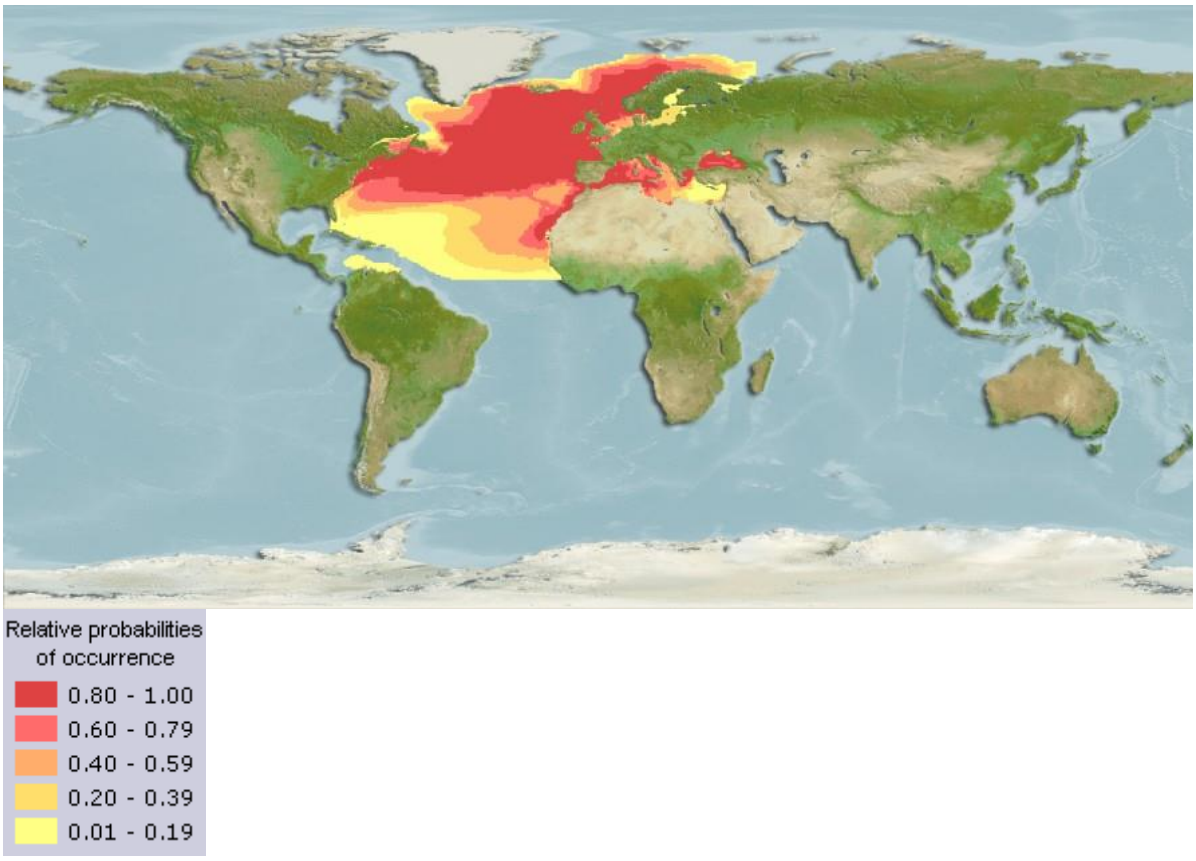


*Fig. 15 Currently known distribution of European eel Anguilla anguilla. Distribution range colors indicate degree of suitability of habitat which can be interpreted as probabilities of occurrence (AquaMaps, 2019)*

### 4.1.1 Biology

As all species of the *Anguilla* genus (Schrank, 1798), the European eel displays a catadromous life cycle, i.e. it spends the adult life stages in freshwater or estuarine waters and undergoes a migration to the Sargasso Sea (offshore Bermudian coasts) of the Atlantic ocean for reproductive purposes. The former phase is known as continental and the latter as oceanic Fig. 16.

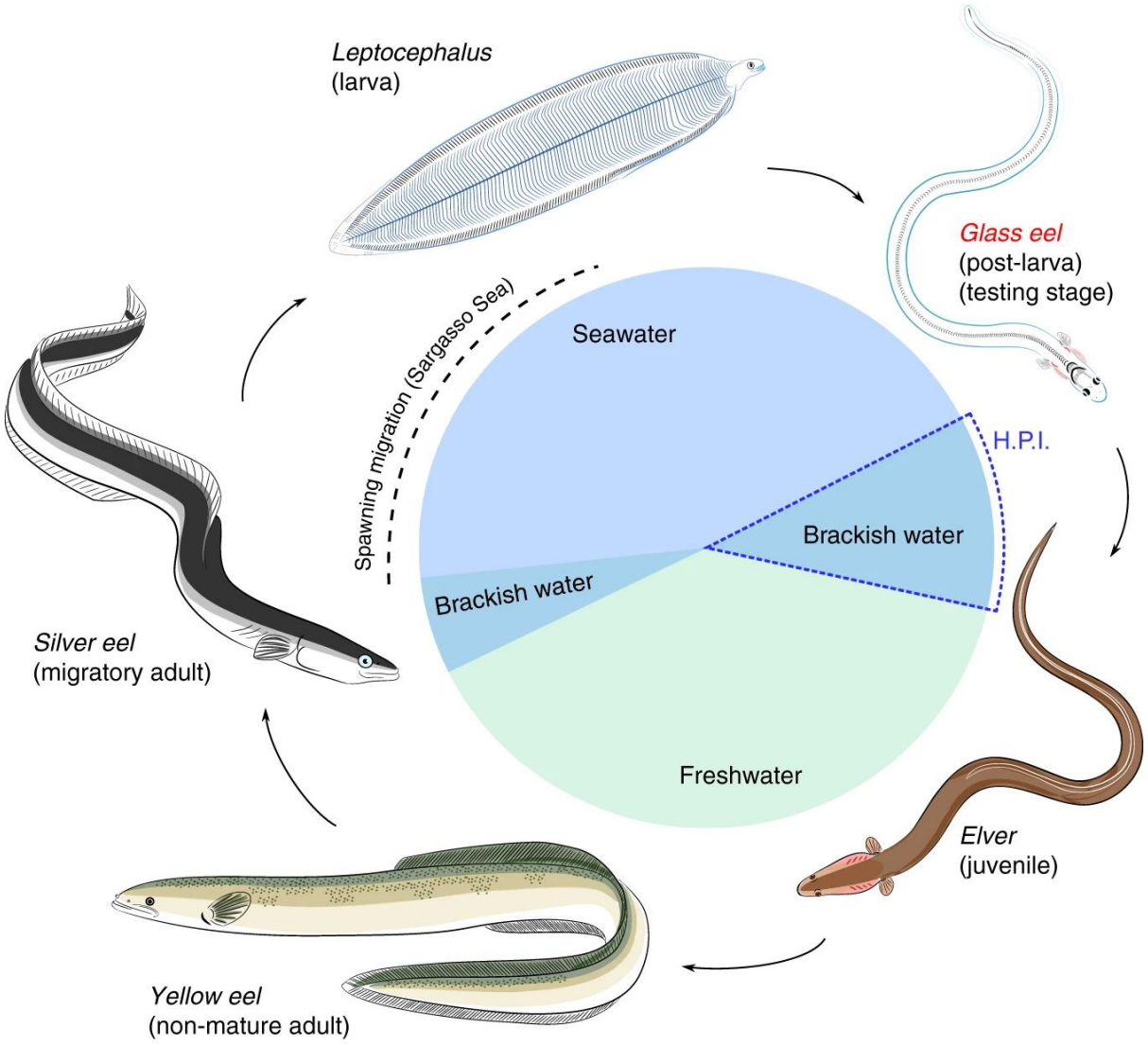


*Fig. 16 Life cycle of the European eel Anguilla anguilla (Cresci et al., 2019). Marked with a dashed blue polygon is the hypothetical period of memory imprinting of the magnetic direction of the prevailing tidal current occurring at estuaries*

Mature females contain an average of 3 million eggs $kg^{-1}$ body weight, which they spawn at a depth of 100-300 m, where epipelagic waters of the Sargasso Sea display an isotherm of 18-19°C that is considered to be the boundary of the spawning depth (Fricke, and Kaese, 1995). The earliest larval stage shows remains of the yolk sac oil droplet, which is reabsorbed completely shortly prior to the start of the independent feeding of transparent larvae known as leptocephali. This leaf-shaped stage is especially suited to long distance migration: by drifting in the Gulf Stream and North Atlantic Drift currents as zooplanktonic organisms, larvae migrate across the continental shelf and eventually reach the North African and

European brackish estuaries in a period of time of 7-24 months. The exact duration of such a period has not yet been determined with certainty by the scientific community (Maitland 1977; Kirkegard et al., 2010). Larvae undergo their first metamorphosis into the so-called glass eel stage just before reaching coastal waters: the body is shortened and its shape becomes cylindrical. Glass eels are the only natural source of supply of the species since reproduction in controlled conditions has not been achieved yet (Pedersen and Ramussen, 2016). The duration of the larval stage varies according to the biogeographic region under consideration, but at its end glass eels grow into so-called elvers (Tabeta and Mochioka, 2003). Some authors use the terms "glass eels" and "elvers" interchangeably, however elvers are easily distinguishable due to the body pigmentation. Elvers are stimulated to migrate upstream where temperatures and salinities are lower (Tosi et al., 1986; Vøllestad et al., 1986). This is the predominant life stage length-wise, the duration of which depends on the sex. Some authors reported that males and females feed and grow for 6-12 years and 9-20 years, respectively (Froese and Pauly 2005), while others defined the earliest age of downstream migrants as 3 year-old (Vøllestad, 1992). Generally, freshwater eels are ubiquitous and show opportunistic behaviour, being able to adapt to and exploit all aquatic habitats. Elvers turn into yellow eels, the sexually-immature adult stage characterized by the yellow-greenish body color.

The reproductive migration from European or North African freshwaters back to the Sargasso sea marks the end of a slow and long growth phase and is triggered in its start by several morphological and physiological changes. With regards to the former, the skin acquires a different structure and color, darkening dorsally and turning to silver ventrally - the silver coloration is considered as the hallmark of sexual maturity; the head becomes smaller; the eyes increase in size and shift in retinal sensitivity; the alimentary tract undergoes degeneration, with a drastic reduction in the numbers of villi and mucosal cells, structural changes in epithelial cells and decrease in size and muscle thickness. With regards to the latter, changes in fat content and in musculature, swim bladder modifications and enlargement and increase of chloride cells in the gills were reported (Aoyama and Miller, 2003). Such metamorphosis from the yellow phase to the so-called silver phase begins weeks to months before the actual start of the migration and was also demonstrated to be reversible. In *Anguilla anguilla*, as well as in other temperate and subtropical species of the *Anguilla* genus, the downstream migration begins as gonad maturation starts. Such migration is usually associated with decreasing water temperatures and increasing flows: the latter factor affects water velocity, turbidity, and conductivity and is likely exploited by *A. anguilla* migrators to optimize energy expenditure and reduce the swimming activity cost (Haro et al., 2003; Sandlund et al., 2017; Cresci et al., 2020). The months in which the above-mentioned environmental conditions are found are usually August throughout December, even though recent studies have theorized that the transition from elver to silver eel is possibly impacted in the timing by climate change scenarios and varying hydrological conditions ((Verreault et al., 2012).

A study in the field of population genetics showed global genetic differentiation caused by isolation by distance, implying the existence of non-random mating and confuting the panmixia hypothesis, i.e. all specimens migrating to the Sargasso Sea for reproduction being

comprised into a single, randomly-mating population; rather, three genetically distinct subpopulations of northern Europe, western Europe (including the Baltic, the Mediterranean and Black Sea) ans southern Europe (including stocks of Morocco) were suggested (Wirth and Bernatchez, 2001).

### 4.1.2 Ecological traits

As seen for many other pelagic organisms, European eels migrating to the Sargasso Sea perform diel vertical migration within the water column, spending the day at ~600 m depth and the night at ~200 m depth, likely for predator avoidance and feeding purposes, respectively. The European eel is indeed a species of predominant nocturnal activity: for instance, in all types of benthic habitats that are connected to the sea where it is naturally found, it remains hidden under stones or burrowed into mud during the daytime. The search for food occurs from dusk throughout the night: its diet is quite diverse and, due to the multiple environments inhabited, includes marine, estuarine and freshwater fauna, with the main preys consisting of invertebrates (e.g. insect larvae, mollusks, worms, and crustaceans) and fishes. Food selectivity increases with age, and larger specimens predominantly feed on fishes, which can also be scavenged and cannibalized. Feeding occurs not only in the aquatic environment, but also on land especially in rainy periods: thanks to its elevated mobility which for instance allow the movement over dams and weirs (McCosker 1989), the species was reported to leave the waters to prey on terrestrial fauna such as slugs and worms (Coad 2005), demonstrating that it is not easily contained (McCosker 1989). The feeding activity is almost completely interrupted during the cold months (Reshetnikov 2003): the species can however survive at freezing temperatures by reducing physiological and metabolic activity to a minimum (Reshetnikov 2003; Froese and Pauly 2005), and the temperature range that ensures survival was reported to span 0-30 °C.

The ecological importance of the European eel is elevated because of the ecosystem services it provides, similarly to all catadromous species: provision of food, regulation of ecosystem functions thanks to nutrient transport across and connectivity among different biomes (Drouineau et al., 2018a), bio-indicator of environmental quality and functionality (Smith et al., 2016), water quality (Amara et al., 2009) and ecological status within the European Water Framework Directive (Delpech et al., 2010).

### 4.1.3 Stock size

Given the broad distribution range of this species, and the extraordinary distances covered during reproductive migrations, multiple factors undermine the health of European eel stocks. Among the anthropogenic and natural threats that are implicated in the cumulative impacts on eel recruitment and stock in the continental phase are fisheries, habitat quality (e.g. hydrology, pollution), pathogenic diseases and barrier to migration posed by water management/use activities including dams, intakes, pumping stations and hydropower plants - this latter category is analyzed in greater detail in the following sections. Climate change scenarios, as anticipated above, will likely influence the oceanic phase (Drouineau et al., 2018b). Most importantly, due to the species' longevity, it is almost impossible to quantify the individual severity of such stressors as well as the effectiveness of corresponding management measures because i) neither of them occur or are implemented in isolation from the rest and ii) possible impacts or positive outcomes on juvenile stages only become evident much later in time at the first and only reproductive event (Belpaire et al., 2019). For these reasons, quantitative data rather than qualitative estimates is hard to achieve (Dekker and Casselman, 2014).

According to several scientific reports or publications, the European eel population as a whole has declined in most geographical areas over the last 50 years and the stock is outside safe biological limits (EIFAC/ICES, 2006; Dekker, 2016). Fisheries, although small-scale, cannot target the species in a sustainable manner due to inherent features: eels are caught both at the yellow/silver stages for direct human consumption, affecting the reproductive potential of the stock, and at glass eel stage for aquaculture purposes and restocking programs, preventing the newly-recruited specimens from establishing in local populations (Kirkegaard et al., 2010). Overfishing practices resulting in indiscriminate mortality over the entire *A. anguilla* life cycle is deemed one of the major threats for the survival of the species (FAO, 2007). The market for eels has surged in demand, causing the product to be transported globally; on the other hand, the management of the resource is run on a local or regional scale and measures are unable to safeguard stock exploitation within safe limits. As a result, the *A. anguilla* stock has shown a steep decline in recruitment and abundance during the past decades in almost all of its distribution area. Such decline was recently regarded as catastrophic or tremendous by some authors: "Abundance of the eel stock for all stages including glass eel, yellow eel and silver eel is at a historical minimum" (ICES, 2009). Although recruitment data significantly increased from zero in the 2011-2019 timeframe, the most recent ICES recruitment index is 98.6% lower in the "North Sea" series, and 94% lower in the "Elsewhere" series, compared to the 1960–1979 reference level (ICES, 2019). A prolonged reduction in recruitment trends is considered as the main driver of the current global status of *A. anguilla* stock (ICES, 2020). Also, the ~ 90% decrease in abundance of adult specimens at the silver stage in the 1975-2010 timeframe (Bevacqua et al., 2015) was attributed, at least partly, to anthropic activities (Feunteun, 2002; Piper et al., 2013). Overall, ICES, already a decade ago, advised that "all anthropogenic impacts on production and escapement of eels should be reduced to as close to zero as possible until stock recovery is achieved" (ICES, 2009).

### 4.1.4 IUCN status and legislative perspective

Despite the life history traits (i.e. catadromy, semelparity, presumed panmixia) of the European eel make the application of the IUCN (International Union for Conservation of Nature) Red List criteria challenging, the last assessment conducted in 2018 during a workshop held at the Zoological Society of London from November 5th–9th identified the species as being Critically Endangered (Pike et al., 2020), confirming the outcomes of the three previous evaluations of 2008, 2010 and 2014 (Fig. 17).

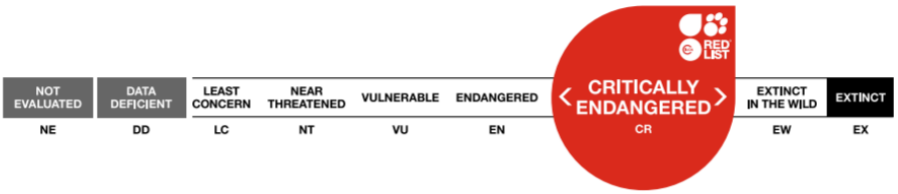


*Fig. 17 IUCN status of Anguilla anguilla*

The species was included in Appendix II of the Convention on International Trade in Endangered Species (CITES, 2021) and in Appendix II of Convention for the Conservation of Migratory Species (CMS, 2020). It is worth mentioning that the former lists species that are not necessarily now threatened with extinction but that may become so unless trade is closely controlled, while the latter covers migratory species that have an unfavourable conservation status and that require international agreements for their conservation and management as well as those that have a conservation status which would significantly benefit from the international cooperation that could be achieved by an international agreement, respectively. From a legislative perspective, measures for the recovery of the stock of European eel were established by Council Regulation No. 1100/2007 of the European Commission.

## 4.2 *Salmo salar* (Linnaeus, 1758)

The Atlantic salmon *Salmo salar* is a teleost species belonging to the order of Salmoniformes. It is typical of temperate and arctic zones in the northern Atlantic Ocean and in all rivers that drain into it. Eastern Atlantic Ocean populations are found from the White and Barents Sea basins through to the Baltic and North Sea basins, including Iceland (Fig. 18).

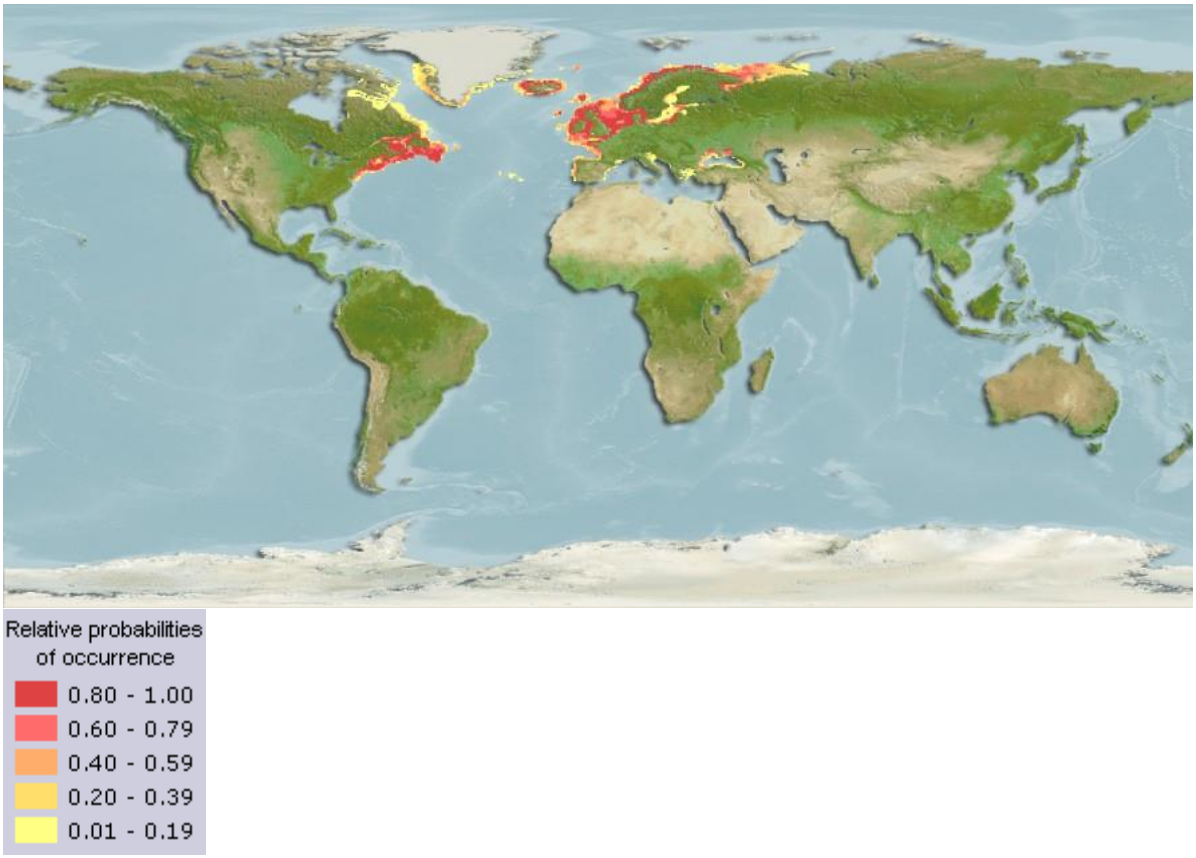


*Fig. 18 Currently known distribution of Atlantic salmon Salmo salar. Distribution range colours indicate degree of suitability of habitat which can be interpreted as probabilities of occurrence (AquaMaps, 2019)*

### 4.2.1 Biology

The Atlantic salmon *Salmo salar* is a species of high socio-economic value. Contrary to the European eel, it is a bentho-pelagic species that displays an anadromous lifestyle, and the key events of reproduction, hatching and early life stages all take place in freshwater environments (Rochard and Elie, 1994; Kangur et al., 2003). Juvenile specimens are found in rivers while the migration to the Atlantic Ocean is achieved for growth and maturation. Spawning occurs exclusively in the freshwater environment of origin. So called "landlocked" (i.e. non-anadromous) populations that feature migrations to and from lakes instead of the sea and can mature in the absence of a sea-ward migration are known (Webb et al., 2007; Hutchings et al., 2019) (Fig. 19).

The preferred temperature range is 4-12 °C and the species is only found in waters that exceed the temperature of 20 °C for a few weeks in the summertime (Kottelat and Freyhof, 2007). Lower and upper lethal temperatures up to -0.7 and 27.8 °C may be also withstood for short periods of time (Bigelow, 1963).

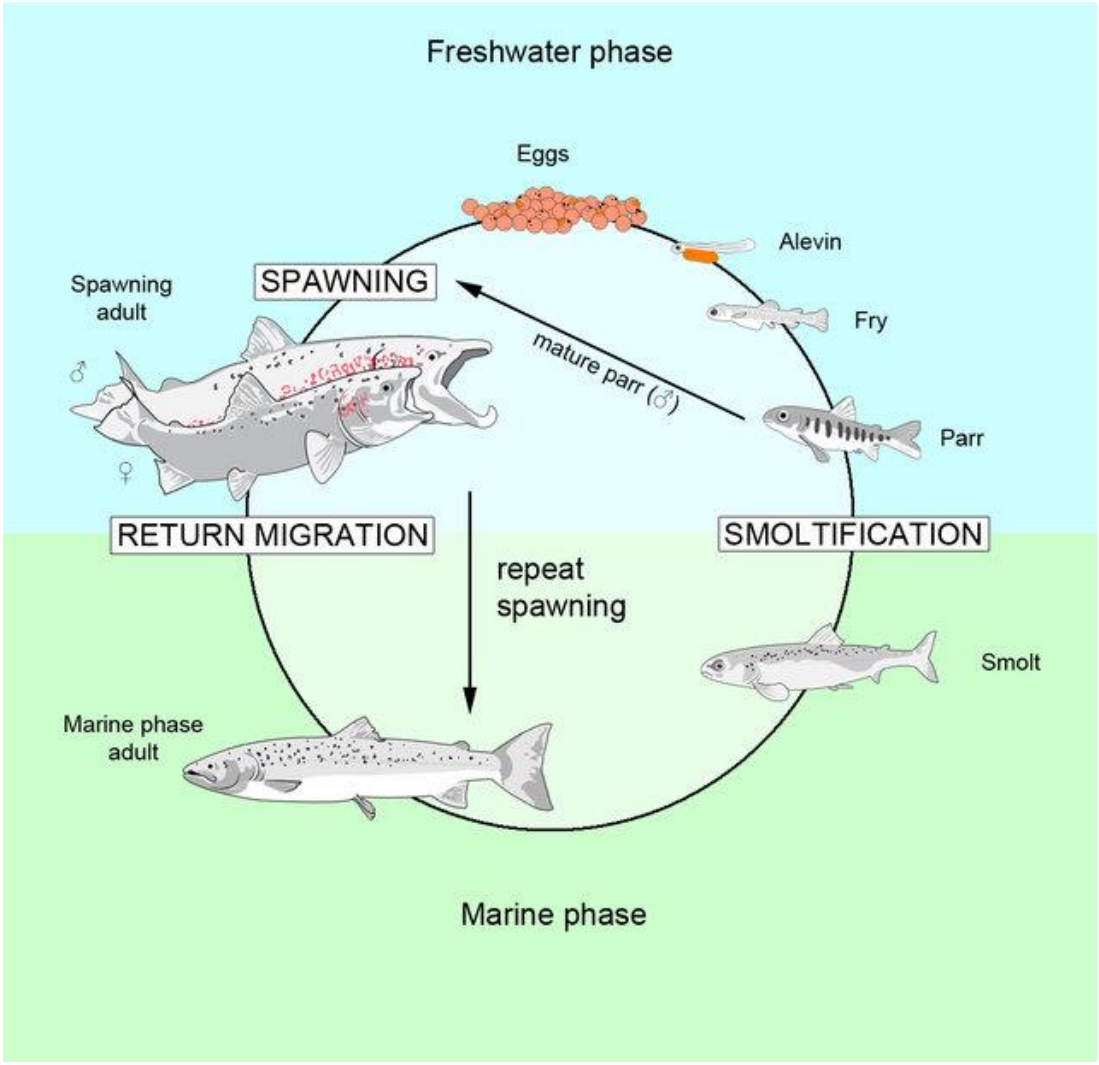


*Fig. 19 Life cycle of the Atlantic salmon Salmo salar (Mobley et al., 2021). The vertical arrow linking spawning adults to adults in the marine phase denotes the existence of repeat spawners over multiple years*

Atlantic salmon females lay 1500-1800 eggs $Kg^{-1}$ of body weight per spawning event and display parental care features exemplified by the digging of shallow nests called redds. These protect the eggs below loose gravel from predators such as eels and other salmonid species. Atlantic salmon males exhibit marked secondary sexual characteristics consisting of a bright red body color for female courtship and the elongation of the lower jaw into the so-called kype for defensive purposes against other spawning males (Witten and Hall, 2003). The eggs are fertilized either by migratory males or sexually-mature juveniles that have never left freshwater yet, and specimens of both sexes predominantly undergo several spawning events at different sites of the same location over 7-10 days across distances of few hundred meters to > 5 Km (Taggart et al., 2001). The reproductive upstream migration may span several hundreds Km: as gonadal development commences, sexually mature adult specimens begin their migration, which can last up to one year. Feeding is interrupted as soon as fish enter the freshwater environment, and energy is hereon entirely allocated to maximizing the chances of a successful reproductive event. Spawning usually occurs in autumn to early winter (October to January) in headwaters, even though salmon may be forced to select additional locations along the migratory route depending on the specimens' health status and energy storage, river fragmentation conditions and habitat suitability (e.g. well-oxygenated water, substrate).

Eggs hatch after 70-160 days (Kottelat and Freyhof, 2007). The developmental stage immediately following hatching is known as alevin. The yolk sac on which their nutrition depends is maintained, and, because they are negatively phototactic, alevins initially maintain a strong relationship with the benthic environment (Kottelat and Freyhof, 2007). They remain in the gravel until the yolk sac is absorbed, a time that corresponds to an increase in locomotory activity. Alevins emerge from gravel in late spring to early summer (May-June). Swim bladder inflation is a critical event that occurs at this time but has paramount implications for all subsequent ones: if abnormally inflated, the shape and size of the organ are indeed affected, with negative consequences on balance and buoyancy (Poppe et al., 1997) and further impairment of energy allocation, growth, and feed conversion, as demonstrated in other species (Schwebel et al., 2018). Autonomous swimming is achieved entirely at the following stage of fry, which, thanks to neutral buoyancy acquired through swim bladder inflation, display the ability to withstand the strong currents of fast-flow rivers and feed exogenously on zooplankton composed of micro-invertebrates and fish larvae (Rochard and Elie, 1994).

From a body length of approximately 5 cm onwards, fish are called parr. This stage is easily recognizable due to the presence of 8-11 dark vertical bars along each side of the body (parr marks) alternating with a row of red spots along the lateral line. Parr continue their life in cool, fast moving streams that ensure the availability of abundant food sources such as aquatic insects for a variable period of time spanning from 1 to 6 years over which their growth is slow.

At a size of 10-25 cm and usually in spring, a morphological and physiological pre-adaptation for the upcoming survival and growth in the marine environment occurs. The above-mentioned morphological markings are lost, and the body becomes silvery with shades of

green, blue and brown on their back depending on the biogeographical region under consideration. Apart from such a macroscopic variation, which however has proven reversible and not necessarily correlated with physiological or biochemical features, major changes were demonstrated at several levels: cytological (water content), biochemical (changes in haemoglobin forms, increase in red blood cells ATP content, increase in low-molecular weight proteins), physiological (intense growth), endocrinological (increase in thyroid stimulating hormone, adrenocorticotropic hormone, prolactin, growth hormone), metabolic (e.g. increase in oxygen consumption, appearance of a marked endogenous circadian rhythm, decreasing concentrations of liver and muscle cholesterol, greater proportion of long-chain polyunsaturated fatty acids) and behavioral (diminished territorial behavior, shift from solitary to shoaling behavior, reduction of fast swimming activity, short permanence in brackish water for gradual adaptation to increased salinity) (Boeuf, 1993 and references therein). Salmon are here known as smolts, and the outlined pre-adaptation process is accordingly termed smoltification.

Adult salmon reach sexual maturation in the marine environment in a minimum of 1 year. Sexually-mature specimens exhibit a strong so-called homing instinct (Hendry et al., 2003) at the end of the oceanic phase that allows them to relocate their spawning grounds. The most accredited factors driving directionality are the earth's magnetic field and/or home stream odors and pheromones released by con-specific in the river that are imprinted along the downstream migration at the end of the riverine phase. Recent literature identified benthic dissolved free amino acids as the primary olfactory clues and demonstrated hatching and emergence from redds as the two key life stages in which fish are early imprinted on the river benthic features (Minkoff, 2019).

Spent specimens, i.e. fish that have completed the spawning process, are known as kelt. Although historically regarded as a semelparous species displaying a single reproductive event, Atlantic salmon actually exhibit a variety of life history strategies with regards to timing of maturation, life stage at spawning and the number of reproductive episodes (Mobley et al., 2021), and repeat spawners were also demonstrated (Niemelä et al., 2006), implying that multiple freshwater-saltwater migrations occur. At the kelt stage, because feeding had been interrupted when entering freshwater and due to the high energetic cost of the gametogenesis and spawning processes, salmon is extremely susceptible to death due to diseases, predators and anthropogenic factors (ICES, 2021; Miccoli et al., 2021). Two contrasting behaviors were recorded: kelts either rest in pools for a few weeks before commencing the downstream migration, or return at once to the ocean, possibly exploiting fast flow rivers for reducing swimming-associated energy expenditure. Habitat degradation and the presence of anthropogenic structures further affect the survival of the species: in particular, the lack of pools or riparian buffers such as natural vegetation along the stream, as well as the obstruction of water passages caused by dams, pumping stations and hydropower plants pose threats to the former and latter behavior, respectively.

### 4.2.2 Ecological traits

*Salmo salar* is profoundly influenced in its life history traits by a multitude of parameters. Following is a summary of the main biotic and abiotic factors which were demonstrated to modulate growth, age at sexual maturation, fertilization rate, embryonic development and survival, larval recruitment, timing of smoltification and successfulness of return migration.

Temperature and photoperiod play a prominent role in all above-mentioned processes regardless of the life stage being considered, even though contrasting information was sometimes produced, especially at embryo or alevin stages. For instance, while incubation temperature did not influence age at maturity in either sex (Jonsson and Jonsson, 2014), embryo incubation at warmer temperatures was demonstrated to affect the timing of the homing migration by two weeks (Jonsson and Jonsson, 2018) and, therefore, the spawning process. The effect of higher temperatures experienced within the incubation period reflect on i) the size of the embryo, with embryos incubated at warmer temperatures being smaller than those incubated in colder water (Peterson et al., 1977), and ii) growth performances at parr stage; however, temperatures experienced following the hatching do not affect the growth of juveniles (Finstad and Jonsson, 2012).

Survival during embryogenesis and at hatching may be limited by dissolved oxygen levels, temperature, sediment infiltration and physiological features: survival rates increase with higher oxygen concentrations and lower temperatures (Hamor and Gardside, 1976); survival of embryos at the pre-eyed, eyed and hatched stages is negatively affected by the amount of fine sediment in the surrounding environment, with early developmental stages being most severely impacted by silts and clays of diameter size smaller than 0.063 mm (Julien and Bergeron, 2006); physiology-wise, significant positive correlations were demonstrated between plasma concentrations of both oestrogen 17-beta estradiol and androgen 11-ketotestosterone in spawning females and embryo survival, which can be as high as 80% (Thayer, 2017). Generally, though, survival in the wild at early developmental stages is estimated within the 0.3-2% range.

Intra-specific competition and predation are the two major factors influencing survival of fry: alevins that emerge sooner from gravel are more susceptible to predation (Brännäs, 1995), but are also the ones to start feeding exogenously earlier than those emerging later. Becoming dominant, the former have a higher optimal growth rate both at fry and at parr (Metcalfe and Thorpe, 1992; Keenleyside and Yamamoto, 1962) and exhibit stronger territorial behavior at juvenile stages (Keenleyside and Yamamoto, 1962). Too strong of an intraspecific competition for food resources leads to dispersion of fry (Brännäs, 1995).

Several biological traits at parr stage are positively modulated by temperature: higher temperatures increase metabolic rates (Oligny-Hébert et al., 2015), food consumption and, consequently, growth rates (Koskela et al., 1997; McCormick et al., 2002). Lipid deposition was shown to correlate positively with increasing temperatures (Koskela et al., 1997). Maturation timing, whose control was unclearly attributed to environmental parameters or genetic contributions to traits associated with maturation initiation such as growth and body

condition until recently, was shown to be explained for up to 25% by temperature (Debes et al., 2019 - research still at pre-print stage at the time of writing).

The triggering of the smoltification process depends both on internal (i.e. endocrinological) and environmental cues (Hoar, 1988; McCormick et al., 2007) but the role of photoperiod seems to be prominent over temperature (McCormick et al., 2002). The former, for instance, seems to underlie the hormonal modulation of insulin-like growth factor and growth hormone associated with smoltification (McCormick et al., 2007). Continuous light provided under experimental conditions drove the highest growth and maturation rates in pre- and post-smolt specimens (Fjelldal et al., 2011; Imsland et al., 2014). Dissolved oxygen concentration and food availability are also crucial at this stage in that they ensure welfare and growth rates of specimens, respectively (Hosfeld et al., 2008; Thorpe and Metcalfe, 1998).

In the marine environment, the importance of temperature, which is undoubtedly the best characterized environmental parameter in salmon life history (Good and Davidson, 2016), remains elevated, but photoperiod and, especially, diet are prominent (Jonsson and Jonsson, 2011). The nutritional status largely contributes to determining the condition factor of specimens. Condition indicators are key to shape several fish life-history traits such as reproduction, growth, and natural mortality, which in turn influence the dynamics and the productivity of a stock. In general, fish having inadequate energy reserves display reduced reproductive potential by means of delayed maturation, reduced fecundity and poor quality of eggs (Lloret et al., 2014), and fish in poor conditions are more likely to direct their energy reserves towards growth than reproduction (Yaragina, 2010).

Provided that the condition factor of adult Atlantic salmon correlates strongly with somatic tissue lipid content (Todd et al., 2008), a limited amount of food resources over the winter results in reduced growth and, most importantly, lower condition index. The consequence is a lower proportion of maturing salmon (Duston and Saunders, 1999) because low-condition salmon are unlikely to enact successful homing behavior or sustain repeat spawning (Todd et al., 2008). Indeed, male Atlantic salmon interrupt their sexual maturation process in case the percentage of mesenterial fat falls below 3%, which appears to be the threshold allowing normal reproduction (Rowe et al., 1991).

At the post-smolt stage, *S. salar* diet is represented by high-lipid prey such as pelagic fish (e.g. herring, capelin) (Rikardsen and Dempson, 2010). A change in their availability caused by climate change scenarios is likely to reflect poorly on fat reserves in salmon: indeed, although ocean warming may directly affect the physiology of fish, it is more likely that negative impacts be explained in a bottom-up manner (Todd et al., 2008). Salmon would suffer from reduced seasonal prey availability; preys, in turn, would be poorer in lipid content because, as demonstrated in the Baltic Sea, climate change is able to shift the composition of phytoplankton species from essential fatty acids-rich diatoms to EFA-poorer flagellates, resulting in lower proportions of such a critical lipid source along the food web and, possibly, reproductive issues in Atlantic salmon (Ahlgren et al., 2005).

### 4.2.3 Stock size

Information on this species' stock status has been generated since the 1980s by the ICES Working Group on North Atlantic Salmon by analyzing and interpreting catch data from more than 2000 rivers draining into the North Atlantic Ocean (Chaput, 2012). The species appears to be extremely vulnerable to human activities because critical biological processes such as spawning and embryo/larval development occur in freshwater environments that are in close connection with densely-populated areas (Parrish et al., 1998).

Atlantic salmon populations can differ much in size depending on the river being considered, and were overall estimated to range between few hundreds to a quarter million individuals (NOAA, 2021). In the last 4 decades, the freshwater annual production of anadromous Atlantic salmon has been lower than 10 million adult-sized specimens (Chaput et al., 2012). Based on the median values of the estimated pre-fishery abundance, the abundance of one-sea-winter (1SW) salmon (i.e. an individual that has spent one winter at sea before returning to freshwater to spawn) in the 1971-2010 period declined by 49, 66, and 40% in North Atlantic Salmon Conservation Organization's N-NEAC (Northern stock complex of North-East Atlantic Commission), S-NEAC (Southern stock complex), and NAC (North American Commission) areas, respectively. With regards to multi-sea-winter (MSW) salmon (i.e. an individual that has spent at least two years at sea before returning to freshwater to spawn), the abundance in the 1971-2009 period declined even more severely by 54% in the N-NEAC area, by 81% for the S-NEAC area, and by 88% for the NAC area (Chaput, 2012). Recently-published data concluded that 7% of analyzed rivers no longer present *S. salar* populations and a further 43% hosts stocks that are considered either to be at risk, threatened in some way, or declining in numbers. Worthy of note, data is not available for 35% of all rivers (NASCO, 2019). The species is currently considered extinct in Belgium, Netherlands, Germany, Czech Republic, Poland, Slovakia and Switzerland, and populations of Ireland, Wales, Scotland, England, Iberian Peninsula, France, Denmark, Sweden, Norway and European Russia declined (Smialek et al., 2021).

The above-mentioned situation was caused by a multitude of factors that interfere with the species' life history, overall resulting in continuously-increasing mortality rates (65-95%), which are unusually higher compared to other marine fish (18% on average). At sea, mortality is highest (up to 71%) within 5-230 km from estuaries in the early marine migration mainly because of predation, while it accounts for less than 10% if the entire marine phase is taken into account (Thorstad et al., 2012). In freshwater, salmon may be lethally threatened by, either directly or indirectly, or experience a delayed downstream migration because of several anthropogenic factors. In general, the most severe anthropogenic factors are hydropower, barriers to migration, habitat alterations (including acidification, introduction of non-native fish species) or destruction, overexploitation, pathogenic diseases from introduced parasites, pollution (both agricultural and chemical), climate change and genetic impoverishment due to i) interspecific hybridization, ii) outbreeding due to immigration of escaped farmed salmons, iii) inbreeding and iv) genetic drift due to reduced population size (Johnsen and Jenser, 1991; Karlsson et al., 2016; Forseth et al., 2017). Worthy of note, the level of threat of the above-mentioned factors was recently ranked by the Norwegian

Scientific Advisory Committee for Atlantic Salmon Management with the aim of prioritizing mitigation measures. The two axes (i.e. effect and development) of such a bi-dimensional classification system describe the effect of each impact factor on the populations and the likelihood for further reductions in population size or loss of additional populations in the future, respectively. Hydropower was regarded as a "stabilized population threat", i.e. a factor that has contributed to populations becoming critically endangered or lost in nature, but that have a low likelihood of causing further reductions than they do already today (Forseth et al., 2017).

### 4.2.4 IUCN status and legislative perspective

The conservation status of *Salmo salar* was assessed as Least Concern following the IUCN Red List criteria (World Conservation Monitoring Centre, 1996) although the assessment report clearly indicates that a revision of the status is needed (Fig. 20).

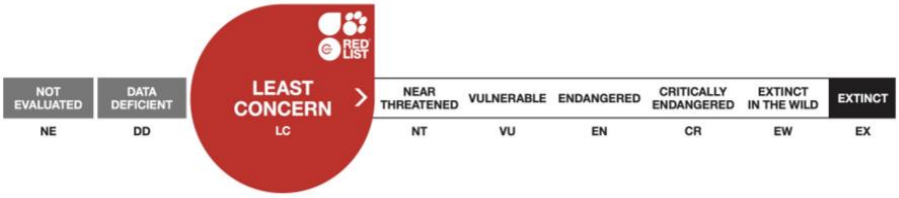


*Fig. 20 IUCN status of Salmo salar*

The species was included in Appendix III of the Bern Convention (Council of Europe, 1979), amendment of 2002, which defines wild fauna species that are protected but can be exploited in a regulated manner according to the Convention. It is also listed in Annexes II and V of the Habitats Directive (European Commission, 1992). The former defines the species that require designation of Special Areas of Conservation, while the latter includes species for which Member States must ensure that their exploitation and taking in the wild is compatible with maintaining them in a favourable conservation status.

# 5 Susceptibility of target fish species to hydropower mechanisms

## 5.1 Rapid decompression

The biological consequences of water pressure change, also known as rapid decompression, have been investigated in a variety of species under controlled conditions. In most cases, researchers have exposed the fish to conditions simulating a realistic situation of increasing water pressures typically associated with passage in the draft tube and sharp decompressions experienced during runner passage. This was achieved by the use of specialized baro-chambers capable of simulating ranges of 0 to 3450 (Harvey, 1963), 600 (Tsvetkov et al., 1972), 690 (Knable and Feathers, 1983), 500 (Turnpenny et al., 1992), 414 (Abernethy et al., 2001) and 200 kPa (Boys et al., 2013). In some cases, the equipment also allowed for an initial acclimation period during which fish can adapt to "environmental" conditions and achieve neutral buoyancy. In all cases, studies aimed at examining the effects of rapid decompression on fish employ absolute pressures since gas expansion follows Boyle's law, which requires such a metric.

The fish species that were examined for susceptibility to pressure-related damages are mostly bluegill *Lepomis macrochirus* (Abernethy et al., 2001; Becker et al., 2003), crucian carp *Carassius carassius* (Meng et al., 2019), white sturgeon *Acipenser transmontanus*, walleye *Sander vitreus* and tiger muskie *Esox masquinongy* (Brown et al., 2015), and some Australian species (Hou et al., 2018). Currently, little information exists on European fish species. With regards to the two target species of this deliverable, research was conducted under controlled conditions only for Atlantic salmon (Tsvetkov et al., 1972; Turnpenny et al., 1992). Data acquired on surrogate species (i.e. American eel *Anguilla rostrata*, and various Salmonidae species) that can provide the reader with the most informative scenario will be presented instead.

In general, the endpoints analyzed can be classified as:

- **Injury**: any sign of barotrauma-related damages such as swim bladder rupture, exophthalmia, eversion of stomach and intestine, emphysema, internal or external hemorrhaging in the fins, musculature and organs (Odeh, 1999; Abernethy et al., 2002; Jacobson et al., 2012; Brown et al., 2014).
- **Mortal injury**: any sign of injuries highly related to death by statistical analysis.
- **Immediate mortality**: occurrence of death or exhibition of moribound behavior (i.e. erratic or burst swimming, inability to regain equilibrium, or persistent cough-like behavior indicative of severe damage to the gills) within 30 minutes from exposure to experimental conditions (Pflugrath et al., 2021).

An additional issue that demands attention is understanding the consequences of fast decompression and barotrauma on reproduction. A recent paper demonstrated that rapid decompression conditions cause eggs to be spawned unintentionally, therefore significantly impacting the fishes' ability to breed, especially if sexual maturity is reached and the gametogenesis process is completed (Pflugrath et al., 2020).

### 5.1.1 European eel *Anguilla anguilla*

No research on the effects of rapid decompression was so far conducted on European eel.

### 5.1.2 Atlantic Salmon *Salmo salar*

Atlantic salmon specimens at the stage of parr or at body lengths of 60-80 mm and 90 mm were employed by Tsvetkov and co-workers (1972) with the aim of evaluating the endpoint of mortality following the application of decompression rates 300, 200 and 100-600 kPa $s^{-1}$, respectively. The highest mortality was reported for parr (death reported in 50% of tested fish), while mortality in salmon of 60-80 mm body length accounted to 20%. The longest of the tested size classes did not show any mortality. These results are somewhat in line with the knowledge related to traits that affect barotrauma, especially life stage: a greater susceptibility is indeed reported for larval stages upon swim bladder inflation (Boys et al., 2016), likely due to the lower ability of releasing gas from the swim bladder than more developed co-specifics.

Atlantic salmon was among the fish species tested by Turnpenny and colleagues (1992). Several experimental groups were initially exposed to a pressure increase to 400 kPa and then rapidly decompressed to nadir pressures ranging from 15 to 90 kPa. The endpoints monitored were immediate mortality, delayed mortality up to 7 days post-treatment, swim bladder rupture and eye and fin haemorrhages. Immediate mortality was not recorded, while 5% delayed 7-day mortality was observed only for fish exposed to the nadir of 75 kPa. Swim bladder rupture was recorded only in the group exposed to the lowest nadir of 15 kPa, although with low occurrence rates.

### 5.1.3 Surrogate species

American eel *Anguilla rostrata* at the yellow (n = 101) and silver (n = 90) phase, body lengths of 230-423 and 216-686 mm, respectively, were tested in rapid decompression experiments at PNNL (Pflugrath et al., 2019). Initial acclimation was allowed for 1 day at 172 kPa, an absolute pressure equivalent to ~ 7 m of depth, and nadir pressures ranged from 8.04 to 57.33 kPa. Because it is a benthic species, eel did not attain a state of neutral buoyancy but rather maintained negative buoyancy to facilitate occupancy on or near the substrate. Silver-phase eel are more likely to be entrained into turbines than yellow-phase eel, because of migratory behavior; however, neither the occurrence of injury nor mortality was found to be significantly correlated to RPC for either phases, suggesting that the species is not majorly affected by rapid decompression in downstream passage and that further sources of mortality must be investigated. It must be noted that the median RPC to which both phases were exposed inflicted a 95% mortality rate in Chinook salmon (Brown et al., 2012a).

Abernethy et al. (2001) tested two Salmonid species, namely rainbow trout *Oncorhynchus mykiss* at ~13 cm body length and Chinook salmon *Oncorhynchus tshawytscha* at ~10 cm body length, in 12 possible conditions based on different combinations of pre-turbine acclimation

pressures (i.e. 101 or 191 kPa), total dissolved gas concentrations (i.e. 100, 120, and 135% saturation), and nadir pressures (i.e. 2-10, ~50, 69 and 97) with the aim of resolving pressure-related concerns about fish passage at hydropower plants. Rainbow trout showed little reaction to the pressure spike during the turbine passage simulation. No fish lost equilibrium or went into convulsions prior to removal from the chambers. No external signs of injury or trauma were evident 1 hr after the turbine passage simulation and swim bladder ruptures were not reported. Mortality was not observed within the 48-hr post-exposure holding period. For Chinook salmon, the major mortality source was represented by the highest percentage of total dissolved gas (TDG) due to gas bubbles in the heart blocking blood flow to the gills. Fish that were exposed to ambient and intermediate TDG concentrations at surface acclimation did not suffer any mortality or injury from the passage-simulated decompression. No depth-acclimated fish at 100% TDG died from the turbine passage simulation. In summary, 7 out of 174 of depth-acclimated fish subjected to the turbine spike had ruptured swim bladders (Table 5).

*Table 5 Mortality and injury rates for fall Chinook salmon based on TDG levels, acclimation depth, and pressure spike from turbine passage (Abernethy et al., 2001, recreated by Pflugrath et al., 2021)*

| Acclimation Pressure (kPa) | Nadir Pressure (kPa) | Injury | | | Mortality | | |
|---|---|---|---|---|---|---|---|
| | | Total Dissolved Gas | | | Total Dissolved Gas | | |
| | | 100% | 120% | 135% | 100% | 120% | 135% |
| 101 | 2–10 | 0% | 2% | | 0% | 0% | |
| 191 | 2–10 | 2% | 2% | 8% | 0% | 5% | 5% |
| 101 | ≈50 | 0% | 3% | | 0% | 0% | |
| 191 | ≈50 | 0% | 0% | 0% | 0% | 0% | 0% |
| 101 | 69 | 0% | | | 0% | | |
| 101 | 97 | 0% | | | 0% | | |
| 191 | 69 | 0% | | | 0% | | |
| 191 | 97 | 0% | | | 0% | | |

Chinook salmon of BL 80–180 mm and 71-205 mm were also investigated at PNNL (Stephenson et al., 2010; Brown et al., 2012a). In the former study, acclimation pressure was set at 175.8 kPa and nadir pressures ranged between 12.1 and 127.9 kPa. The authors monitored the occurrence of gill emboli, swim bladder rupture, mortality, and internal haemorrhaging as end points. As nadir pressures decreased, higher incidence of immediate mortality, emboli in the gills, swim bladder rupture and haemorrhage in liver, heart or kidney were observed. However, in all cases, negatively buoyant fish were less exposed to the risks than neutrally buoyant ones. Nadir, buoyancy state, interaction between nadir and buoyancy and body length were identified as statistically significant predictors in the models developed following simulated turbine passage. In the latter study, fish were exposed to varied acclimation pressures (i.e. 116.5, 146.2 and 175.8 kPa) and subsequent nadir pressures (i.e. ranging from 6.4 to 144.8 kPa) and, in addition, TDGs of 115% and 125% along with several and biotic factors (i.e. condition factor, body length and weight) were tested. LRP, TDG, condition factor, RPC and the interaction effects of TDG × condition factor were all found to be statistically significant predictors of mortal injuries including

haemorrhaging in the pericardium, liver, or kidney, ruptured swim bladder, blood or bile secretions from the vent and emboli in the gills or pelvic fins. Haemorrhaging from vasculature associated with the swim bladder was the most common injury and, in general, the likelihood of mortal injury increased with higher pressure ratios. In fact, LRP on its own explained the large majority (i.e. 89.7%) of the total deviance of the model, therefore indicating that Log Ratio Pressure Change alone can be used as a valid predictor of mortal injury in juvenile Chinook salmon (Fig. 21). Dose-response equations were produced from both studies.

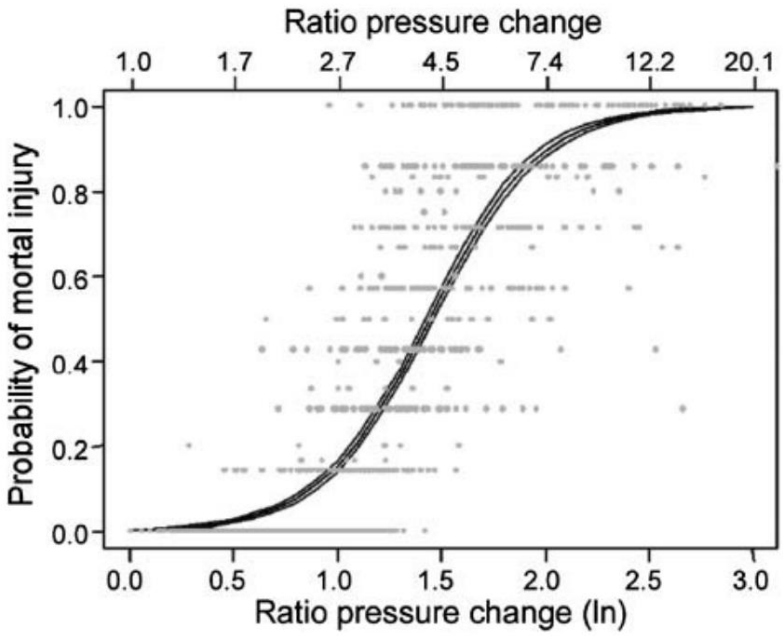


*Fig. 21 Probability of mortal injury from simulated turbine passage along a range of LRP (natural log of the ratio of acclimation to nadir pressures) for juvenile Chinook salmon (Brown et al., 2012a)*

As demonstrated for Sockeye salmon *Oncorhynchus nerka*, the rapidity of the decompression period is key in determining the actual susceptibility of fish to water pressure change (Harvey, 1963). Indeed, no barotrauma-induced mortality was recorded for fish that were gradually decompressed up to 16.7 kPa, likely due to their ability to evacuate gas from the swim bladder.

Three salmonid species, namely *Oncorhynchus tshawytscha* (n = 3882, 100–170 mm, data gathered from literature), *Oncorhynchus nerka* (n = 200, 113–166 mm) and *Oncorhynchus mykiss* (n = 194, 104–156 mm), were recently tested by PNNL in a surrogacy validation oriented work (Beirão et al., 2021). Fish were subjected to rapid decompression within 1.1 to 2.6 s to nadir values ranging from 9.8 to 149.96 kPa. Immediate mortality occurred in 5 *O. nerka* specimens, which did not allow for the development of a mortal injury dose-response equation. *O. nerka* had the lowest and *O. tshawytscha* the highest mortal injury probability at low LRPs. Swim bladder rupture was the most frequent injury recorded. Of the three, rainbow trout was the least susceptible species to mortal injury caused by extreme decompression in simulated turbine passage and no immediate mortality was reported. However, its response to low LRP (higher nadir pressures) rapid decompressions was similar to the other two

salmonids, resulting in overall similar predicted adverse passage probabilities in the Kaplan turbine operation scenarios simulated using the BioPA tool.

Turnpenny and colleagues (1992) also tested the response of brown trout *Salmo trutta* to the initial pressure increase to 400 kPa and the rapid decompression ranging from 15 to 100 kPa. Immediate mortality was not shown by any group. At the lowest nadir pressure, delayed 7-day mortality was observed only for 3 specimens and swim bladder rupture occurred in 5 specimens. Swim bladder rupture was also recorded in two specimens exposed to a nadir of 45 kPa.

## 5.2 Shear

The biological consequences of shear have been investigated using several dedicated apparatus to simulate realistic shear conditions experienced by fish during passage. They allowed the testing of distinct jet exit velocities ranging from 17.5 to 28 (Johnson, 1972), 20 (Turnpenny et al., 1992), higher than 20 (Neitzel et al., 2004) or 18.3 m $s^{-1}$ (Boys et al., 2014). A typical testing apparatus is shown in Fig. 22.

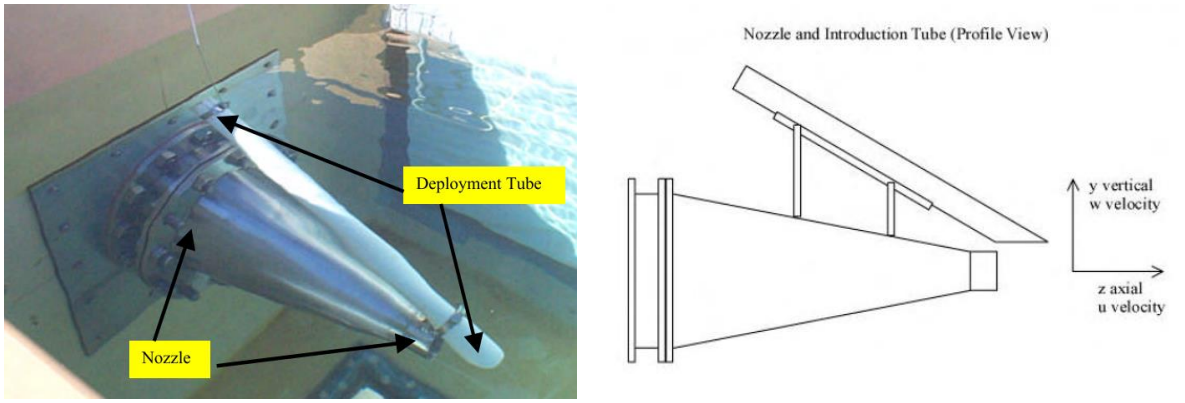


*Fig. 22 Close-up (left) and schematic representation (right) of the test flume nozzle (stainless-steel, 25.4 cm and 6.35 cm base and exit diameters, respectively) employed for generating jet velocities, and the deployment tube through which fish specimens were inserted just above the stream (Neitzel et al., 2000).*

Susceptibility to shear stress was tested experimentally on over 20 fish species, including American (e.g. American eel *Anguilla rostrata*, American shad *Alosa sapidissima*) European (e.g. Atlantic herring *Clupea harengus*, many salmonid species, European eel *Anguilla anguilla*, common carp *Cyprinus carpio*) and Australian (e.g. golden perch *Macquaria ambigua*, Australian smelt *Retropinna semoni*) species. Currently, little information exists on the European eel and Atlantic salmon, while a higher number of studies is available on their surrogate species.

### 5.2.1 European eel *Anguilla anguilla*

Adult *Anguilla anguilla* specimens were tested by Turnpenny et al. (1992) against a velocity range of 5.4 to 20.9 m $s^{-1}$, equivalent to strain rates of 300-1161 $s^{-1}$ (this and all subsequent velocity-shear conversion performed by considering a Δy of 1.8 cm). The European eel did not show any susceptibility to mortality and did not present any external injury except for slight mucus loss, which was however regarded as a minor injury. These findings suggest that the species is not impacted by shear during downstream passage. Based on this data, both β0 and β1 coefficients for equation predicting the likelihood of injury, major injury and mortality were 0, and no dose-response equation could be developed so far (see section 7.4 - Biological response models / 7.4.2 - Shear).

### 5.2.2 Atlantic salmon *Salmo salar*

Turnpenny et al. (1992), using the same testing apparatus as above, generated data also on Atlantic salmon. Mortality-wise, a rate of 12% was observed within 7 days from the exposure to the greatest strain rate of 1161 $s^{-1}$. The type and extent of injuries experienced, instead, varied with the applied shear dose: while descaling was always documented, eye damages and mucous loss were only observed after exposure to the two greatest strain rates of 911 and 1161 $s^{-1}$.

### 5.2.3 Surrogate species

Forty American eel *Anguilla rostrata* specimens ranging from 265 to 453 cm BL were exposed to a water jet simulating severe fluid shear with strain rates equivalent to 833 and 1000 $s^{-1}$. These conditions are comparable to the hydrodynamic stress encountered during actual downstream passage (Neitzel et al., 2004). Following exposure, fish were analyzed for behavioral changes, loss of equilibrium or more serious injuries such as vertebral fractures, and held for the next 48 hours to record possible delayed damages or mortality. In line with data acquired on its European congener, no adverse outcome was observed either immediately or at 48 h post-exposure. Excess mucus production was noted, but authors attributed such a response to the handling of specimens and regarded it as minor.

Chinook salmon *Oncorhynchus tshawytscha* was tested thoroughly for susceptibility to shear at different body lengths. Specimens of 127-178 mm BL were not impacted, either minorly or severely, by a strain rate of 974 $s^{-1}$ (Johnson, 1970). By employing a more dispersed sample length-wise (i.e. BL up to 229 mm) and applying several shear doses (i.e. 972, 1111, 1333.3 and 1555.5 $s^{-1}$), mortality rates increased with shear stress up to 25.8%, with smaller specimens being the most susceptible ones (Johnson, 1972). Among the injuries recorded were, in order of severity, torn operculum, eye damage, vertebral fractures and decapitation, and generally increased resistance to injury was correlated with increased size. It is worth noting that shear was not the only simulated hydropower mechanism produced in the testing apparatus, as cavitation was acknowledged by the author especially when producing the two greatest strain rates. Because cavitation could have contributed to the severity of impacts on

fish, a focused understanding of the biological consequences of shear stress alone was not achieved. However, injuries such as eye damage, loss of equilibrium and, particularly, torn operculum, were reproduced in additional studies (e.g. Deng et al., 2005), contributing to elucidating the biological consequences of shear on its own starting at a strain rate of 933 $s^{-1}$. Torn operculum, in particular, was found in up to 90% of specimens tested against a rate of at least 844.4 $s^{-1}$.

Contrary to the findings of Johnson (1972), Neitzel et al. (2004) concluded that larger fall Chinook salmon smolt of 123-152 mm BL had an increased susceptibility to fluid shear relative to the smaller pre-smolt fall Chinook specimens of 85-95 mm, suggesting that a smaller body length is not always correlated with a higher severity of damages.
To obtain the most complete overview on species sensitivity, the orientation of the fish must be considered as a critical factor when assessing the effects of shear. Data produced by Neitzel et al. (2000) demonstrate that, at a similar size class of 140 mm BL, major injuries and mortalities of Chinook salmon start at a strain rate of approximately 688 $s^{-1}$ when introduced in the testing apparatus head-first, while no significant proportions of major injuries and mortalities were found when fish were subject to shear stresses of 688 to 1008 $s^{-1}$ tail-first. In any case, there were no significant injuries to any fish subjected to rates of strain of less than 517 $s^{-1}$.

Coho salmon *Oncorhynchus kisutch* was tested by Johnson (1972) at 1111, 1333.3 and 1555.5 $s^{-1}$. Dose-dependent mortality rates were observed also in this species, but coho salmon of tested BLs (i.e. 76-229 mm) appeared way more susceptible than the congener *O. tshawytscha*, in that the highest mortality rates accounted for 78%. There was a high degree of similarity between the injury type experienced by these two species, and it must be remembered that the influence of cavitation cannot be ruled out.

In an attempt to highlight possible differences in shear sensitivity of congener species, Johnson (1972) also conducted tests on rainbow trout *Oncorhynchus mykiss*. Specimens of 76-305 mm BL (i.e. a size class quite similar to that of *O. kisutch*) were exposed to 1111, 1333.3 and 1555.5 $s^{-1}$. Dose-dependency was observed also on this species, with mortality rates ranging from 0.7% to 30.1%. Based on mortality rates, these results highlight that rainbow trout is more similarly susceptible to shear to Chinook than coho salmon.
Rainbow trout yearlings and smolts of 155 and 215 mm average BLs were tested in a headfirst only orientation by Neitzel et al. (2000) against 688, 852, 1008 and 1150 $s^{-1}$ strain rates and assessed for direct injury and mortality as well as for indirect mortality due to predation by larger conspecifics within the 15 minutes following exposure of juvenile rainbow trout to the no-observed-effect level (NOEL) or lowest-observed-effect level (LOEL) strain rates. With regard to yearlings, the highest strain rate not causing any statistically significant minor injury was 688 $s^{-1}$, with higher strains causing minor injuries to 28% and 33% of fish. No major injuries were detected in test fish exposed to strain rates up to 688 $s^{-1}$, and higher strain affected 6 and 7% of fish, even though no significant differences from controls were found. Smolts appeared more susceptible to minor injuries, as a statistically significant 18% proportion of injury was found compared to controls at 688 $s^{-1}$, and 67% and 100% of fish exhibited such damage at higher rates. On the other hand, no statistically-supported major

injuries were recorded. Importantly, neither yearling nor smolts suffered from any shear-related mortality. Smolts were also tested tailfirst at 852 and 1008 $s^{-1}$, resulting in 20% of minor injuries (the proportion at headfirst was 100%) and any statistically-supported mortality.
One-year old rainbow trout were also tested by Turnpenny et al. (1992) against 911 and 1161 $s^{-1}$. Minor injuries such as scale and mucous loss occurred at both velocities, and more serious ones such as eye and gill damages occurred only at the highest velocity in low proportions i.e. 0.3% and 2%, respectively.

Turnpenny et al. (1992) also tested brown trout *Salmo trutta* at the additional strain rate of 578 $s^{-1}$. Minor and major damages to scales, eyes and gills were also observed, and the most lethal strain rate causing approximately 20% mortality was 911 $s^{-1}$.

## 5.3 Blade strike

The biological consequences of blade strike have been investigated with laboratory settings in a variety of species overall belonging to 9 taxonomic families. The experiments were carried out to decipher the relevance of the blade strike impact variable by including different strike locations (i.e. head, mid-body and tail), body orientation (i.e. dorsal, ventral and lateral) and angle of impact (i.e. 45, 90 and 135°).

The family for which most of the knowledge was generated was Salmonidae, with rainbow trout *Oncorhynchus mykiss*, brown trout *Salmo trutta*, brook trout *Salvelinus fontinalis* and Atlantic salmon *Salmo salar* as species, here listed in decreasing order of completeness of data. Rainbow trout, in particular, was thoroughly tested, as the species was included in several experiments by multiple authors over the last 25 years (Turnpenny et al., 1992; EPRI, 2008; Bevelhimer et al., 2019; Saylor et al., 2020; Amaral et al., 2020). Further well-investigated species with reference to the consequences of blade strike impact are gizzard shad *Dorosoma cepedianum* (Bevelhimer et al., 2019; Saylor et al., 2020), hybrid striped bass *Morone saxatilis* x *M. chrysops* (Bevelhimer et al., 2019) and bluegill sunfish *Lepomis macrochirus* (Saylor et al., 2019). This set of species is in fact the only one for which data on all of the above-mentioned 9 levels of locations, orientation and blade angle exist.

One set of data is also available for the European eel *Anguilla anguilla* (Turnpenny et al., 1992).

Data acquired on surrogate species (i.e. American eel *Anguilla rostrata* and Salmonidae species) that can provide the reader with the most integrated scenario will also be presented. In the case of blade strike, surrogacy must be clearly defined due to the key role that fish characteristics such as fish-blade interaction as well as morphological and behavioral traits play in determining susceptibility to such a mechanism (see section 5.3 - Blade strike). For this reason, surrogacy can be safely established between species based on shared biological, behavioral, physiological features and of course taxonomic classification: in this regard, the availability of data on American eel is precious for expanding the knowledge on European eel *Anguilla anguilla*, which was reported to suffer mortality at European hydropower projects (Calles et al., 2010; Jansen et al., 2007). Instead, intra-species surrogacy based on size is not advisable.

In general, the endpoints analyzed can be classified as:

- **1-hour mortality**: also referred to as instantaneous mortality.
- **Functional mortality**: evaluation of severe injuries in specimens surviving the exposure to strike that, however, typically lead to mortality. These include, for example, vertebral fractures, which profoundly impair fish biological processes (e.g. feeding, swimming, defense).
- **Latent mortality**: evaluation of signs of severe injuries likely leading to mortality that are suffered at a given life stage but do not manifest in their ultimate consequence until later life stage (Beckerman et al., 2002). This is the most difficult hydropower impact to evaluate in the wild due to the difficulty in isolating the individual sources

of injury and tracking specimens, especially migrators, over long distances and timeframes. To this end, fish are usually exposed to different treatments and then monitored in their post-treatment survival rates through time under controlled conditions.

- **External assessment**: evaluation of gross sign of typical strike-related injuries such as contusions, lacerations, amputation of fins and head, eye damage, scale and mucous loss, hemorrhaging, blood clotting. This is the easiest endpoint to check: all 17 fish species tested for blade strike damages were externally assessed for injury following the simulated turbine passage.
- **Internal necropsy**.

### 5.3.1 European eel *Anguilla anguilla*

Only one data set informing about blade strike impacts on the European eel was retrieved from literature.

Turnpenny et al. (1992), in a laboratory study, aimed at investigating the processes of approach and 90° collision between fish and various blade profiles. *A. anguilla* specimens of 320-720 mm in length were exposed to 4 blades differing in the width of the tip profiles (i.e. 10, 20, 40 and 100 mm) as a proxy of impacts occurring at different locations along the blade (from tip to hub, respectively). The range of blade velocities was 5.2-7.1 m $s^{-1}$, reproducing the collision velocities that a fish would experience near the hub but not near the periphery of a full-sized turbine. The endpoints considered were latent mortality and assessment of external injuries. At the lowest velocity and with the 100 mm blade width, the extent of injuries was minor and no mortality was observed. On the contrary, at the higher spectrum of collision velocities and using the 10, 20 and 40 mm-wide blades, moderate to severe injuries such as mucous loss, bruising, eye damages, internal hemorrhaging and vertebral fractures were reported.

### 5.3.2 Atlantic salmon *Salmo salar*

Atlantic salmon was also tested by Turnpenny et al. (1992) under the same experimental conditions as above. The impacts of the above-mentioned 4 blade tip profiles were tested on specimens of 150-1000 mm BL. In line with previous findings, thinner and faster blades were more injurious than thicker and slower ones: fish exhibited diverse injury types such as mucous loss, bruising, eye damage, internal bleeding and broken spines.

### 5.3.3 Surrogate species

Laboratory experiments employing surrogates of the two target species of the present deliverable have been conducted extensively by several authors (Fig. 23). Data on American

eel will be presented to infer information about the congener European eel, while studies performed on rainbow trout and brook trout will inform about Atlantic salmon.

Two somewhat complementary studies on American eel have investigated the effects of blade strike by considering all above-mentioned endpoints and exploring how strike locations and fish orientation determine the species' susceptibility. In the first one, specimens of 285-795 mm BL were exposed to three blade tip profiles (i.e. 25, 50 and 150 mm) at two blade strike velocities (i.e. 10.7 and 12.2 m $s^{-1}$) (EPRI, 2008). Such laboratory data demonstrated that the species is apparently resistant to strike impacts up to the highest of the tested velocities, even though possible internal injuries leading functional or latent mortality were not assessed and, most importantly, overall mortality after a 96-h observation period increased to 70% for mid-body struck specimens (EPRI, 2008); this suggests that American eel may be severely threatened by turbine passage in terms of delayed mortality, functional mortality or short-term latent mortality. In the second study, even more extreme experimental settings were used, as specimens of about 550 mm in BL were exposed to thinner blades (i.e. 19 and 26 mm) with higher blade strike velocities (i.e. 12 and 13.6 m $s^{-1}$), in an attempt to simulate typical conditions experienced between the hub and blade tip and with the aim to produce a mid-body strike to assess injuries on most internal organs (Saylor et al., 2019) . The species was found to be extremely resistant to blade strike velocities up to 13.6 m $s^{-1}$, likely due to its anatomical and biomechanical properties (i.e. peculiar body shape, skeletal architecture, muscle thickness and integument quality with regards to skin thickness and scale type). Using the 19 mm-thick blade at 13.6 m $s^{-1}$, the highest observed mortality rate was 45.5% when struck dorsally. However, only an accurate assessment of internal injuries revealed that specimens suffered major damages, the most common of which were haemorrhaging from mouth and organs, lacerations, vertebral fractures (i.e. in some case causing an internal decapitation) or contusions, once again implying that functional death is the major consequence of downstream passage and that mortality rates were only apparently low due to the evaluating criteria defined to the authors.

In general, it is also important to highlight that the strike velocities investigated on American eel in both studies are the highest ones tested to date on any fish species under controlled conditions.

Rainbow trout, as stated above, is the species for which the greatest amount of data on blade strike impacts exists. Together with brook trout, it appears as the most susceptible species to blade strike. Very recently, data was produced on both species to estimate mortality as a function of turbine blade velocities and verify the reliability of surrogacy in similar controlled experiments (Saylor et al., 2020). Two size classes of specimens for rainbow trout (i.e. 114 and 258 mm BL) and one size class for brook trout (i.e. 242 mm BL) were exposed to semi-circular leading edge blades of 26, 52, or 76 mm in width and 4.7 to 9.7 m $s^{-1}$ strike velocities. Several variables of strike location, orientation and angle were also taken into account. Large brook and rainbow trout were most susceptible, with mortality occurring already at the lowest velocity of 4.9 m $s^{-1}$, while small rainbow trout represented the most resistant group in the study, even though the velocity of 8.7 m $s^{-1}$ and a lateral mid-body strike at 90° was the most impactful on them. As amply discussed, thicker blades were less injurious than thinner

ones: the latter produced nearly a 100% mortality in rainbow trout of both size classes at 6.6 m $s^{-1}$. The smaller size class of rainbow trout was more resistant (15.8% mortality) to strike than the larger one (55% mortality) at the velocity of 6.7 m $s^{-1}$. The large rainbow trout specimens and brook trout, comparable in their BLs, also displayed similar susceptibility to mid-body lateral strikes at 90° with a 52 mm blade, as indicated by similar slopes in the dose response mortality curves and $ED_{50}$ values (6.59 compared to ~6 m $s^{-1}$). Injury-wise, few major injuries (i.e. vertebral and rib fractures, injuries to internal organs and muscle, mouth and operculum haemorrhaging) were found in rainbow trout survivors of both size classes. Frequency and number of spinal fractures differed between rainbow trout size classes, with internal decapitation having been recorded only in large specimens. In addition to statistically validating surrogacy in salmonids, the study suggested that rainbow and brook trout mostly display immediate rather than functional mortality following downstream turbine passage.

Rainbow trout specimens of 173 mm BL were also employed by Bevelhiver et al. (2019) to elucidate the consequences of blade thickness, strike velocity, strike location and orientation on mortality in three species of fish and to correlate adverse outcomes to specific injuries. Different combinations of the above variables were tested. Strike velocities ranged between 5.8 and 9.8 m $s^{-1}$ (7.7 and 8.2 for the first dataset) for both semi-circular leading edge blades, whose widths were 26 and 52 mm, in line with EPRI (2008) and Saylor et al. (2020). Following simulated passage, fish were monitored for visible injuries as well as for immediate, 1-h and functional mortality.

Regardless of blade velocity, head and midbody strikes always caused higher mortality rates than tail strikes, which resulted in few mortalities not statistically different from controls. This is most certainly due to vital organs being damaged by the blade strike path; for this reason, angled strikes not in line with the center of gravity generally deflect fish without causing any mortal injury. Thinner blades were statistically demonstrated to result in greater mortality rates than thicker ones. With regards to the relationship between injury and mortality, higher mortality was significantly related to gill damage, heart haemorrhaging and swim bladder injury.

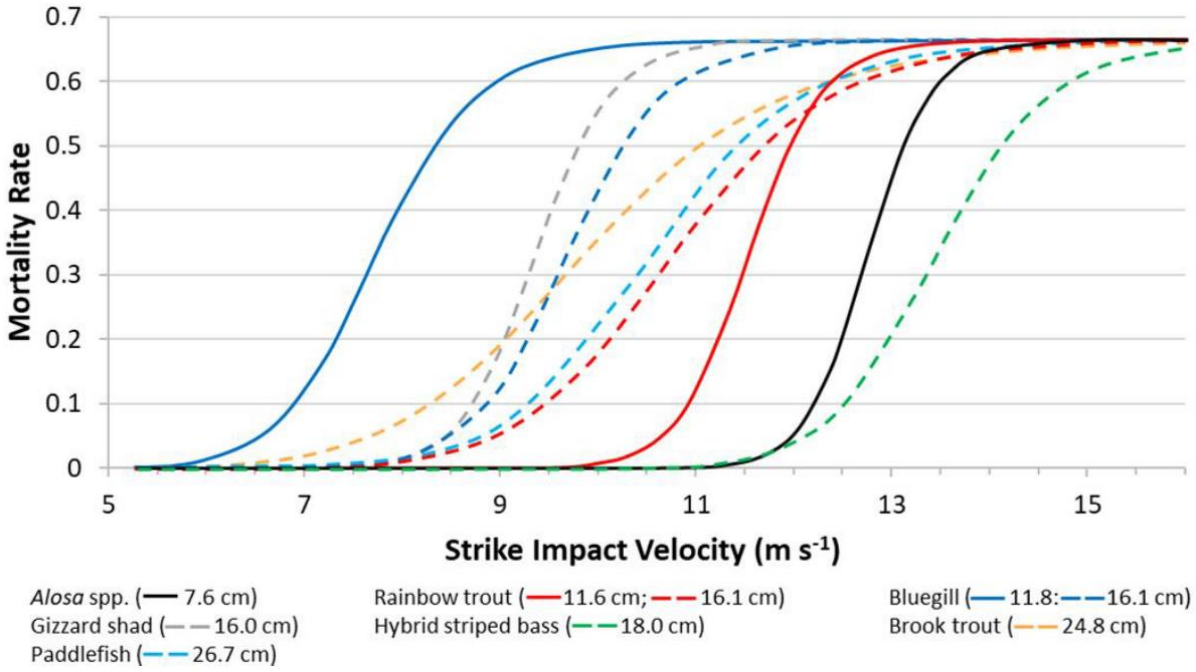


*Fig. 23 Dose-response mortality curves in several fish species, including surrogate species for Atlantic salmon, i.e. rainbow trout and brook trout. American eel was not included in the plot. Please note that the larger size class of rainbow trout was 25.8 and not 16.1 cm (Pflugrath et al., 2021)*

# 6 FPHI - Fish Population Hazard Index tool

## 6.1 Introduction

Hydropower is often considered as a “green” source contributing to the decarbonization process of the European energy system. Nevertheless, the pressure caused on aquatic ecosystems is significant due to habitat fragmentation, impoundments, hydropeaking, and water abstraction. Water abstraction, for instance, leads to a reduction of flow velocities, therefore changing a river’s specific flow characteristics and flow variability. On the other hand, hydropower management of reservoirs, due to the sudden release of water, may damage downstream benthic and fish communities. Furthermore, as discussed above, the passage of fish through water intakes and turbines is associated with several damage mechanisms that impact welfare and survival of specimens, ultimately compromising the structure of fish populations. Therefore, when planning or renewing hydropower plants (HPP), it is critical to increase the knowledge related to them and objectively assess in advance their potential impact on the aquatic ecosystem processes. In this context, a useful tool is the Fish Population Hazard Index (FPHI), produced by the EU-funded H2020 FIThydro - Fishfriendly Innovative Technologies for Hydropower, a project aimed at exploring and developing measures for mitigating the impacts of HPP.

## 6.2 General description

The Fish Population Hazard Index (FPHI) is a first-step decision and management tool for environmental impact assessment of hydropower plants. Its outcome is based upon the weighing of site-specific effects of hydropower plants, the susceptibility of fish species to hydropower-induced mortality as well as overarching environmental and societal development targets. FPHI leads to the identification and assessment of eight aspects involved in the construction and operation of hydropower plants that have an impact on the welfare of fish species (Wolter et al., 2020).

The FPHI assessment approach is based on the ordinal, categorical “low, moderate or high” scores, depending on the typical impact thresholds obtained from available datasets. In addition, a set of technical and operational mitigation measures have been integrated into the index, including design of a fine screen, a downstream bypass and adjusting in a more fish-friendly way the operational regime of the HHP. The implementation of these mitigation measures leads to lowering the score by 0.1 to 0.3 points, which may shift the score to a lower hazard class.

## 6.3 Technical description

The output of FPHI is a classification of HPPs in terms of low, moderate or high risk. This score is in function of the species-specific sensitivity to the damage mechanisms generated by hydropower that can be retrieved from literature and / from dedicated sections of the present deliverable.

This is clearly a coarse classification, but it permits to model various combinations of site-specific factors and overcomes possible shortage of species-specific empirical data on the effect of single hydropower aspects. In summary, the tool focuses on parameters that exclusively concern the constructive, operational and technical aspects of an HPP which are presented as follows:

1. **Type of the plant**: Specific impacts on the river stream may rise from different types of hydropower plants, to which they are closely linked. FPHI differentiates among storage plants, runoff plants and diversion plants, which, due to their operating conditions, size and functioning of structures and presence of reservoir, are scored from high- to low-risk, respectively.

2. **Height of the barrier/dam**: A structure located in the river stream, regardless of its use for the generation of electricity or regulation of the water level, generates severe impact on many fish species, due to habitat fragmentation, impoundment and direct mortality during downstream passage. The hazard scoring of the barrier height is (Fig. 24):

| Risk class | Low | Moderate | High |
|---|---|---|---|
| Barrier height (m) | <2 | 2-10 | >10 |

*Fig. 24 Risk scoring of the dam height (Wolter et al., 2020)*

3. **Installed to average discharge ratio**: In principle, the probability that fish pass through the turbines is higher when the amount of stream water that is guided to the turbines increases, with less amount going through the sluice gates, spillways, bypass channels or fish passes. The ratio of the installed to mean discharge is considered an important predictor for actual turbine fish passage (Fig. 25).

| Risk class | Low | Moderate | High |
|---|---|---|---|
| Discharge ratio ($\frac{Q_{installed}}{Q_{mean}}$) | ≤0.5 | >0.5-<1 | ≥1 |

*Fig. 25 Risk scoring the probability of entrainment (Wolter et al., 2020)*

4. **Type of the installed turbines**: Different types of turbines have been developed to fulfil the requirement of each single scenario in which the HPP is located. Available water head and discharge are the two main parameters used for the design of a hydropower turbine. As described in section “Hydropower as source of damages on downstream migrating fish”, distinct turbine types are associated with different degrees of injury/mortality in fishes accounting for null/low (i.e. Archimede screws),

moderate (i.e. Minimum Gap Runner turbine) to extreme (i.e. Francis or Pelton turbines) impacts. The score assigned with this factor is shown in Fig. 26.

| Risk class | High | Moderate | Low |
|---|---|---|---|
| based on strike mortality for Kaplan and Francis turbines | $M_{Monten}$>20% | $M_{Monten}$=10-20% | $M_{Monten}$<10% |
| based on other turbine types | • Ossberger,<br>• Pelton,<br>• Kaplan (bulb) | • Archimedes screw<br>• Kaplan (MGR)<br>• Kaplan (VLH)<br>• Pentair Fairbanks | • Water wheel |

*Fig. 26 Risk scoring for turbine type and blade strike rate (Wolter et al., 2020)*

5. **Blade strike rates**: Predicting when and where a fish is hit by any physical part during turbine passage is very difficult but, in general, the probability of strike by turbine blade can be evaluated most accurately in the cases of Kaplan and Francis turbines. Models to estimate turbine-related mortality can be grouped into empirical models and physically based models. According to physically based models, the probability of a strike increases with fish length, number of blades and rotational speed of the turbine. On the other hand, it decreases with increasing space between single blades. Usually, rotational speed decreases with turbine size. FPHI applies the blade-strike models as provided by the equations developed by Montén (1985). The strike mortality according to Montén (1985) is categorized into three risk classes. Due to the fact that strike mortality can only be calculated for standard Kaplan and Francis turbines, other turbine types were categorized into appropriate risk classes based on a weight of evidence approach from literature data (Fig. 26).

6. **Mode of operation**: FPHI takes into account three operating conditions:
    1. **Hydropeaking*:*** this mode consists in a periodical release of water due to temporary electricity demands, which generates a downstream hydrograph of very high and very low flows that alternate on an hourly, daily or weekly basis. Generally, high up- and down ramping rates cause impacts such as the displacement of fishes, dewatering of fish habitats, increased turbidity of waters and geomorphological degradation of the river stream. These consequences translate into direct habitat losses and severe impacts on macroinvertebrate populations, ultimately disrupting food webs. The risk associated with the hydropeaking mode is high, regardless of the plant type.
    2. **Regular release*:*** this mode refers to HPPs regularly releasing water. For this reason, the impact on fish communities is lower than hydropeaking and the score is dependent upon the type of plant (Fig. 27).
    3. **Pump storage:** HPPs with such operating conditions can be used both to store energy by pumping water, in times of peak production, and to generate electricity as turbine mode in times of high demand. They are compensating for differences in the production in the power grid and can in part substitute peak-load power plants, avoiding hydropeaking effects. Pump storage is considered to have a rather low to no impact on the fish community, for any type of plant.

| | | Mode of operation | | |
|---|---|---|---|---|
| | | Hydropeaking | Regular release | Pump storage |
| Plant type | Diversion | High | Low | Low |
| | ROR | High | Moderate | Low |
| | Storage | High | High | Low |

*Fig. 27 Risk scoring of the plant type and operation mode (Wolter et al., 2020)*

7. **Availability of an upstream migration facility**: Connectivity is a prerequisite before any other measures and fish migration facilities are currently accepted as standard practice. Therefore, FPHI considers the presence of a fishway as a basic element of a hydropower plant. Successful upstream migration of fishes through a barrier is mainly achieved by means of fishways. Due to the highly variable and hardly predictable fishway passage efficiency, the tool does not score the related hazard species-specifically but only as yes (i.e. an upstream migration facility is installed and operational) or no.

8. **Mitigation measures**: FPHI also accounts for existing or planned measures to reduce specific hazards to fish communities. The mitigation measures considered in the evaluation are the following:
    1. **Guiding structures*:*** defined as structures with fine screens that are located in the upstream part of the power plant to prevent fishes from entering the penstock, installed at a horizontal angle with the streamflow less than 45°. Flow velocity at the screen should usually not exceed 0.5 m $s^{-1}$. The distance between the bars determines the maximum width of a fish being able to pass it.
    2. **Downstream bypasses*:*** are structures allowing fishes to migrate downstream, avoiding the passage through the turbines.

    The scores associated with the above mitigation measures are shown in Fig. x.

| | | With bypass | | | Without bypass | | |
|---|---|---|---|---|---|---|---|
| Horizontal installation angle (°) | | <45 | 45-<90 | 90 | <45 | 45-<90 | 90 |
| Bar space (mm) | <10 | -0.2 | -0.1 | 0 | 0 | 0 | 0 |
| | 10-15 | -0.1 | -0.1 | 0 | 0 | 0 | 0 |
| | >15 | 0 | 0 | 0 | 0 | 0 | 0 |
| Vertical installation angle (°) | | <45 | 45-<90 | 90 | <45 | 45-<90 | 90 |
| Bar space (mm) | <10 | -0.1 | -0.0.5 | 0 | 0 | 0 | 0 |
| | 10-15 | -0.05 | -0.0.5 | 0 | 0 | 0 | 0 |
| | >15 | 0 | 0 | 0 | 0 | 0 | 0 |

*Fig. 28 Score for fine screen and downstream bypass (Wolter et al., 2020)*

## 6.4 FPHI calculation

To compute the Fish Population Hazard Index, all the features of the hydropower plant have to be specified in a dedicated "Input" Excel sheet. These input values are used to generate the parameter-specific impact classes "Low", "Moderate" or "High". Next, the computed impact classes are then contrasted with the species-specific sensitivity score (Fig. 29) to provide score values for the final assessment. The species sensitivity is a matrix that integrates the results of the sensitivity analysis with the species status assigned by the IUCN. Worthy of note, both *Anguilla anguilla* and *Salmo salar* have high biological sensitivity, but only the former is a critically endangered species (van Treeck et al., 2017).

| Impact class | Species' sensitivity | | | | |
|---|---|---|---|---|---|
| | Highest | High | Average | Moderate | Low |
| High | 3 | 3 | 2 | 2 | 1 |
| Moderate | 3 | 2 | 2 | 1 | 1 |
| Low | 2 | 2 | 1 | 1 | 1 |

*Fig. 29 Matrix for contrasting the impact classes with the species-specific sensitivity score*

Finally, an impact parameter-specific hazard score is then calculated by transforming the hazard values 1, 2 and 3 into decimal numbers of 0, 0.5 and 1 and then averaged across all the fish species of the sample, with the number of species considered by the tool being five at most per run. This computation is repeated for each impact. The resulting average hazard values are again averaged.

The principal impact classification is classified as "low, medium and high risk", while the decimal scoring between 0 and 1 allows for more differentiated cause-effect analyses and further use of the index in cumulative impact assessments, such as a decision support system integrating technical solutions (Fithydro DSS, 2022).

# 7 BioPA – Biological Performance Assessment tool

## 7.1 General description

The Biological Performance Assessment (BioPA) is a tool developed by the Pacific Northwest National Laboratory (PNNL) within the framework of Hydropassage (www.hydropassage.org), a collaborative project whose ultimate goals are to increase hydropower efficiency, lower the cost of deploying hydropower and improve downstream fish passage, with clear benefits for both the industry and the environment.

The toolset enables the evaluation of the influence of the turbine passage on fish, therefore supporting the design, operation and evaluation of hydropower facilities. It integrates information from the computational fluid dynamics (CFD) model of the hydraulic conditions of a given turbine type, the passage distribution of fish and known damage mechanisms related to specific turbine types (see section 2.1 - Mechanisms affecting mortality of fish during turbine passage for details on sources of damage encountered by fish during turbine passage) to ultimately quantify the physical stress experienced by fish during downstream passage by resolving dose-response equations. BioPA is able to evaluate the biological performance of Kaplan and Francis turbine types on over 20 species of fishes.

Exposure distributions are generated from CFD models in two steps: first, particles are run through the model to calculate expected fish trajectories. Each trajectory is analyzed to determine the occurrence and magnitude of a stressor event. From these trajectories, distributions are generated for each physical stressor (i.e. strike, rapid decompression, fluid shear and turbulence). A preliminary knowledge about fish response to physical stressors is needed to predict the likelihood of injury, mortal injury (i.e. injuries statistically determined to be highly associated with and significant predictors of mortality) or mortality following the exposure to a certain stressor, effectively allowing the translation of a hazard characterization to a species-specific probabilistic risk of damage (Fig. 30). To this end, PNNL has developed 99 dose-response models for exposure to blade strike, rapid decompression and fluid shear for several fish species employing data generated from dedicated experiments under controlled conditions or gathered from scientific literature. The catalog of species for which dose-response equations are available currently encompasses over 31 fish species (Table S1 of Pflugrath et al., 2021), and additional ones may be included in future versions of the software as soon as their dose-response equations are generated.

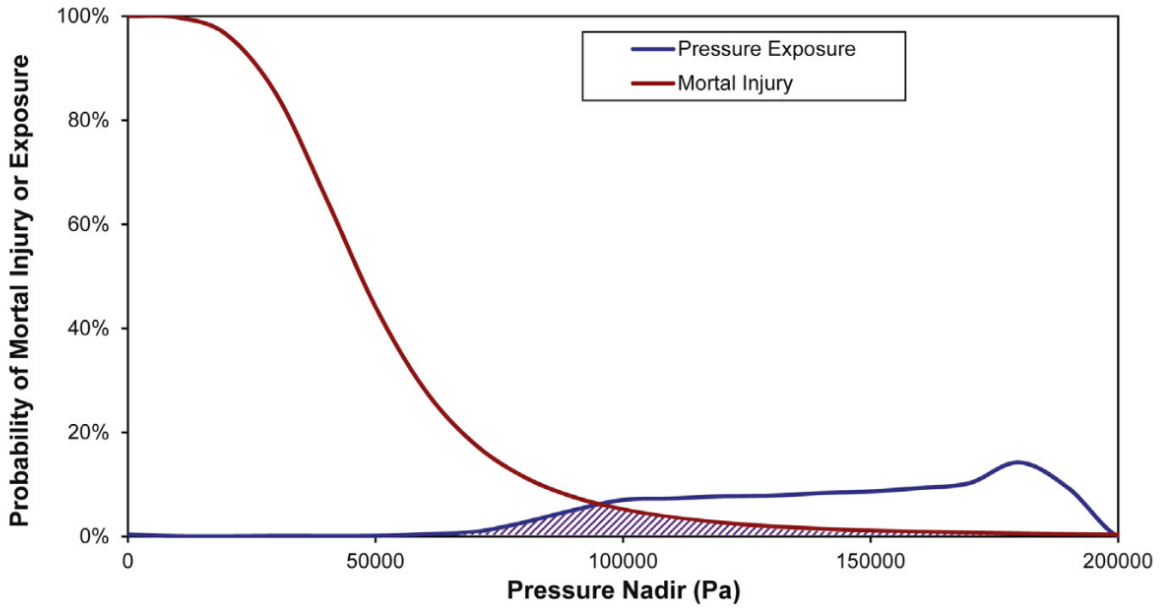


*Fig. 30 Example of probability of expected mortality (hatched area under the curves) determined by a given pressure probability distribution in BioPA (Richmond et al., 2014)*

Combining the exposure probability of stressors determined through streamtrace sampling with biological response models information obtained from laboratory studies, BioPA returns a performance score, or Passage Quality Index - a relative risk of fish damage. This can be used to evaluate and compare different turbine designs and hydropower operating conditions. It is important to specify that the BioPA PQI score is not an estimate of fish passage survival nor an indication of the absolute risk of fish injury following downstream migration through a turbine. Rather, it represents a relative risk specific of a given species for a given stressor in a given turbine design or hydraulic condition. This information allows stakeholders to best investigate the design and operating conditions to ultimately improve fish passage. For instance, Hydropassage led to the development of hydropower turbines with a very low impact on fish that allowed for nearly 99% predicted fish passage survival.

The performance score is dependent upon several factors:

- **Fish species and size/life stage**: fish species of varying body length differ in their response to specific stressors.
- **Turbine design**: the turbine type and geometry impose distinct hydraulic stressors.
- **Hydraulic conditions**: several variables that vary according to the operating configuration (e.g. discharge flow velocity, blade orientation) contribute to the severity of specific stressors.

Such a toolset has been used to evaluate the biological performance of Kaplan and Francis turbines in many hydropower plants in the Pacific Northwest region in the United States and is being used for research and development purposes by Andritz Hydro, Voith and Natel Energy. University of Tuscia purchased a one-year license of BioPA v. 2.1 and 3 in June 2021 and attended two training sessions on August 5$^{th}$, 2021. Recordings of the two sessions can be made available upon request to Dr. Andrea Miccoli (University of Tuscia).

## 7.2 Technical specifications

BioPA integrates well with commercial software packages such as Microsoft Excel. Previous versions of BioPA relied on Tecplot360 CFD post-processing software to compute stream trace trajectories. In the latest version (v.3 at the time of writing of this deliverable, released in December 2019), the use of Tecplot360 is waived and the package utilizes directly computed trajectories and collision boundary sampling data following data extraction from the CFD simulation by means of custom post-processing Java scripts.

The BioPA toolset consists of the following components:

1. **Model and trajectories**: The CFD model that describes the hydraulic environment and the particle trajectories using the flow-particle interaction method. Contrary to v.2, which was based on stream traces in the flow field, BioPA v.3 employs particle trajectories calculated from CFD simulations conducted with the Lagrangian particle tracking method. Particle trajectories are regarded as equivalent to estimated fish trajectories, and stressor information is exported from the CFD model along the simulated fish trajectories. Scalar stressors (i.e. nadir pressure, strain and turbulence) and collision data are exported in this order. Collision data must be extracted using a Javascript plugin in any CFD software.

2. **Probabilities**: Calculation of exposure probabilities to hydraulic performance metrics of turbines (i.e. net head, efficiency and torque) and biological stressors (i.e. collision/strike, pressure, hydraulic shear and turbulence). The statistics from the exported stressors are extracted before loading into the BioPA Excel application for converting CFD output to BioPA input

3. **Dose-response models**: Employing data either generated on purpose or gathered from the literature, dose-response equations were generated that allow the relation of the extent of biological stressor to damages suffered by fish during passage. The available dose-response models are shown in the “Input Information” worksheet of the BioPA Workbook. A unique dose-response code is given to each stressor, species and adverse effect under investigation. For Atlantic salmon *Salmo salar* and European eel *Anguilla anguilla*, only fluid shear dose-response models were produced based on data from Turnpenny et al. (1992). Nevertheless, models for all three stressors are available for rainbow trout *Oncorhynchus mykiss* and American eel *Anguilla rostrata* based on data from several experiments (Saylor et al., 2019; Pflugrath et al., 2019; EPRI, 2011 and 2008; Saylor et al., 2020; Amaral et al., 2020; Beirão et al., 2021; Neitzel et al., 2004). Because they belong to the same families (Salmonidae and Anguillidae) and display morphological (i.e. body shape), anatomical (i.e. physostomous vs. physoclistous), physiological or behavioral features (acclimation depth) similar to our species of interest (see section 4 - Description of target species), rainbow trout and American eel are considered surrogate species of Atlantic salmon and European eel, respectively. The same worksheet also includes the depth weighting function generator tool that can be used to simulate vertical distribution of fish at the passage entrance according to linear, gaussian and sigmoidal functions.

4. **Passage Quality Index**: Conversion of exposures to a Passage Quality Index (PQI) using biological response data. The PQI for each stressor is calculated as a function of both the probability of exposure (Pe) and the probability of adverse response at a given exposure (Pm) according to the following equation:

$$PQI = 500 * \sum_{i=1}^{N} (1 - Pe, i * Pm, i)$$

The PQI score ranges from 0 to 500, with lower PQIs corresponding to lower estimates of survival rates (i.e., higher likelihood of injury). Instead, in case of no adverse effect estimated, the equation returns a PQI value of 500.

PQIs can be compared across different operating conditions or among different stressors. In the former case, statistically significant differences are indicated by the lack of overlap among 95% confidence intervals of PQIs; in the latter, the experimental approach followed in the establishment of the mathematical relationships must be identical (i.e. fish species, body length/life stage and injury type modeled) for all stressors that are to be compared.

## 7.3 Calculation process

The next paragraphs report the road-map for the implementation of the BioPA tool in the ALPHEUS project, based on the indications reported in the BioPA User Guide.

### 1. Selection of the case study

The first step concerns the selection of the project layout for the analysis with BioPA (i.e. contra-rotating propeller and/or the positive displacement turbine) (Fig. 31). The working stage of the hydraulic machine - either stationary or transient - flow regimen, has to be chosen, as well.

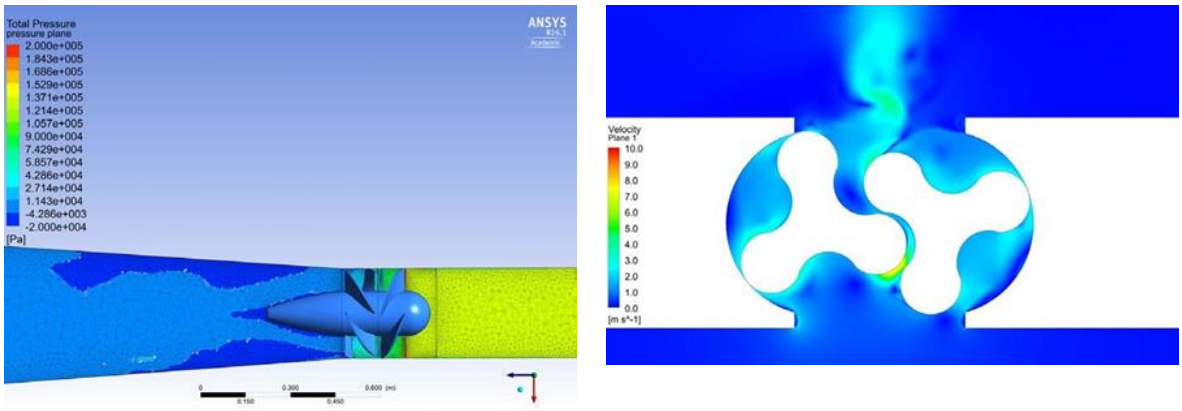


*Fig. 31 CFD simulations for the contra-rotating propeller (left) and the turbine positive displacement turbine (right)*

### 2. Definition of the seeding array

The extraction of the appropriate stressor's values (i.e. rapid decompression, fluid shear, turbulence and collision) is based on first calculating representative fish trajectories through the passage route. The number of trajectories modeled in the CFD must be sufficient to achieve a robust Passage Quality Indices (PQI) estimate. Therefore, a suitable representation of density and distribution of the approaching fish population (e.g. vertical distribution, etc.) leads to the selection of a seeding array at the beginning of the study domain, i.e. the turbine intake (Fig. 32).

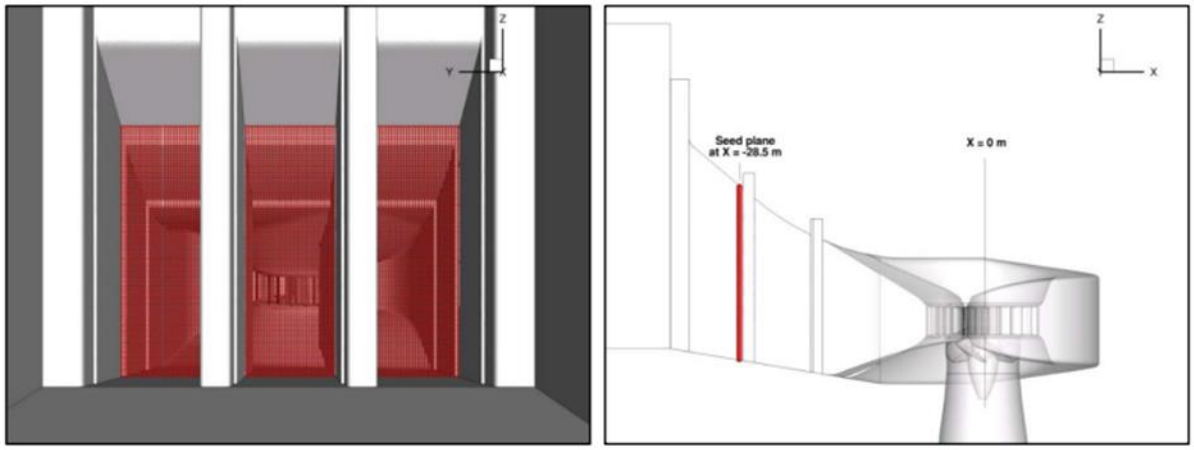


*Fig. 32 Example of seeding array with 0.2 m spacing (left), located in the intake of a representative Kaplan turbine passage (right)*

## 3. Computation of passage trajectories within CFD

In BioPA v.3, the trajectories representing the fish passage are expected to be calculated using particle tracking functionality within the CFD software, whereby individual particles are modeled and tracked within the flow field from an array of seeding locations to an exit boundary. This method is usually referred to as Lagrangian particle tracking and discrete element modeling. The seeding location is typically located at the entrance to the intake or distributor as shown in Fig. 32 and Fig. 33, respectively. Fig. 32 also shows the coordinate convention used within the BioPA tool, whereby X is the primary flow direction of the intake, Z is oriented vertically up, and Y is based on the direction of X and Z using the right-hand coordinate convention.

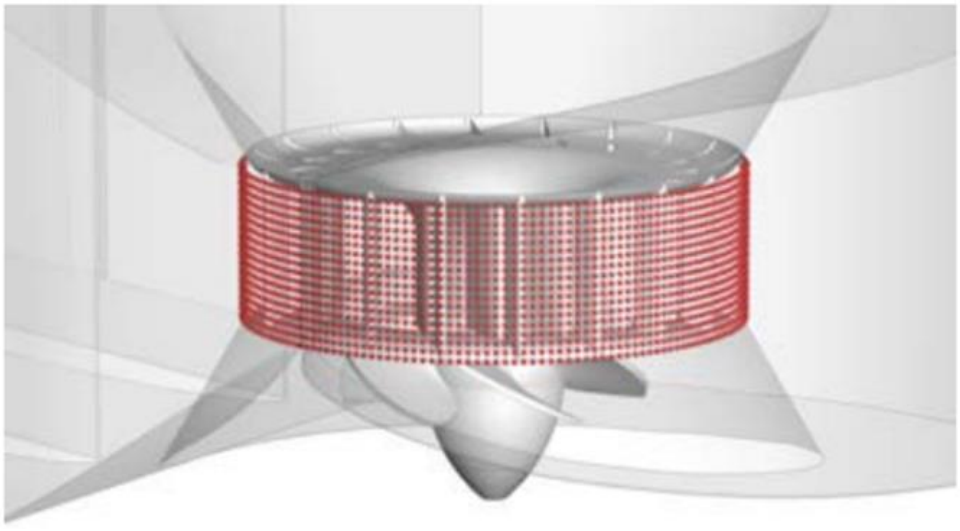

*Fig. 33 Example of seeding array located just upstream of the distributor to represent trajectories that sample the entire stay vane, wicket gate, and runner blade zones*

## 4. Export of stressors data from CFD

The CFD model results are exported in a way that outputs stressor information along the simulated fish trajectory. This is typically achieved in two steps: first, the export of the scalar

stressors (CFD nadir pressure, maximum strain, and maximum TKE) as trajectory data; second, the export of the collision data (implemented in BioPA v.3 as a collision flag and impact intensity). The steps to export these files are outlined in more detail in the following subsections.

## 5. Conversion of CFD results to BioPA statistics file

The statistics from the exported stressor data must be extracted before loading into the BioPA tool. The pre-processing step can be done using the provided Excel macro or other software of the user's choice.

The key statistics for each trajectory are defined as follows:

N: Incremental counter of the number of trajectories simulated in the CFD.

Seed: Unique ID number for the individual trajectory, usually generated by the CFD.

Seed_X: X-ordinate of trajectory start location. The X-direction of the CFD model is defined as the primary direction of flow (often perpendicular to the inlet or seeding plane).

Seed_Y: Y-ordinate of trajectory start location. The Y-direction of the CFD model is defined by the directions of the X and Z directions, using the right-hand coordinate convention.

Seed_Z: Z-ordinate of trajectory start location. The Z-direction of the CFD model is defined as "up" (positive in the opposite direction to gravity).

End_X: X-ordinate of trajectory termination point (m).

End_Y: Y-ordinate of trajectory termination point (m).

End_Z: Z-ordinate of trajectory termination point (m).

Nadir: Minimum total pressure encountered along the trajectory (Pa).

Strain: Maximum magnitude of the strain tensor encountered along the trajectory ($s^{-1}$).

TKE: Maximum TKE encountered along the trajectory (J/kg).

Collision: Binary flag to indicate whether the trajectory included a collision with a structural element (= 1) or not (= 0).

Intense: Maximum magnitude of the normal velocity component of the collision event (velocity of the fish relative to the velocity of the collision object).

Thick: Representative thickness of the collision object. BioPA v.3 currently assumes a constant value for this parameter, which is entered as an input variable to the dose response.

## 6. Using the BioPA application

The conversion of the CFD output into a BioPA v.3 input format can be achieved with the Microsoft Office Excel application. The user specifies the column numbers required in each of the trajectory and collision data files through the input table shown below (Fig. 34).

| Column Parameter | Units | CSV Column # | |
|---|---|---|---|
| | | Trajectory File | Hits File |
| Particle ID | --- | 1 | 1 |
| X Location | m | 9 | 4 |
| Y Location | m | 10 | 5 |
| Z Location | m | 11 | 6 |
| CFD Pressure | Pa | 3 | |
| CFD TKE | J/kg | 5 | |
| CFD Strain | 1/s | 4 | |
| CFD Collision Velocity (X) | m/s | | 12 |
| CFD Collision Velocity (Y) | m/s | | 13 |
| CFD Collision Velocity (Z) | m/s | | 14 |
| | | | |
| Include Collision Analysis with *_Coll file? | | | Yes |
| Convert Pressure to Absolute Value? | | | Yes |
| | | $Z_{ref}$ (m) | 0 |
| | | $P_{ref}$ (Pa) | 101300 |
| | | $P_{CFD@ref}$ (Pa) | 0 |

*Fig. 34 Input table for CFD output to BioPA v.3*

The BioPA toolset comprises a broad dose-response library, as shown in the "Input Information" worksheet of the BioPA Workbook. This table lists the stressor, species, adverse effect, and any additional information regarding each dose-response model available. Dose-response models are identified by unique codes, which also appear in the dose-response drop-down menus in the "Case" worksheets to specify the dose response to be used in the calculation of the PQI.

BioPA enables the prediction of adverse effects by hydropower turbines on fish populations by taking into account multiple incident distributions of fish. For example, downstream migrating fish may swim closer to the water surface and hence be distributed with a greater density towards the ceiling of the turbine intake. However, if a uniform seeding is used in the CFD calculation, the "Input Information" worksheet also provides the opportunity to weight the results by user-defined weighting functions that are designed to model the vertical distribution of the fish at the passage intake. These functions can be selected from the following forms: None, Linear, Gaussian and Sigmoidal (Fig. 35). It is important to specify that each test "Case" study worksheet allows the selection of distinct weights models.

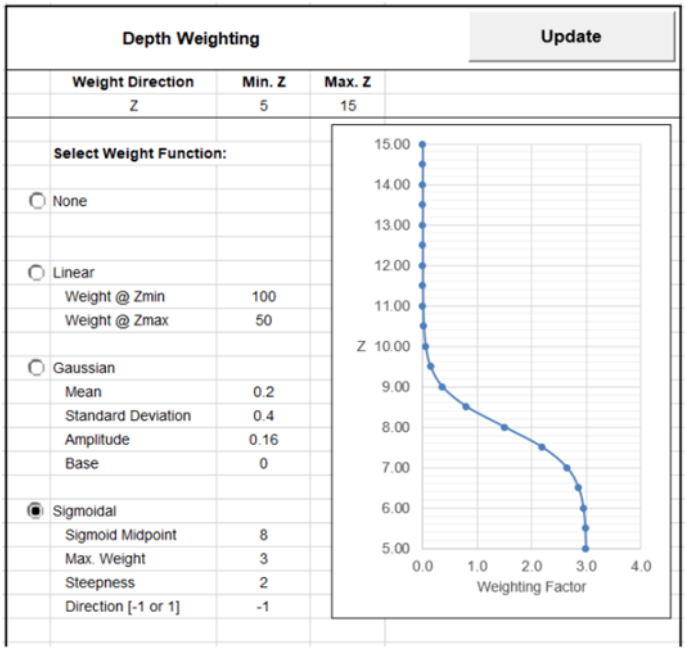


*Fig. 35 Weighing function tool*

Next, Passage Quality Indices (PQIs) are computed as a function of both the probability of exposure (Pe) and the probability of adverse response to that level of exposure (Pm) (see equation at bullet 4 of section "Technical specification" above). Importantly, comparisons of PQI values between different stressors is only possible if the dose-response specifications (species, life stage, injury mechanism, etc.) are identical for those stressors.

## 7.4 Biological response models

BioPA v.3 currently encompasses 99 biological response models, classified by stress mechanism and fish species. Below, general information on equations per stress mechanisms are provided, and selected dose response model coefficients developed for both target fish species and surrogate species presented in damage-specific tables (i.e. injury, major injury, mortal injury, immediate mortality, depending on the damage being modeled).

### 7.4.1 Rapid decompression

Rapid decompression biological response models are not currently available for the two target species of the present deliverable. However, equations that predict the likelihood that fish will be subject to injury (Fig. 36), mortal injury (Fig. 37) and immediate mortality (Fig. 38) when exposed to given RPC were developed for up to three surrogate species, namely American eel, Chinook salmon and rainbow trout (Pflugrath et al., 2021) (see section 5.1 - Rapid decompression). Worthy of note, American eel appeared to not be impacted in any of the endpoints considered by rapid decompression in downstream turbine passage. All three above-mentioned species have an open swim bladder, i.e. they are physostomous. For this reason, they tend to experience lower injury rates than physoclistous species, but their mortality rates do not necessarily follow the same trend.

The general form of the equation is:

$$P(X) = \frac{e^{\beta 0 + \ \beta 1 * \ln(\mathrm{Pa}/\mathrm{Pn})}}{1 + e^{\beta 0 + \ \beta 1 * \ln(\mathrm{Pa}/\mathrm{Pn})}}$$

where P(X) is the probability of occurrence of the selected endpoint, $\beta_0$ and $\beta_1$ are endpoint-specific coefficients determined by logistic regression analyses, and Pa and Pn are acclimation and nadir pressures, respectively.

The endpoint-specific β0 and β1 coefficients for the three surrogate species are included in Table 6.

*Table 6 Coefficients to be used for predicting the probability of adverse effects caused by rapid decompression, per species and endpoint (recreated from Pflugrath et al., 2021). NA: not available. Zero denotes models for which minimal or no endpoint was observed.*

| Fish species | $\beta_0$ and $\beta_1$ coefficients for injury | | $\beta_0$ and $\beta_1$ coefficients for mortal injury | | $\beta_0$ and $\beta_1$ coefficients for immediate mortality | | Reference |
|---|---|---|---|---|---|---|---|
| ***Anguilla rostrata*** | 0 | 0 | 0 | 0 | 0 | 0 | Pflugrath et al., 2019 |
| ***Oncorhynchus tshawytscha*** | -4.735 | 3.485 | -5.560 | 3.850 | -7.700 | 3.878 | Brown et al., 2012a |
| ***Oncorhynchus mykiss*** | -4.956 | 3.276 | -5.118 | 2.927 | NA | NA | Beirão et al., 2020 |

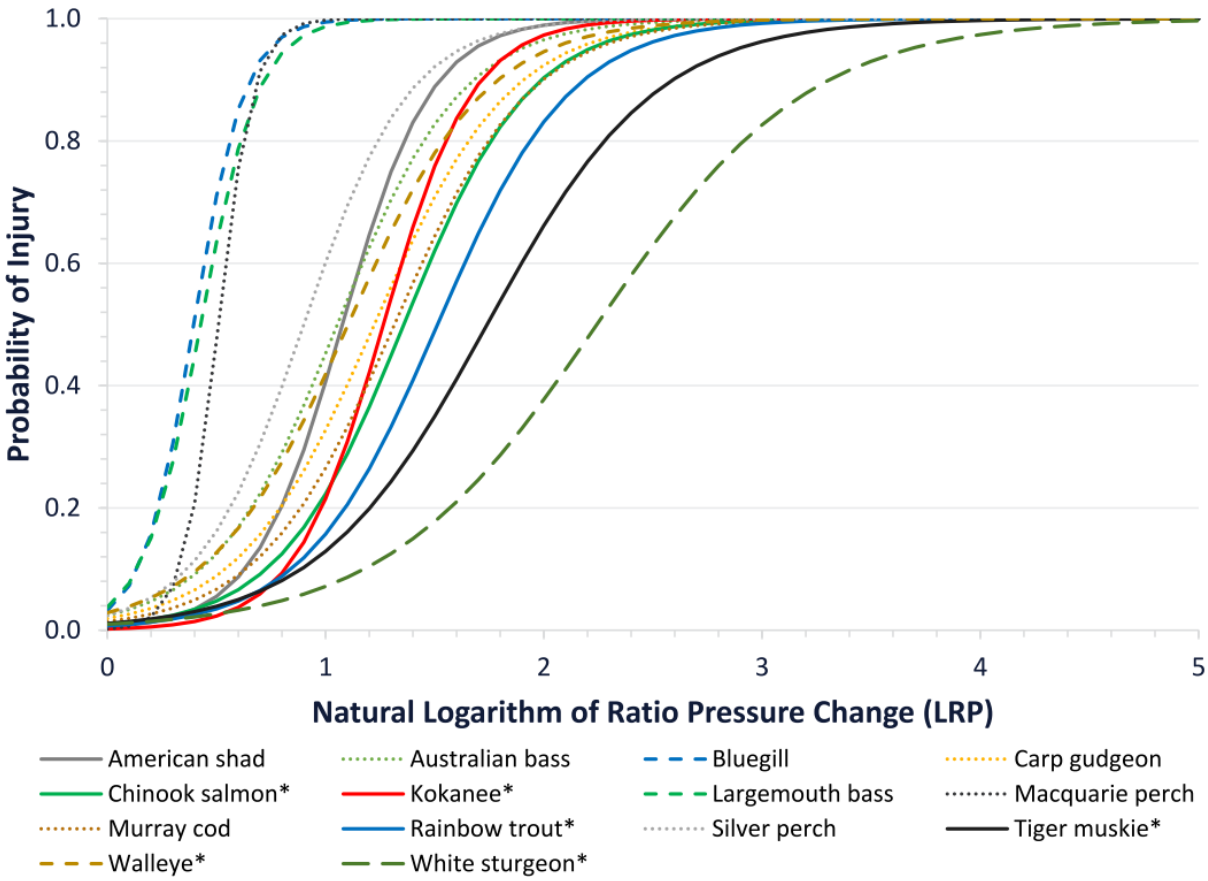


*Fig. 36 Probability of injury over LRP for selected fish species including 2 surrogate species of Atlantic salmon. Physostomous and physoclistous species are represented with solid and dotted lines, respectively (Pflugrath et al., 2021)*

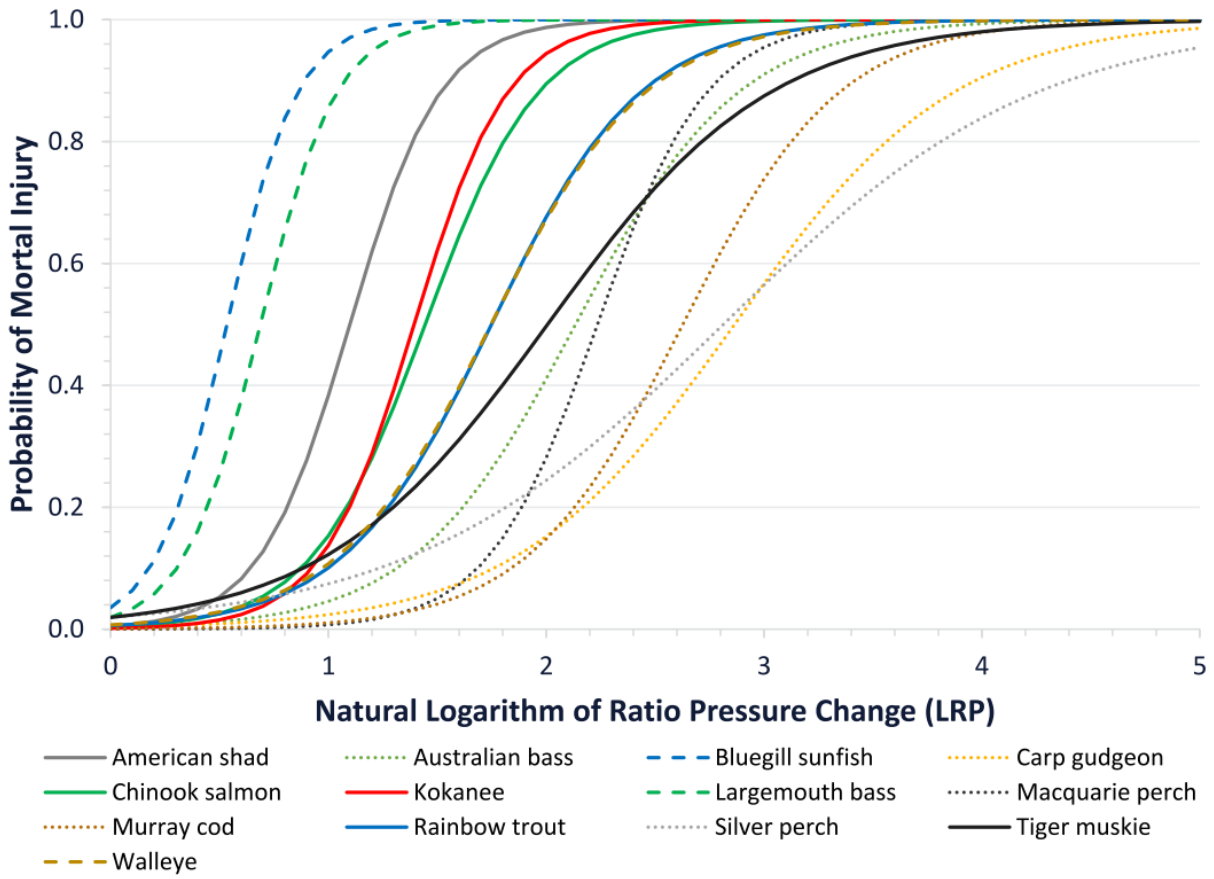


*Fig. 37 Probability of mortal injury over LRP for selected fish species including 2 surrogate species of Atlantic salmon. Physostomous and physoclistous species are represented with solid and dotted lines, respectively (Pflugrath et al., 2021)*

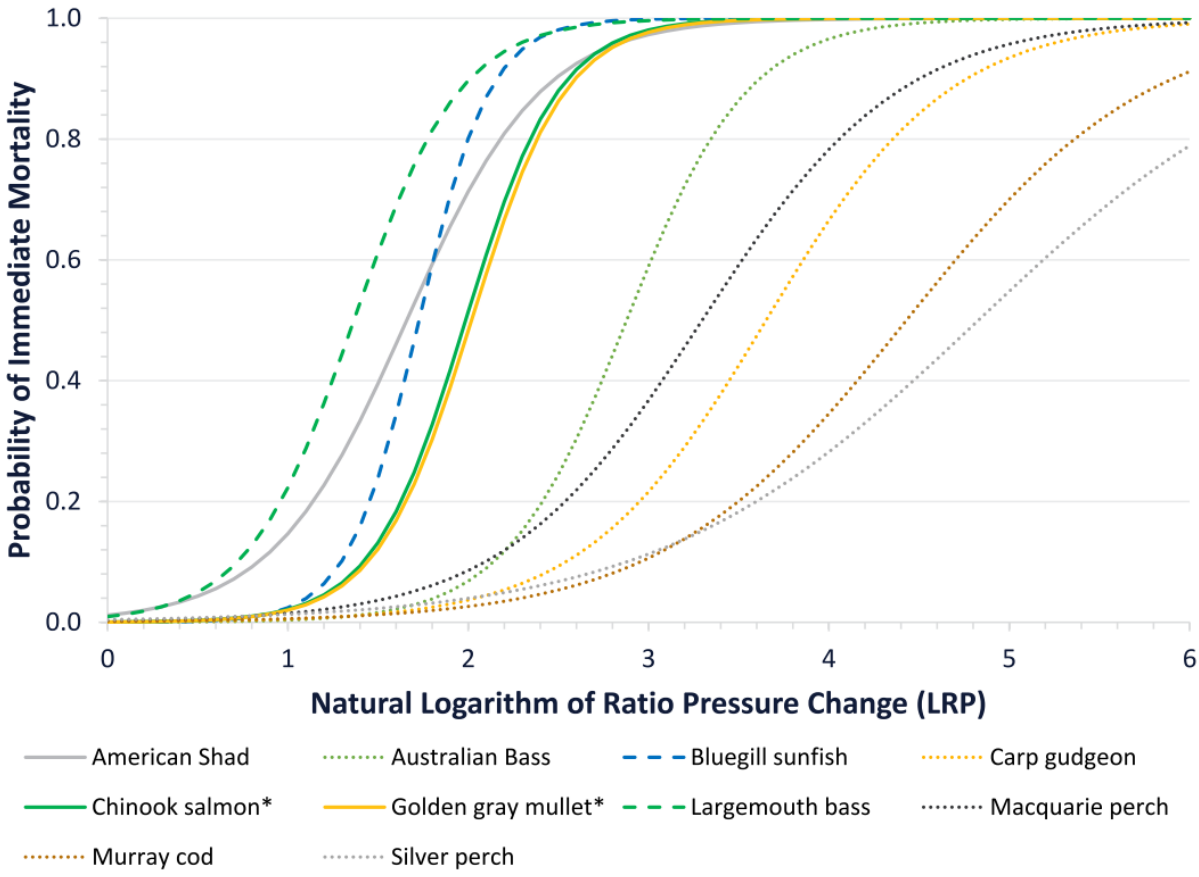


*Fig. 38 Probability of immediate mortality LRP for selected fish species including 1 surrogate species of Atlantic salmon. Physostomous and physoclistous species are represented with solid and dotted lines, respectively (Pflugrath et al., 2021). * : model developed by Pflugrath et al. (2021) from data published by Brown et al. (2012a)*

### 7.4.2 Shear

Biological response models predicting the consequences of exposure to shear stress are available for both target species of the present deliverable, depending on the selected endpoint, i.e. injury (Fig. 39), major injury (Fig. 40) and mortality (Fig. 41). Only mortality can be predicted for Atlantic salmon, while all three endpoints were monitored for European eel under controlled conditions. Datasets produced on five surrogate species (i.e. American eel, Chinook salmon, coho salmon, rainbow trout and brown trout) have allowed the development of equations predicting fish damage based on shear ($s^{-1}$) (Pflugrath et al., 2021) (see section 5.2 - Shear), therefore allowing fluid shear associated with passage through hydropower facilities to be successfully used as a predictor of damage in several fish species. In the case of Chinook salmon, a surrogate species of Atlantic salmon, a fine level of prediction was achieved by modeling biological responses in three different size classes, namely fall/subyearling, fall/yearling and spring. Worthy of note, neither American eel nor European eel suffered from any of the above-mentioned endpoints imposed by fluid shear in downstream turbine passage likely due to the absence of external scales (eels do have scales, but these are embedded within their skin so that their surface is smooth and mucous) and vulnerable structures: minimal or no susceptibility was observed in controlled experiments (Table 7) and for this reason no curve is available in Fig. 39-Fig. 41 for these two species.

The general form of the equation is:

$$P(X) = \frac{e^{\beta 0 + \beta 1 * \ln(S)}}{1 + e^{\beta 0 + \beta 1 * \ln(S)}}$$

where P(X) is the probability of occurrence of the selected endpoint, $\beta_0$ and $\beta_1$ are endpoint-specific coefficients determined by logistic regression analyses, and S is fluid shear expressed as strain rate ($s^{-1}$).

The endpoint-specific β0 and β1 coefficients for the three surrogate species are included in Table 7.

*Table 7 Coefficients to be used for predicting the probability of adverse effects caused by fluid shear, per species and endpoint (recreated from Pflugrath et al., 2021). NA: not available. Zero denotes models for which minimal or no endpoint was observed*

| Fish species | $\beta_0$ and $\beta_1$ coefficients for injury | | $\beta_0$ and $\beta_1$ coefficients for major injury | | $\beta_0$ and $\beta_1$ coefficients for mortality | | Reference |
|---|---|---|---|---|---|---|---|
| ***Anguilla anguilla*** | 0 | 0 | 0 | 0 | 0 | 0 | Turnpenny et al., 1992 |
| ***Salmo salar*** | NA | NA | NA | NA | -7.555 | 0.005 | Turnpenny et al., 1992 |
| ***Anguilla rostrata*** | 0 | 0 | 0 | 0 | 0 | 0 | Pflugrath et al., 2021b |
| ***Oncorhynchus tshawytscha*** **(fall/subyearling)** | -8.272 | 0.01 | -27.534 | 0.028 | -40.981 | 0.039 | Neitzel et al., 2004 |
| ***Oncorhynchus tshawytscha*** **(fall/yearling)** | -7.148 | 0.01 | -10.502 | 0.011 | -10.251 | 0.009 | Neitzel et al., 2004 |
| ***Oncorhynchus tshawytscha*** **(spring)** | -9.845 | 0.014 | -10.053 | 0.010 | -13.992 | 0.012 | Neitzel et al., 2004 |
| ***Oncorhynchus kisutch*** | NA | NA | NA | NA | -12.588 | 0.008 | Johnson, 1972 |
| ***Oncorhynchus mykiss*** | -5.352 | 0.005 | -9.156 | 0.0068 | 0 | 0 | Neitzel et al., 2004 |
| ***Salmo trutta*** | NA | NA | NA | NA | -5.087 | 0.003 | Turnpenny et al., 1992 |

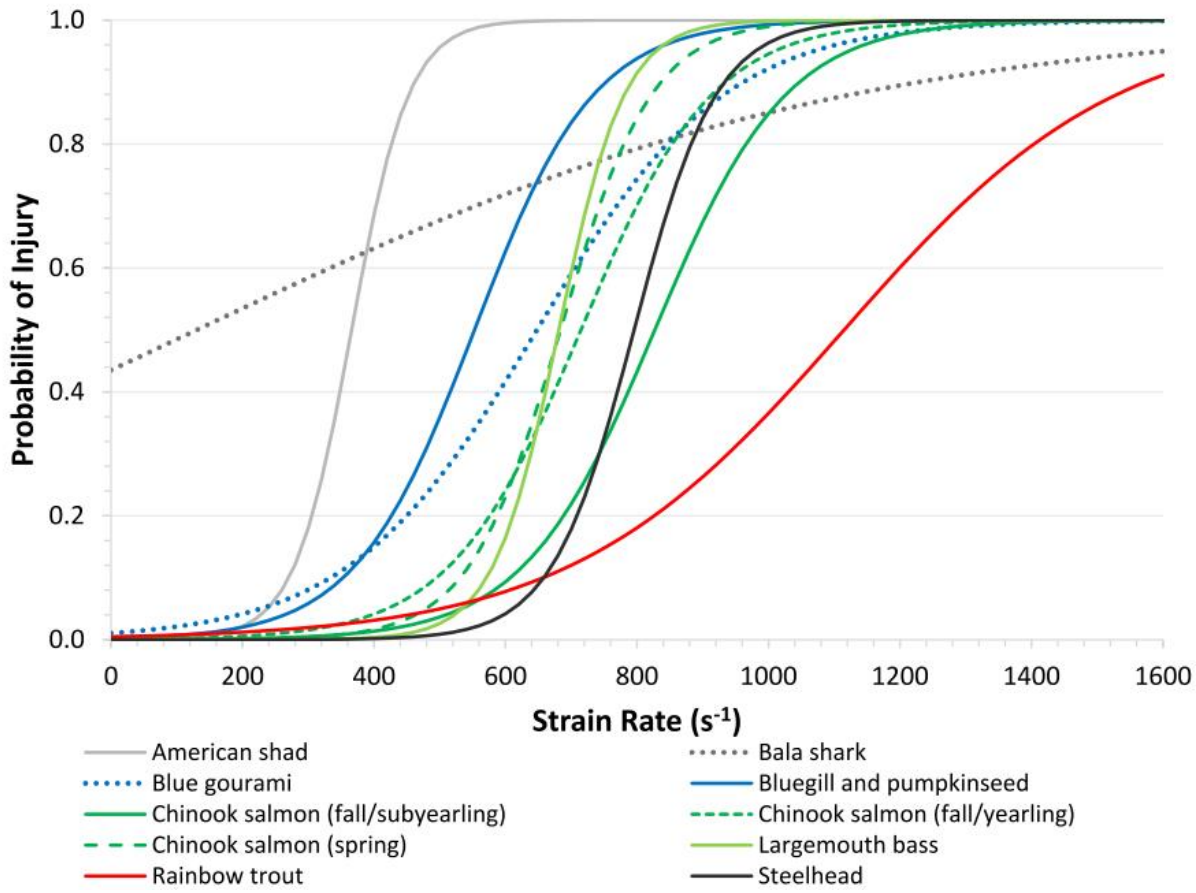


*Fig. 39 Probability of injury over fluid shear for selected fish species including 2 surrogate species of Atlantic salmon, namely Chinook salmon and rainbow trout (Pflugrath et al., 2021)*

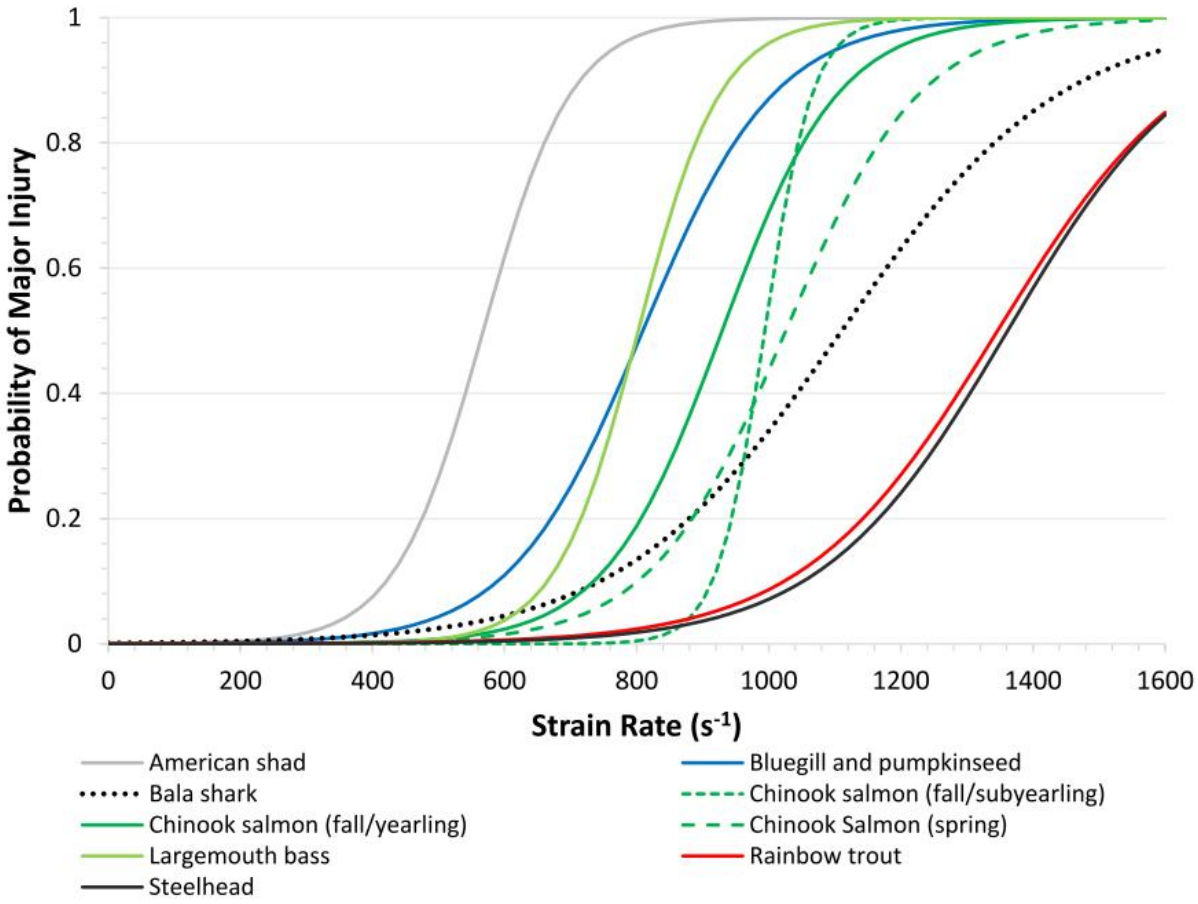


*Fig. 40 Probability of major injury over fluid shear for selected fish species including 2 surrogate species of Atlantic salmon, namely Chinook salmon and rainbow trout (Pflugrath et al., 2021)*

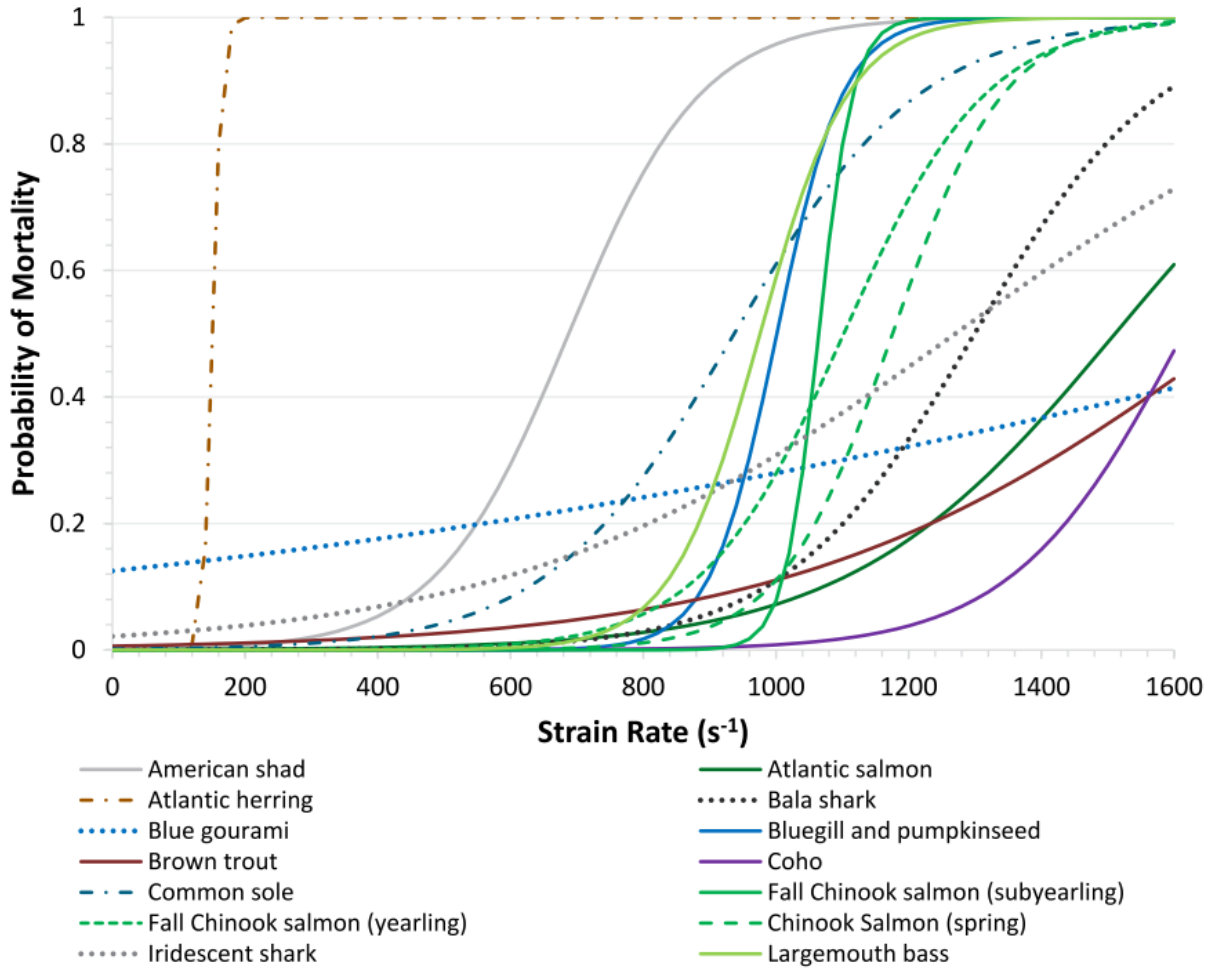


*Fig. 41 Probability of mortality over fluid shear for selected fish species including one of the two target species of this deliverable, Atlantic salmon, and 4 surrogate species for it, namely Chinook salmon, coho salmon, rainbow trout and brown trout (Pflugrath et al., 2021)*

### 7.4.3 Blade strike

Blade strike biological response models are not currently available for the two target species of the present deliverable. However, equations that predict the likelihood of fish mortality based on strike velocity (m $s^{-1}$) and/or blade ratio were developed for two surrogate species, namely American eel and rainbow trout (Pflugrath et al., 2021) (see section 5.3 - Blade strike). Blade ratio could be used as a predictor of mortality only for rainbow trout.

It must be noted that the two surrogate species exhibited opposite trends of susceptibility to blade strike, with American eel being the most resistant species tested as indicated by the highest LD50 blade velocity (lethal dose at which mortality was recorded for 50% of tested specimens) (Fig. 43). The model of rainbow trout was built upon the largest amount of data available for blade strike-related endpoints.

Two different equations were used for modeling the likelihood of mortality.

- A multiple linear regression model was applied to data produced on rainbow trout by EPRI (2011) where fish survival was assessed following blade strike conducted with a fish-to-blade angle of 90 degrees (Fig. 42).

  The general form of the equation is:

  $$if\ V \leq Vcrit: P(M) = 0$$
  $$if\ V > Vcrit: P(M) = m(V - Vcrit)$$

  where m is the slope of specific L/t ratios, Vcrit is the critical velocity at which survival starts to decrease and P(M) is the probability of occurrence of mortality as a function of strike velocity (V).

- A curvilinear model was built for both American eel and rainbow trout from the whole-fish biological response model based on log-logistic and linear regressions (Fig. 43). The initial whole-fish biological response equation was developed to account for 36 mortality rate parameters, i.e. 12 different combinations of location and orientation of striking and three impact angles for each. These were then reduced to 8 to generate a simplified model. The general form of the resulting equation is:

  $$if\ V \leq x: P(M) = \frac{f}{1 + \left(\frac{V}{e}\right)^b}$$
  $$if\ V\ > x: P(M) = \frac{f}{1 + \left(\frac{V}{e}\right)^b} + m(V - x)$$

  where P(M) is the probability of occurrence of mortality as a function of strike velocity (V) and b, e, f, m and x are species-specific coefficients.

The species-specific coefficients for the two surrogate species are included in Table 8.

*Table 8 Coefficients to be used for predicting the probability of mortality as a function of strike velocity, per species and model (recreated from Pflugrath et al., 2021)*

| | Coefficients (multiple linear regression) | | | Coefficients (curvilinear model) | | | | | Reference |
|---|---|---|---|---|---|---|---|---|---|
| **Fish species** | L/t ratio | Vcrit | m | b | e | f | m | x | |
| ***Anguilla rostrata*** | NA | NA | NA | -26.9 | 14.2 | 0.38 | 0.0119 | 11.4 | Saylor et al. (2019) |
| ***Oncorhynchus mykiss*** | 0 | 100 | 0 | -12.33 | 7.06 | 0.54 | 0.0089 | 5.08 | EPRI (2011); Saylor et al. (2019) |
| | 0.75 | 10 | 0.01 | | | | | | |
| | 1 | 7.5 | 0.05 | | | | | | |
| | 2 | 5 | 0.06 | | | | | | |
| | 4 | 4.9 | 0.11 | | | | | | |
| | 10 | 4.8 | 0.21 | | | | | | |
| | 25 | 4.8 | 0.90 | | | | | | |

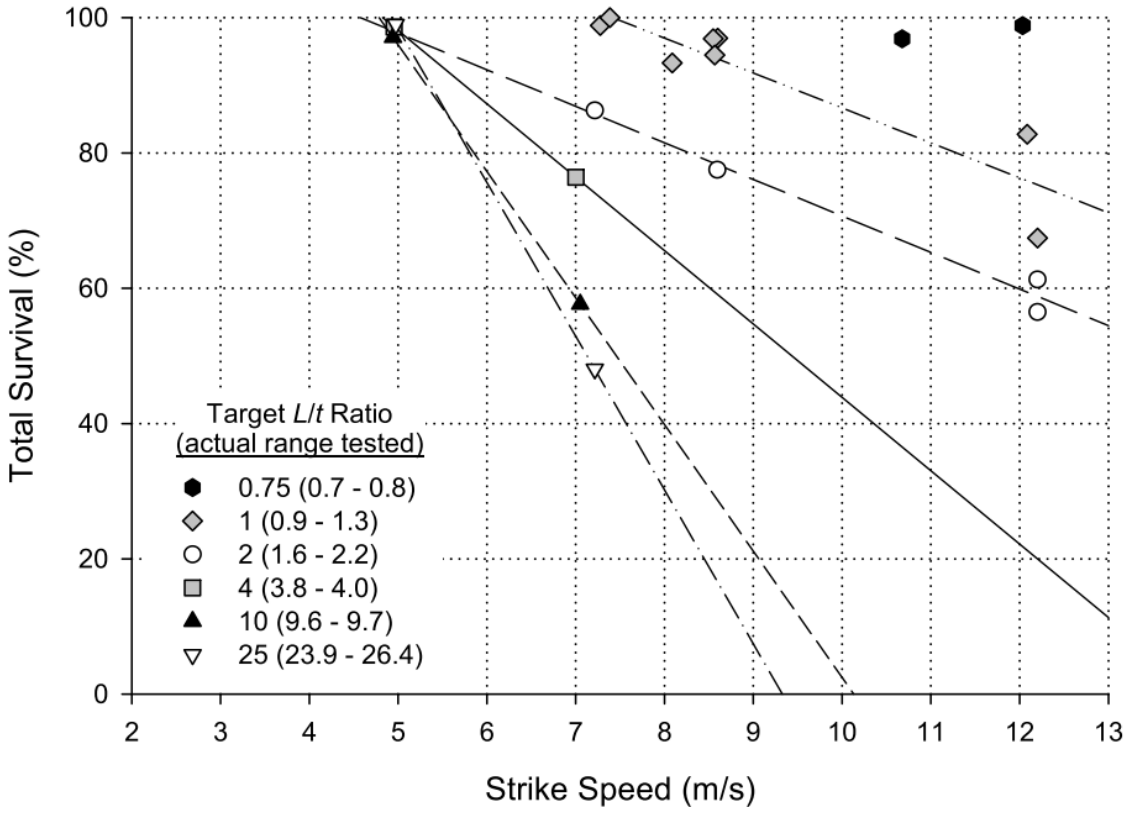


*Fig. 42 Survival rates over strike velocities tested across a broad L/t ratio range at a fish-to-blade angle of 90 degrees using the multiple linear regression model (EPRI, 2011). For L/t ratio below 1, a reliable regression line could not be fitted due to extremely low survival and small sample size*

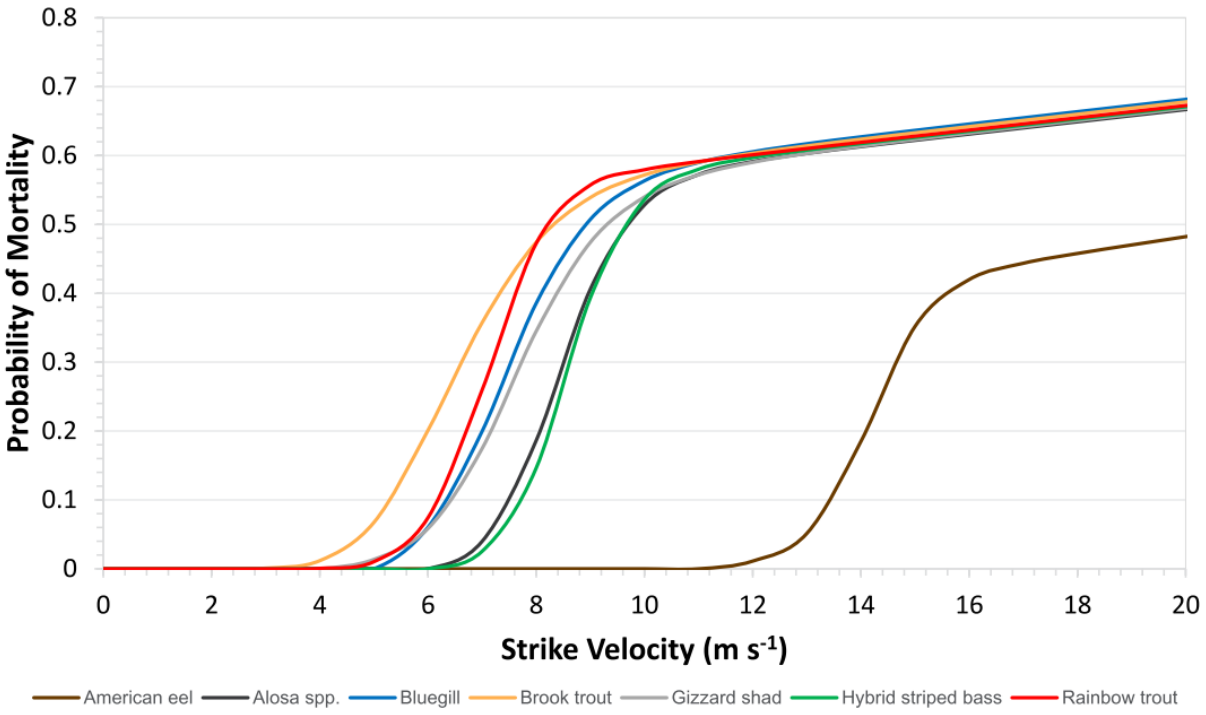


*Fig. 43 Probability of functional and immediate mortality over strike velocities for selected fish species including 1 surrogate species for European eel and 1 for Atlantic salmon, using the curvilinear model. (Pflugrath et al., 2021)*

# 8 The BioPA-based ALPHEUS case study

## 8.1 Turbine design

The ALPHEUS project studies the following three promising Reversible Pump Turbine (RPT) technologies for a low to ultra-low head (i.e. 1 - 20 m) operating conditions:

1. Shaft-Driven variable-speed Contra-Rotating propeller RPT (SDCRRPT)
2. Rim-Driven variable-speed Contra-Rotating propeller RPT (RDCRRPT)
3. Positive displacement RPT

ALPHEUS deliverables D2.1 and D2.2 provide a detailed description of the design process for the SDCRRPT (Fig. 44) and RDCRRPT (Fig. 45), respectively, along with the performance data of the initial designs and the optimized model scale designs. A brief summary of this is given below.

Advance Design Technology's (ADT) turbomachinery design software TURBOdesign Suite was used for the design of both RPTs. The design process started with the meanline design in pump mode at prototype scale using TURBOdesign Pre software based on an operating head of 9 m at a power of 10 MW. At design conditions, the two rotors operate at different speeds with a speed ratio of 0.9 between them. The resulting machine had a shroud diameter of approximately 6 m. Meanline design was followed by the design of 3D blade geometry of both rotors using TURBOdesign1. This software is based on the 3D inverse design approach where a blade design satisfying the user specified blade loading (pressure distribution over the blades) is produced (Zangeneh, 1991; Zangeneh et al., 1996; Bonaiuti et al., 2010). The initial design was analyzed in both pump mode and turbine mode of operation in steady state Computational Fluid Dynamics (CFD) analysis using ANSYS CFX software. An efficiency of more than 90% was obtained in both modes across a range of flow rates for the SDCRRPT. The RDCRRPT has a hollow center which resulted in secondary flows and related losses and hence was less efficient in pump mode compared to the SDCRRPT; it has a comparatively flatter characteristics with a smaller efficiency drop from best efficiency point (BEP) for a wide range of flows. A finite element analysis for stress evaluation of both SD- and RDCRRPT were done using ANSYS Workbench with Stainless Steel as material, showing that the stresses are well within the material limits.

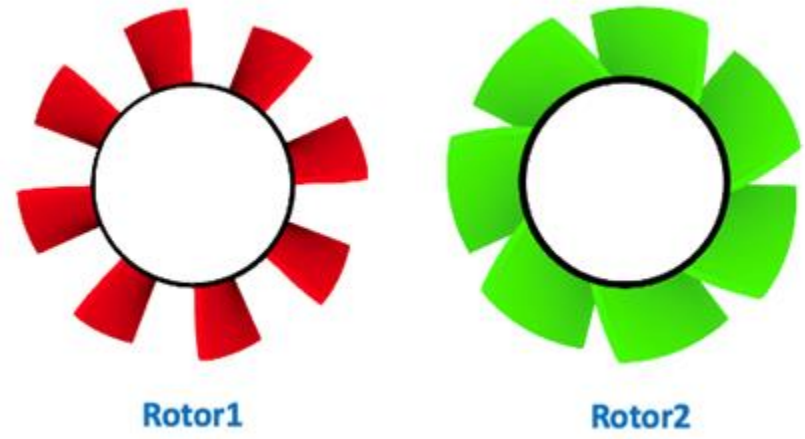


*Fig. 44 Geometry of initial SDCRRPT design*

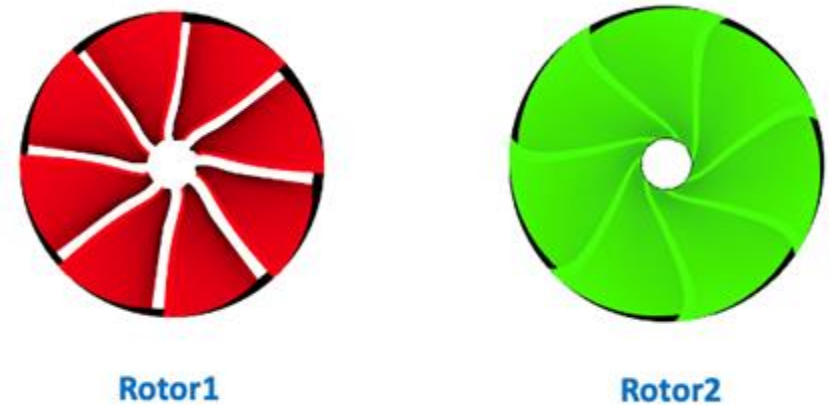


*Fig. 45 Geometry of initial RDCRRPT design*

Laboratory testing of a model scale SDCRRPT is to be performed at TU Braunschweig to validate the CFD results. Standard scaling laws were used to scale down the initial prototype to model scale. An optimization to maximize the efficiency was performed at the model scale for both SD- and RDCRRPT; optimized SDCRRPT will be used for the testing. The optimization process of the SDCRRPT consisted of an initial sensitivity study to identify important design parameters. Then a design matrix was generated using the Design of Experiments (DoE) method. For each design in the design matrix, CFD simulations were performed at multiple operating points in both pump and turbine mode and performance data was obtained. This data was used for a surrogate model based approximation followed by an optimization using Multi-objective Genetic Algorithm (Bonaiuti and Zanganeh, 2009). For the RDCRRPT, the design was improved based on several manual design iterations. For both configurations, the optimizations produced better performing designs. A scaled-up version of the optimized design will be used for further studies such as system level operation performance and cost analysis including the reservoir, fish friendliness analysis, mechanical design and behavior analysis, mode switching dynamics etc. The final design optimization in prototype scale will include additional parameters to meet the system level requirements.

## 8.2 Fish friendliness study

For the fish friendliness study, the BioPA developed by Pacific Northwest National Laboratory (PNNL) (USA) was used. BioPA enables users to evaluate potential impact to fish based on the CFD models of the hydraulic conditions of a turbine design (see dedicated subsections of "BioPA - Biological Performance Assessment Tool" for general approaches and technical details). Various turbine designs can be ranked based on the BioPA score, a proxy of fish friendliness.

BioPA versions allow the use of CFD models with different fidelities; higher fidelity models produce more accurate results but require higher computational resources. In the current study BioPA version 2.1 and BioPA version 3.0 are used for the fish friendliness assessment. BioPA 2.1 was initially used since it uses a low fidelity steady state single phase CFD analysis, which is cheaper and faster. BioPA 2.1 uses the steamtrace statistics from CFD solution for evaluating the BioPA scores. This version needs a third party application (i.e. Tecplot360) for computing the streamtrace statistics from the CFD solution. For establishing the BioPA workflow, the initial SDCRRPT design was chosen; an operating point in the turbine mode with a volume flow rate of 143 $m^3$ $s^{-1}$ and an output power of 10 MW at the design speed, as indicated by red marker in the power vs. volume flow rate plot, is used (Fig. 46).

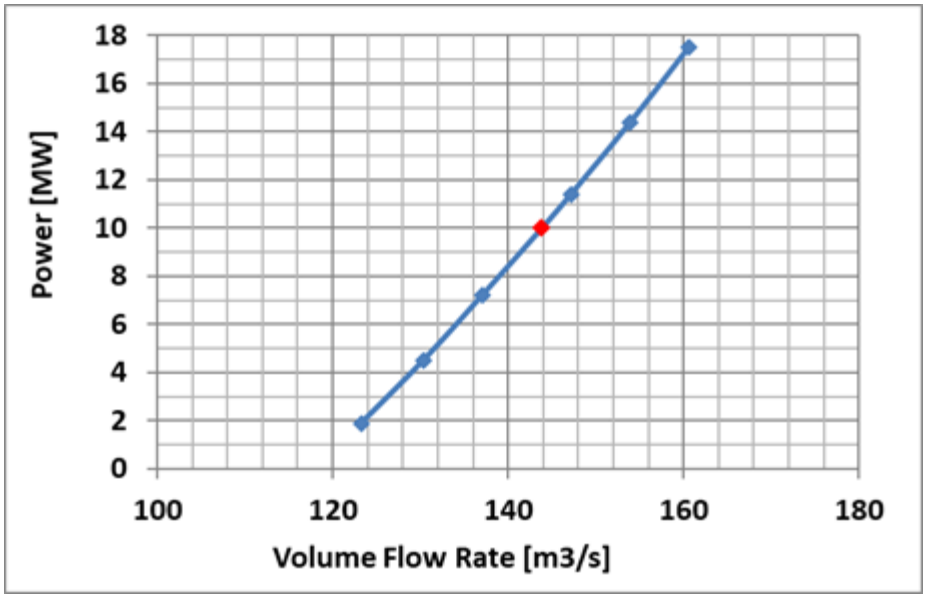


*Fig. 46 SDCRRPT initial design turbine mode power vs flow rate plot*

### 8.2.1 CFD setup for BioPA v.2.1

CFD simulations were performed using Ansys CFX software. Steady state full wheel simulations were performed; CFD domain as shown in Fig. 47 consisted of 2 stationary domains S2 and S1 and 2 rotating domains R2 and R1. Meshing was done using Ansys Turbogrid with hexahedral elements, total mesh size was ~7 million elements. K-omega SST turbulence model used and a y+ < 30 was ensured on the blade surfaces. Mass flow rate at inlet, static pressure at outlet and no slip wall was used as the boundary conditions. Incompressible flow Reynolds Averaged Navier Stokes (RANS) solver was used. All of the above settings as well as the orientation of the rotors comply with BioPA v.2.1 CFD modeling guide (BioPA User Manual, Version 2.1). A single point CFD solution took less than 4 hours to attain convergence. Results were converted to ".cgns" format for use in Tecplot360.

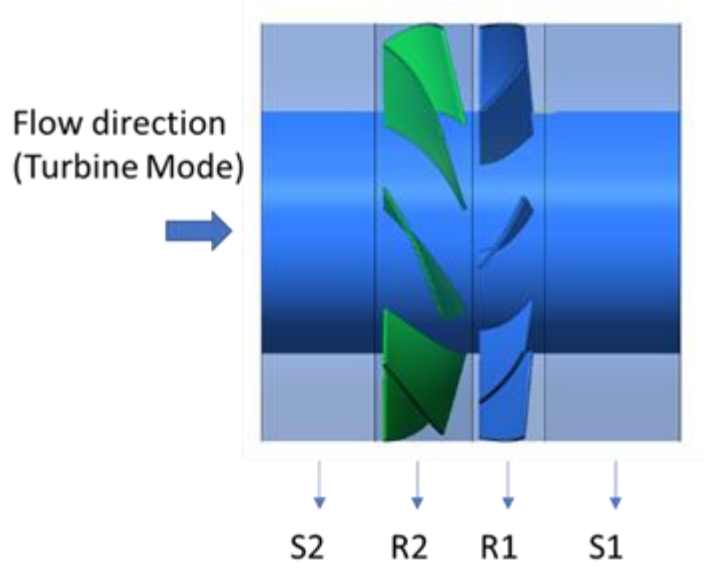


*Fig. 47 SDCRRPT CFD analysis domain*

Multiple problems were encountered during the execution of Tecplot360 and BioPA v2.1, which could not be solved as the tool has become obsolete. It was hence decided to proceed with BioPA v.3 for further studies.

### 8.2.2 CFD setup for BioPA v.3

BioPA v.3 requires a discrete particle CFD modeling approach for obtaining the data required for the fish friendliness assessment. The main advantage of BioPA v.3 over the previous version is the better prediction of collision events of particles with solid structures of the turbine although volitional collision avoidance behavior of the fish is not captured (Romero-Gomez and Richmond, 2014). Since blade striking is more probable for a contra-rotating turbine, BioPA v.3 is preferred over v.2.1. Two discrete particle modeling approaches can be used, namely Lagrangian or a Discrete Element Method (DEM). Lagrangian modeling is based on a center of mass collision, while DEM is based on a surface-to-surface collision. DEM is a higher fidelity method which also resolves the surface contact force during collision but, on

the downside, it requires considerably higher computational costs. Hence, the Lagrangian approach was followed in the current study.

The Lagrangian multiphase unsteady RANS CFD analysis with moving reference frame (MRF) approach was performed using Siemens Star CCM+ software. CFD domain, as shown in Fig. 47, consisted of 2 stationary domains S2 and S1 and 2 rotating domains R2 and R1. Meshing was performed in Star CCM+ with polyhedral elements and prism layers close to the walls, total mesh size was ~8 million elements. K-omega SST turbulence model used and a y+ < 30 was ensured on most of the blade surfaces. A timestep of 0.01 s corresponding to less than < 3° rotation of the blade was chosen. Velocity at inlet, static pressure at outlet and no slip wall was used as the boundary conditions. All of the above settings as well as the orientation of the rotors comply with BioPA v.3 CFD modeling guide (BioPA User Manual, Version 3.0). A single point CFD solution with 12 s of physical simulated time took ~16 hours to complete; this can vary depending on the total physical time simulated.

Initially a steady CFD simulation was conducted to achieve the steady state condition; this solution served as the initial condition for the following unsteady simulation with particle injection. Particles were injected from a specified injector plane, injection locations/cells on the plane are randomly assigned by the software based on a specified point inclusion probability parameter. Fourteen particles were injected at a 0.1 s-interval for a total of 10 s amounting to a total sample size of 1400 particles. Particles were modeled as neutrally buoyant spheres (i.e. with a specific gravity of 1). Particle diameters were calculated based on the fish mass, as per the modeling proposed by Romero-Gomez and Richmond (2014). From the CFD simulation, particle trajectory data and collision data were exported for use in BioPA v.3. Track data was calculated based on the following momentum equation:

$$Mparticle\ \frac{dUparticle}{dt} = Fd + Fp + Fg + Fvm$$

where Mparticle is the mass of the particle, Uparticle is the velocity, Fd is the drag force, Fp is the force due to pressure gradients, Fg is the gravity force and Fvm is the virtual mass force (Romero-Gomez and Richmond, 2014). More details regarding formulation in Star CCM+ can be referred from the BioPA user manual. Boundary sampling technique helps to obtain the collision data of the particle from the simulation. A sample plot record of collision events is shown in Fig. 48. Fig. 49 shows the particle movement through the turbine. Based on the particle trajectory data and collision data, BioPA v.3 can evaluate the fish friendliness score.

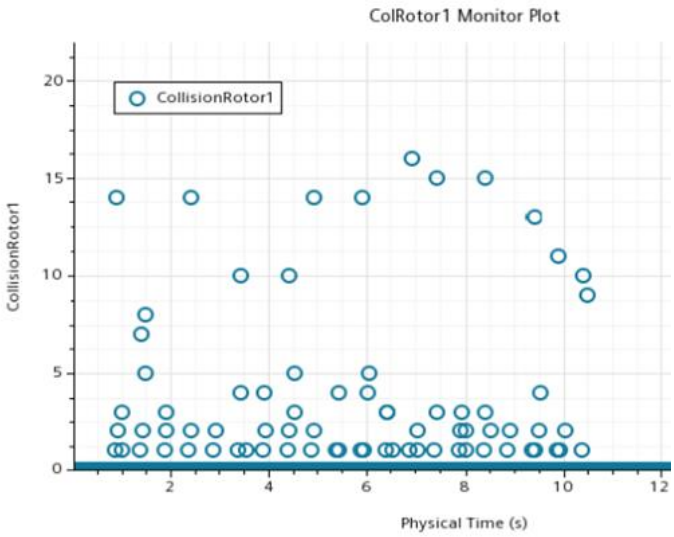


*Fig. 48 A sample collision plot*

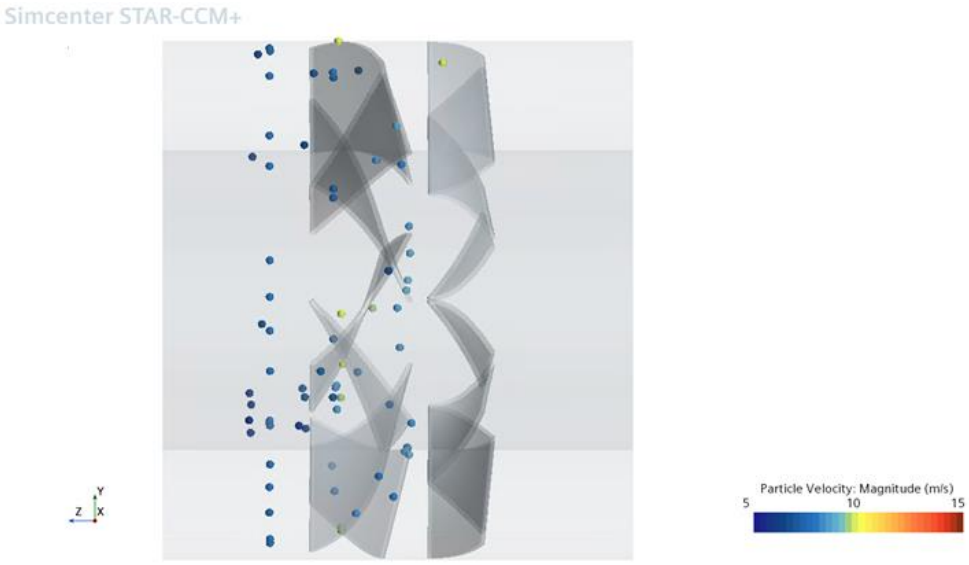


*Fig. 49 A sample picture of particle movement through the turbine*

Fish friendliness analysis is conducted and comparisons are made for 2 different designs, 2 different operating conditions and for 2 different fish species. The different fish species considered are Atlantic salmon *Salmo salar* with a BL of 150 mm and European eel *Anguilla anguilla* with a BL of 300 mm. As per the modelling equation in Romero-Gomez and Richmond (2014), the particle diameters are calculated to be 0.053 m and 0.086 m for salmon and eel, respectively. The two configurations chosen are the initial SDCRRPT design, called Prototype 0, and a scaled version of the optimized design, called Prototype 1. Both of these designs are simulated in CFD for an operating condition in turbine mode at a full load power output of approximately 10 MW. For this power output, Prototype 0 operates at rotational speed of 45 rev $min^{-1}$ for rotor R2 and -50 rev $min^{-1}$ for rotor R1 at a flow rate of 143 $m^3 s^{-1}$. Prototype 1

operates at rotational speed of 34.6 rev $min^{-1}$ for R2 and -46 rev $min^{-1}$ for R1 at 138 $m^3$ $s^{-1}$ flow rate. Besides this, another simulation is conducted for Prototype 0 at the same operating speeds but at a flow rate of 130 $m^3$ $s^{-1}$ at a part load power output of approximately 5 MW. The BioPA v.3 fish friendliness performance was compared for the contrasts below and will be presented in the subsequent section:

- Prototype 0 vs Prototype 1 at 10 MW (comparing 2 designs at full load power output), for salmon and eel;
- Prototype 0 – 10 MW vs 5 MW (comparing 2 operating conditions – full load vs part load for same design), for salmon and eel

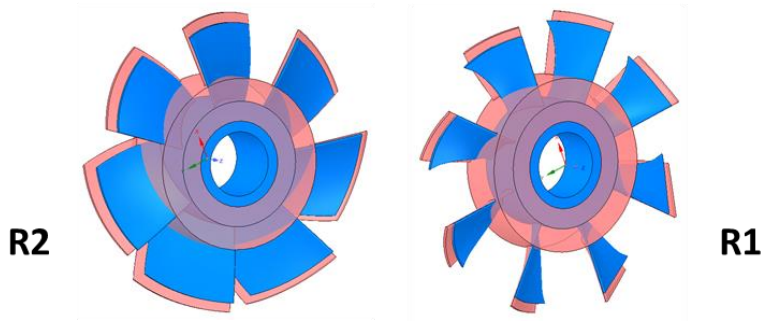


*Fig. 50 SDCRRTP – Prototype 0 (Orange) vs Prototype 1 (Blue)*

Eel and salmon, which are the two target species of the present deliverable, were selected for the BioPA-based fish friendliness analysis based on conservation importance and different susceptibility to stressors. Both species were analyzed for susceptibility to rapid decompression, shear and collision, while only *S. salar* was analyzed for susceptibility to turbulence because no biological model is available for the European eel or its surrogate species. No biological response models are so far available for *S. salar* and *European eel*, hence the ones developed for Chinook or Rainbow trout and American eel were used for the former and the latter, respectively, based on surrogacy. Turbulence was not examined for eel because no surrogate biological response model was developed for it. No depth weighting was applied for this analysis of Prototype 0 and 1 for each particle track. Blade thickness of 60 mm was input for collision models. For this preliminary analysis, the most severe endpoint of mortality was selected for all stressors response models, except for the estimation of the effects of rapid decompression on *S. salar*: in this case, the biological response model predicting the probability of mortal injury (i.e. injuries highly associated with and likely to predict mortality) was used (Table 9).

*Table 9 Summary of the biological response models employed for estimating adverse effects per target species, with indication of the surrogate species for which the models were developed, when appropriate*

| Stressor | Adverse effect | Ref. | Species | Surrogate species |
|---|---|---|---|---|
| **Rapid Decompression** | Mortal injury | Brown et al. (2012a) | *Salmo salar* | Chinook salmon |
| | Mortality | Pflugrath et al. (2021b) | *Anguilla anguilla* | American eel |
| **Fluid Shear** | Mortality | Nietzel et al. (2004) | *Salmo salar* | Fall Chinook salmon |
| | Mortality | Pflugrath et al. (2021b) | *Anguilla anguilla* | American eel |
| **Collision** | Mortality | EPRI (2011) | *Salmo salar* | Rainbow Trout |
| | Mortality | Not publicly available | *Anguilla anguilla* | American eel |
| **Turbulence** | Mortality | Odeh et al. (2002) | *Salmo salar* | NA |

The probability of exposure (Pe) is calculated from the statistics file data for each stressor. The distribution data for each stressor is a calculation of the probability of response (Pm) at the various stressor magnitudes. The probability of adverse passage is then calculated by multiplying the probability of exposure by the probability of response for the full range of stressor magnitudes based on the chosen response model (i.e. Pe*Pm) (see section 7.2 - Technical specifications). The cumulative sum of adverse passage is a prediction of the overall likelihood that a fish will exhibit the selected response when exposed to the stressor. The probability of adverse passage in terms of above-mentioned endpoints was calculated for each stressor for the two selected species and the two operating conditions: 5 MW and 10 MW for Prototype 0 (rotors R1 and R2), and 10 MW for Prototype 1 (rotor R1 and R2). An example of the BioPA worksheet set up for calculating the probability of adverse passage through P1 R1 at the 10 MW operating condition of salmon, with corresponding exposure and extent of biological response, is shown in Fig. 51.

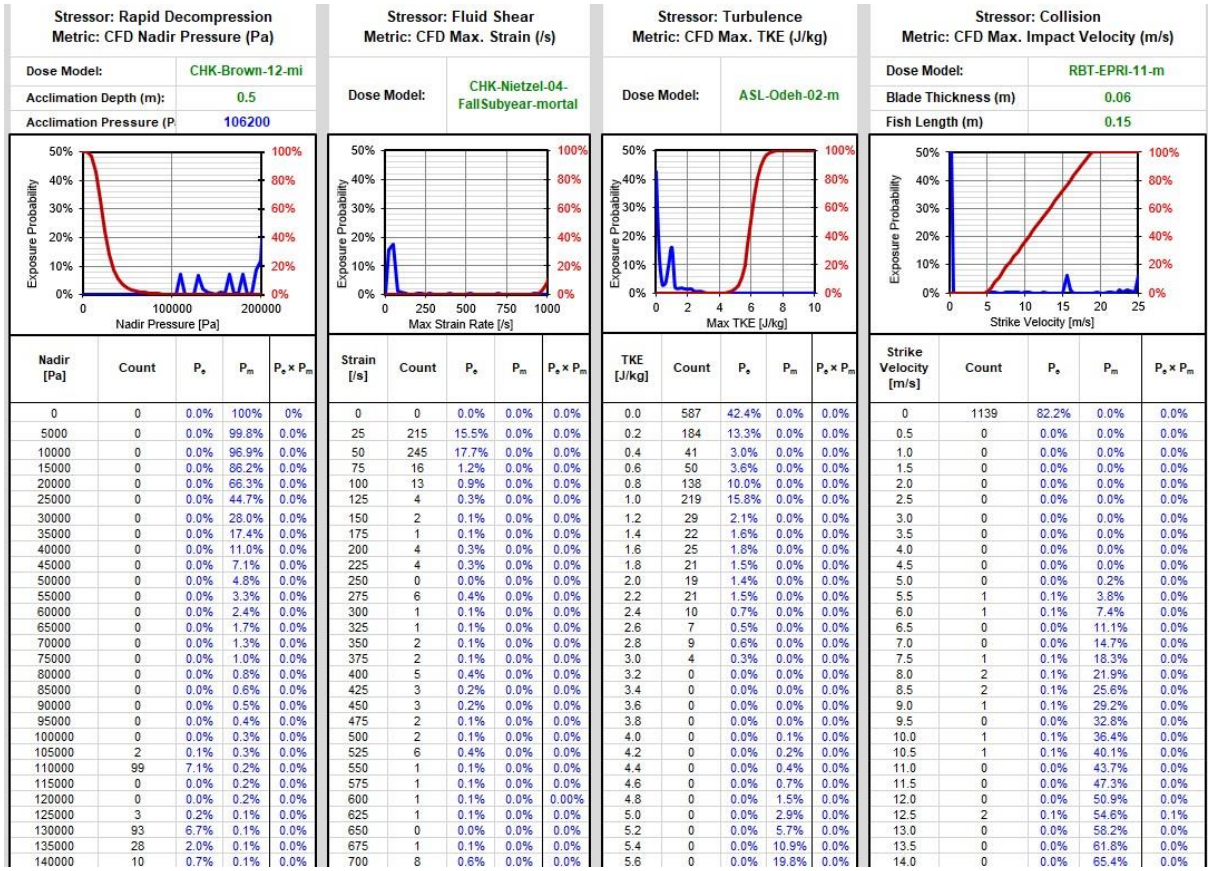


| Nadir [Pa] | Count | $P_e$ | $P_m$ | $P_e \times P_m$ |
|---|---|---|---|---|
| 0 | 0 | 0.0% | 100% | 0% |
| 5000 | 0 | 0.0% | 99.8% | 0.0% |
| 10000 | 0 | 0.0% | 96.9% | 0.0% |
| 15000 | 0 | 0.0% | 86.2% | 0.0% |
| 20000 | 0 | 0.0% | 66.3% | 0.0% |
| 25000 | 0 | 0.0% | 44.7% | 0.0% |
| 30000 | 0 | 0.0% | 28.0% | 0.0% |
| 35000 | 0 | 0.0% | 17.4% | 0.0% |
| 40000 | 0 | 0.0% | 11.0% | 0.0% |
| 45000 | 0 | 0.0% | 7.1% | 0.0% |
| 50000 | 0 | 0.0% | 4.8% | 0.0% |
| 55000 | 0 | 0.0% | 3.3% | 0.0% |
| 60000 | 0 | 0.0% | 2.4% | 0.0% |
| 65000 | 0 | 0.0% | 1.7% | 0.0% |
| 70000 | 0 | 0.0% | 1.3% | 0.0% |
| 75000 | 0 | 0.0% | 1.0% | 0.0% |
| 80000 | 0 | 0.0% | 0.8% | 0.0% |
| 85000 | 0 | 0.0% | 0.6% | 0.0% |
| 90000 | 0 | 0.0% | 0.5% | 0.0% |
| 95000 | 0 | 0.0% | 0.4% | 0.0% |
| 100000 | 0 | 0.0% | 0.3% | 0.0% |
| 105000 | 2 | 0.1% | 0.3% | 0.0% |
| 110000 | 99 | 7.1% | 0.2% | 0.0% |
| 115000 | 0 | 0.0% | 0.2% | 0.0% |
| 120000 | 0 | 0.0% | 0.2% | 0.0% |
| 125000 | 3 | 0.2% | 0.1% | 0.0% |
| 130000 | 93 | 6.7% | 0.1% | 0.0% |
| 135000 | 28 | 2.0% | 0.1% | 0.0% |
| 140000 | 10 | 0.7% | 0.1% | 0.0% |

| Strain [/s] | Count | $P_e$ | $P_m$ | $P_e \times P_m$ |
|---|---|---|---|---|
| 0 | 0 | 0.0% | 0.0% | 0.0% |
| 25 | 215 | 15.5% | 0.0% | 0.0% |
| 50 | 245 | 17.7% | 0.0% | 0.0% |
| 75 | 16 | 1.2% | 0.0% | 0.0% |
| 100 | 13 | 0.9% | 0.0% | 0.0% |
| 125 | 4 | 0.3% | 0.0% | 0.0% |
| 150 | 2 | 0.1% | 0.0% | 0.0% |
| 175 | 1 | 0.1% | 0.0% | 0.0% |
| 200 | 4 | 0.3% | 0.0% | 0.0% |
| 225 | 4 | 0.3% | 0.0% | 0.0% |
| 250 | 0 | 0.0% | 0.0% | 0.0% |
| 275 | 6 | 0.4% | 0.0% | 0.0% |
| 300 | 1 | 0.1% | 0.0% | 0.0% |
| 325 | 1 | 0.1% | 0.0% | 0.0% |
| 350 | 2 | 0.1% | 0.0% | 0.0% |
| 375 | 2 | 0.1% | 0.0% | 0.0% |
| 400 | 5 | 0.4% | 0.0% | 0.0% |
| 425 | 3 | 0.2% | 0.0% | 0.0% |
| 450 | 3 | 0.2% | 0.0% | 0.0% |
| 475 | 2 | 0.1% | 0.0% | 0.0% |
| 500 | 2 | 0.1% | 0.0% | 0.0% |
| 525 | 6 | 0.4% | 0.0% | 0.0% |
| 550 | 1 | 0.1% | 0.0% | 0.0% |
| 575 | 1 | 0.1% | 0.0% | 0.0% |
| 600 | 1 | 0.1% | 0.0% | 0.00% |
| 625 | 1 | 0.1% | 0.0% | 0.0% |
| 650 | 0 | 0.0% | 0.0% | 0.0% |
| 675 | 1 | 0.1% | 0.0% | 0.0% |
| 700 | 8 | 0.6% | 0.0% | 0.0% |

| TKE [J/kg] | Count | $P_e$ | $P_m$ | $P_e \times P_m$ |
|---|---|---|---|---|
| 0.0 | 587 | 42.4% | 0.0% | 0.0% |
| 0.2 | 184 | 13.3% | 0.0% | 0.0% |
| 0.4 | 41 | 3.0% | 0.0% | 0.0% |
| 0.6 | 50 | 3.6% | 0.0% | 0.0% |
| 0.8 | 138 | 10.0% | 0.0% | 0.0% |
| 1.0 | 219 | 15.8% | 0.0% | 0.0% |
| 1.2 | 29 | 2.1% | 0.0% | 0.0% |
| 1.4 | 22 | 1.6% | 0.0% | 0.0% |
| 1.6 | 25 | 1.8% | 0.0% | 0.0% |
| 1.8 | 21 | 1.5% | 0.0% | 0.0% |
| 2.0 | 19 | 1.4% | 0.0% | 0.0% |
| 2.2 | 21 | 1.5% | 0.0% | 0.0% |
| 2.4 | 10 | 0.7% | 0.0% | 0.0% |
| 2.6 | 7 | 0.5% | 0.0% | 0.0% |
| 2.8 | 9 | 0.6% | 0.0% | 0.0% |
| 3.0 | 4 | 0.3% | 0.0% | 0.0% |
| 3.2 | 0 | 0.0% | 0.0% | 0.0% |
| 3.4 | 0 | 0.0% | 0.0% | 0.0% |
| 3.6 | 0 | 0.0% | 0.0% | 0.0% |
| 3.8 | 0 | 0.0% | 0.0% | 0.0% |
| 4.0 | 0 | 0.0% | 0.1% | 0.0% |
| 4.2 | 0 | 0.0% | 0.2% | 0.0% |
| 4.4 | 0 | 0.0% | 0.4% | 0.0% |
| 4.6 | 0 | 0.0% | 0.7% | 0.0% |
| 4.8 | 0 | 0.0% | 1.5% | 0.0% |
| 5.0 | 0 | 0.0% | 2.9% | 0.0% |
| 5.2 | 0 | 0.0% | 5.7% | 0.0% |
| 5.4 | 0 | 0.0% | 10.9% | 0.0% |
| 5.6 | 0 | 0.0% | 19.8% | 0.0% |

| Strike Velocity [m/s] | Count | $P_e$ | $P_m$ | $P_e \times P_m$ |
|---|---|---|---|---|
| 0 | 1139 | 82.2% | 0.0% | 0.0% |
| 0.5 | 0 | 0.0% | 0.0% | 0.0% |
| 1.0 | 0 | 0.0% | 0.0% | 0.0% |
| 1.5 | 0 | 0.0% | 0.0% | 0.0% |
| 2.0 | 0 | 0.0% | 0.0% | 0.0% |
| 2.5 | 0 | 0.0% | 0.0% | 0.0% |
| 3.0 | 0 | 0.0% | 0.0% | 0.0% |
| 3.5 | 0 | 0.0% | 0.0% | 0.0% |
| 4.0 | 0 | 0.0% | 0.0% | 0.0% |
| 4.5 | 0 | 0.0% | 0.0% | 0.0% |
| 5.0 | 0 | 0.0% | 0.2% | 0.0% |
| 5.5 | 1 | 0.1% | 3.8% | 0.0% |
| 6.0 | 1 | 0.1% | 7.4% | 0.0% |
| 6.5 | 0 | 0.0% | 11.1% | 0.0% |
| 7.0 | 0 | 0.0% | 14.7% | 0.0% |
| 7.5 | 1 | 0.1% | 18.3% | 0.0% |
| 8.0 | 2 | 0.1% | 21.9% | 0.0% |
| 8.5 | 2 | 0.1% | 25.6% | 0.0% |
| 9.0 | 1 | 0.1% | 29.2% | 0.0% |
| 9.5 | 0 | 0.0% | 32.8% | 0.0% |
| 10.0 | 1 | 0.1% | 36.4% | 0.0% |
| 10.5 | 1 | 0.1% | 40.1% | 0.0% |
| 11.0 | 0 | 0.0% | 43.7% | 0.0% |
| 11.5 | 0 | 0.0% | 47.3% | 0.0% |
| 12.0 | 0 | 0.0% | 50.9% | 0.0% |
| 12.5 | 2 | 0.1% | 54.6% | 0.1% |
| 13.0 | 0 | 0.0% | 58.2% | 0.0% |
| 13.5 | 0 | 0.0% | 61.8% | 0.0% |
| 14.0 | 0 | 0.0% | 65.4% | 0.0% |

*Fig. 51 An example of the BioPA worksheet set up for calculating the probability of adverse passage through P1 R1 at the 10 MW operating condition of salmon*

Rapid decompression was the least impacting stressor, regardless of the species considered. Both rotors in all operating conditions produced high values of Nadir pressure, which were related to minimum risk of mortality and injuries.

Turbulence was not a particular concern for salmon: Pe values ranged from 0 to 3 J $Kg^{-1}$ for both Prototypes and were related to 0% mortality likelihood according to the selected response model.

The stressor raising the greatest concern was shear, at least for one species: mortal injury rates in the simulated passage of salmon ranged from 42.82 to 56.32%, while damages for eel were negligible.

The collision stressor showed a different extent depending on the species, the operating conditions and the rotors. For salmon, the 10 MW operating condition had different probability of adverse passage for R1 and R2 (i.e. 8.13% and 4.93% for P0 and 15.54 for P1 R1). The probability of adverse passage for the 5 MW operating condition was much higher for R1 (i.e. 19.39%). Eel appeared to be little exposed to this stressor in the 10 MW operating condition (i.e. 3.04% – 4.73%), while collision exposure was higher for R1 than R2 (i.e. 5.71% vs. 0.0%) within the 5 MW operating condition. Prototype 1 R1 displayed higher probabilities

of adverse passage for many stressors than the same rotor for Prototype 0 for both species. Results are reported in Table 10 and Table 11.

*Table 10 Probability of adverse passage for Anguilla anguilla*

| **Mechanism** | **P0 R1 10 MW** | **P0 R2 10 MW** | **P0 R1 5 MW** | **P0 R2 5 MW** | **P1 R1 10 MW** | **P1 R2 10 MW** |
|---|---|---|---|---|---|---|
| Rapid decompression | 0.00% | 0.00% | 0.00 | 0.00% | 0.00% | 0.00% |
| Fluid Shear | 0.00% | 0.00% | 0.00 | 0.00% | 0.00% | 0.00% |
| Collision | 4.73% | 3.04% | 5.71% | 0.00% | 8.34% | 0.00% |

*Table 11 Probability of adverse passage for Salmo salar*

| **Mechanism** | **P0 R1 10 MW** | **P0 R2 10 MW** | **P0 R1 5 MW** | **P0 R2 5 MW** | **P1 R1 10 MW** | **P1 R2 10 MW** |
|---|---|---|---|---|---|---|
| Rapid decompression | 0.10% | 0.00% | 0.00% | 0.00% | 0.00% | 0.00% |
| Fluid Shear | 47.01% | 42.82% | 49.97% | 42.74% | 56.32% | 35.69% |
| Collision | 8.13% | 4.93% | 19.39% | 0.00% | 15.54% | 0.12% |
| Turbulence | 0.01% | 0.00% | 0.00% | 0.00% | 0.00% | 0.00% |

Because it is uncertain how exposure to multiple stressors during passage through a hydropower facility will actually affect a fish susceptibility, a performance score is given by the BioPA toolset. This PQI (Passage Quality Index) score is a relative value that allows the comparison between various operating conditions of the hydropower plant. The PQI is based on a scale of 0 to 500 with a higher score representing a better biological performance.

The decompression and shear PQIs for eels had the highest values of 500 in all simulated runs. The PQI values for collisions ranged from 458 to 500, with rotor R2 always resulting more fish friendly than the corresponding rotor R1 within the same operating condition (478 - 485 for P0 - 10 MW, 458 - 500 for P1 - 10 MW and 471 - 500 for P0 - 05 MW) (Fig. 52).

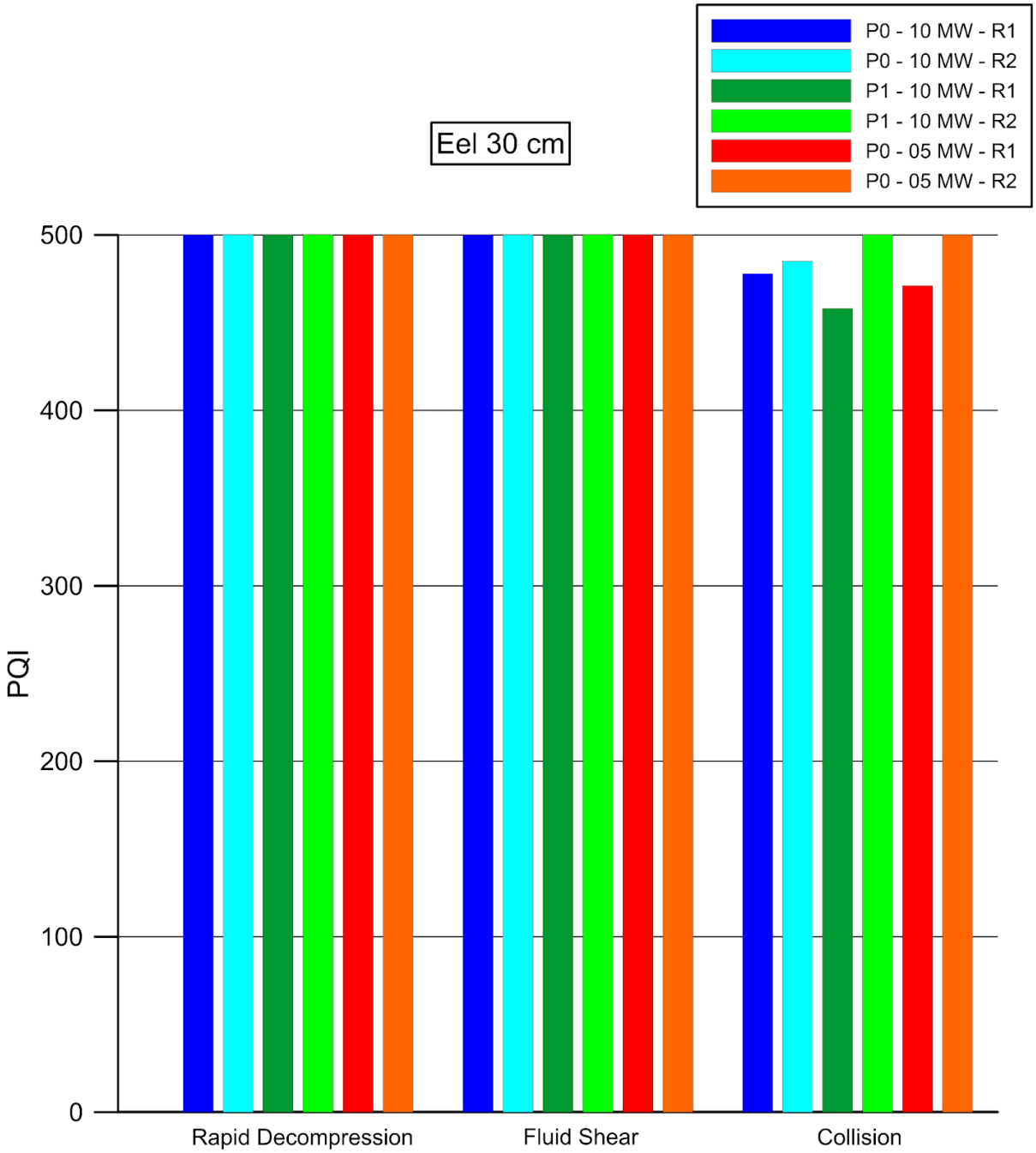


*Fig. 52 Anguilla anguilla PQIs for SDCRRPT prototype designs and rotor types per damage mechanism*

In all simulated configurations, maximum decompression and turbulence PQIs were returned for salmon. As in the case of eel, the greater fish friendliness of rotor R2 compared to rotor R1 was confirmed. The lowest PQI values (i.e. greatest expected biological impact) were related to shear exposure: while PQIs of the P0 runs either at the full or part load power outputs of 10 MW or 5 MW were similar (i.e. 265 vs. 286) and 5 MW (250 - 286), the difference between PQI values resulting from R1 and R2 simulations of P1 was much more pronounced (i.e. 218 - 322). Very large ranges of PQI values were also shown in collisions. For rotor R2, they ranged from 475 (P0 - 10 MW) to 500 (P1 - 10 MW and P0 - 5 MW); for rotor R1, the lowest values were found for P1 - 10 MW with 422 and for P0 - 05 MW with 403 (Fig. 53).

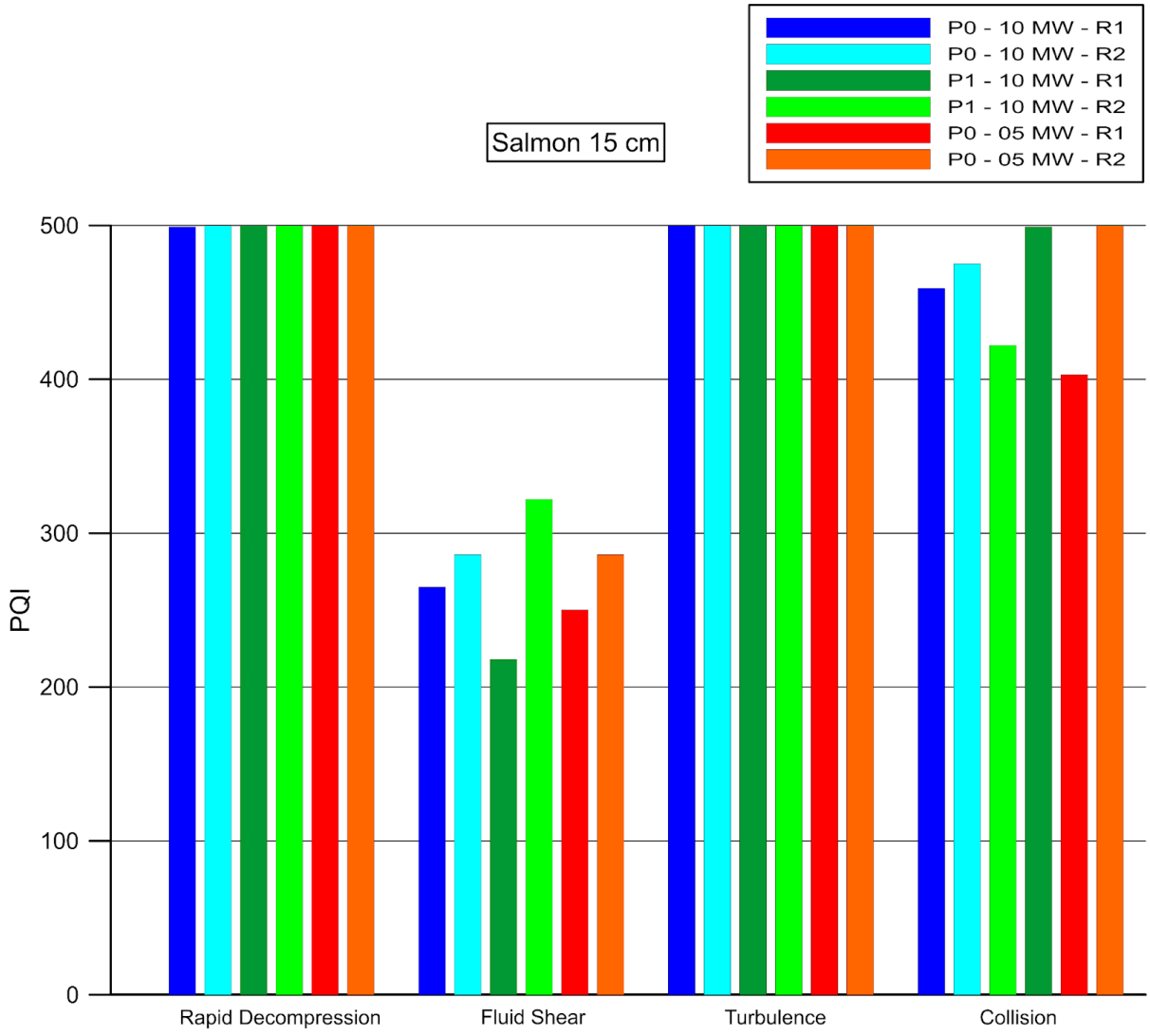


*Fig. 53 Salmo salar PQIs for SDCRRPT prototype designs and rotor types per damage mechanism*

Overall, the cumulative PQIs for salmon and eel (Fig. 54) followed a similar trend to those of the individual damage mechanisms, confirming the higher fish friendliness of rotor R2 than rotor R1 in all simulations. Rotor R2 of the scaled version of the SDCRRPT optimized prototype design (i.e. P1) at full load power output of approximately 10 MW is associated with the greatest fish friendliness scores. Similar PQIs were obtained following the simulated passage through rotor R2 of the initial SDCRRPT design (i.e. P0) operating at a part load power output of 5 MW. The difference between the two rotors is more evident in the case of salmon, especially in the configuration P1 - 10 MW (i.e. 413 - 447) and for prototype 0 in the 5 MW condition (410 - 455). For eel, no marked differences were reported among operating conditions, prototypes or rotors, and the PQIs were always very high, ranging from 486 to 500.

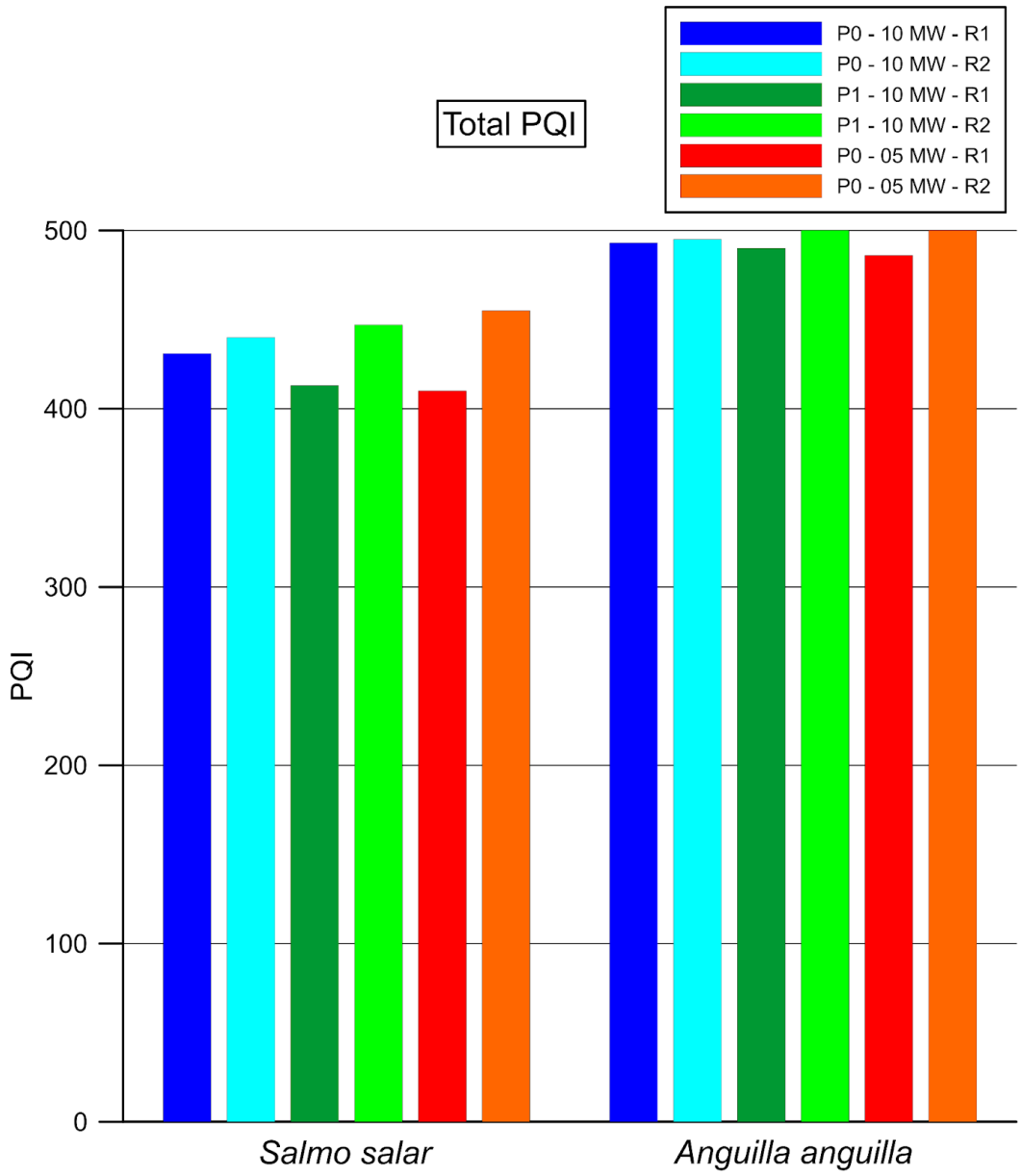


*Fig. 54 Passage Quality Indexes per target species, operating condition and rotor*

# 9 References

Aarestrup, K. and Koed, A. (2003). Survival of migrating sea trout (*Salmo trutta*) and Atlantic salmon (*Salmo salar*) smolts negotiating weirs in small Danish rivers. Ecology of Freshwater Fish, 12, 169– 176. https:// doi.org/10.1034/j.1600- 0633.2003.00027.x.

Abernethy, C.S. (2002): Simulated Passage through a Modified Kaplan Turbine Pressure Regime: A Supplement to "Laboratory Studies of the Effects of Pressure and Dissolved Gas Supersaturation on Turbine-Passed Fish, Pacific Northwest National Laboratory.

Abernethy, C.S., Amidan, B.G., Čada, G.F. (2001). Laboratory Studies of the Effects of Pressure and Dissolved Gas Supersaturation on Turbine-Passed Fish. U.S. Department of Energy, PNNL-13470. https://doi.org/10.2172/782074.

Abernethy, C.S., Amidan,, B.G. and Čada, G.F. (2003). Fish Passage Through a Simulated Horizontal Bulb Turbine Pressure Regime: A Supplement to" Laboratory Studies of the Effects of Pressure and Dissolved Gas Supersaturation on Turbine-Passed Fish". No. PNNL-13470-B. Pacific Northwest National Lab.(PNNL), Richland, WA (United States).

Acou, A. (1999). L'anguille européenne (*Anguilla anguilla* L. 1758): dynamique et déterminisme de la migration catadrome dans un bassin versant anthropisé de Bretagne (Frémur). Thèse de l'Université de Rennes 1.

Adam, B. and Brujis, M. (2006). General requirements of fish protection and downstream migration facilities: investigations on the river Meuse system. Free Passage for Aquatic Fauna in Rivers and Other Water Bodies, 70.

Ahlgren, G., Nieuwerburgh, L., Wänstrand, I., Pedersén, M., Boberg, M. & Snoeijs, P. (2005). Imbalance of fatty acids in the base of the Baltic Sea food web: a mesocosm study. Canadian Journal of Fisheries and Aquatic Sciences 62: 2240–2253. https://doi.org/10.1139/f05-140.

Albayrak, I., Kriewitz, C.R., Hager, W.H., and Boes, R.M. (2018). An experimental investigation on louvres and angled bar racks. Journal of Hydraulic Research, 56(1), 59-75. https://doi.org/10.1080/00221686.2017.1289265.

Amara R., Selleslagh J., Billon G., Minier C. (2009). Growth and condition of 0-group European flounder, *Platichthys flesus* as indicator of estuarine habitat quality. Hydrobiologia 627:87-98. DOI : 10.1007/s10750-009-9717-9.

Amaral, S., Coleman, B., Rackovan, J., Withers, K., Mater, B. (2018). Survival of fish passing downstream at a small hydropower facility. Mar Freshwater Res. 69(12): 1870–1881. https://doi.org/10.1071/MF18123.

Amaral, S., Perkins, N., Giza, D., McMahon, B. (2011). Evaluation of Fish Injury and Mortality Associated with Hydrokinetic Turbines (Report No. 1024569). Report by Alden Research Laboratory. Report for Electric Power Research Institute (EPRI).

Amaral, S.V., Watson, S.M., Schneider, A.D., Rackovan, J. and Baumgartner, A. (2020). Improving survival : injury and mortality of fish struck by blades with slanted, blunt leading edges. Journal of Ecohydraulics. https://doi.org/10.1080/24705357.2020.1768166.

Amaral, S.V., Winchell, F.C., McMahon, B.J. and Dixon, D.A. (2003). Evaluation of angled bar racks and louvers for guiding silver phase American eels. Conference Proceedings, American Fisheries Society Symposium (pp. 367-376). American Fisheries Society

Aoyama, J. and Miller, M.J. (2003). The Silver Eel. In Eel Biology, eds. Aida, K., Tsukamoto, K., Yamauchi, K. Springer Japan, Tokyo. doi:10.1007/978-4-431-65907-5.

AquaMaps (2019). Computer generated distribution maps for *Anguilla anguilla* (European eel), with modelled year 2050 native range map based on IPCC RCP8.5 emissions scenario. Retrieved from https://www.aquamaps.org.

Ball, I., Hendricks, D., Jawaid, T.S., Rutz, D., Steller, J. (2020). Small hydropower technologies - European state-of-the-art innovations. HYPOSO report, ISBN 978-3-936338-75-1.

Becker, J.M., Abernethy, C.S. and Dauble, D.D. (2003). Identifying the effects on fish of changes in water pressure during turbine passage. Hydro review (HCL PUBLICATIONS) 22 (2003): 32-42.

Beckerman, A., Benton, T.G., Ranta, E., Kaitala, V. and Lundberg, P. (2002). Population dynamic consequences of delayed life-history effects. Trends in Ecology and Evolution 17:263–269. https://doi.org/10.1016/S0169-5347(02)02469-2.

Beirão, B., Pflugrath, B.D., Harnish, R.A., Harding, S.F., Richmond, M.C. and Colotelo, A.H. (2021). Empirical Investigation into the Applicability of Surrogacy for Juvenile Salmonids (*Oncorhynchus* spp.) Exposed to Hydropower Induced Rapid Decompression. Ecological Indicators, 121. https://doi.org/10.1016/j.ecolind.2020.107090.

Bell, M.C., DeLacy, A.C. and Copp, H.D. (1972). A compendium on the survival of fish passing through spillways and conduits. Report prepared for U. S. Army Corps of Engineers, Portland, OR.

Belpaire, C., Hodson, P., Pierron, F., Freese, M. (2019). Impact of chemical pollution on Atlantic eels: Facts, research needs, and implications for management. Curr. Opin. Environ. Sci. Heal. doi:10.1016/j.coesh.2019.06.008.

Ben Ammar, I., Cornet, V., Houndji, A., Baekelandt, S., Antipine, S., Sonny, D., Mandiki, S.N.M., Kestemont, P. (2021). Impact of downstream passage through hydropower plants on the physiological and health status of a critically endangered species: The European eel *Anguilla anguilla*. Comp Biochem Physiol A Mol Integr Physiol. Apr;254:110876. doi: 10.1016/j.cbpa.2020.110876.

Bevelhimer, M.S., Pracheil, B.M., Fortner, A.M. and Deck, K.L. (2017). An Overview of Experimental Efforts to Understand the Mechanisms of Fish Injury and Mortality Caused by Hydropower Turbine Blade Strike. United States. doi:10.2172/1425338.

Bevelhimer, M.S., Pracheil, B.M., Fortner, A.M., Saylor, R. and Deck, K.L. (2019). Mortality and Injury Assessment for Three Species of Fish Exposed to Simulated Turbine Blade Strike. Canadian Journal of Fisheries and Aquatic Sciences. https://doi.org/10.1139/cjfas-2018-0386.

Bigelow, H.B. (1963). Fishes of the Western North Atlantic. Sears Foundation for Marine Research, Denmark.

Biological Performance Assessment (BioPA) User Manual, Version 2.1

Biological Performance Assessment (BioPA) User Manual, Version 3.0

Boes, R.M., Albayrak, I., Kriewitz, C.R., and Peter, A. (2016). Fish protection and downstream fish migration by means of guidance systems with vertical bars: Head loss and bypass efficiency. Wasserwirtschaft, 106(7-8), 29-35.

Boeuf, G. (1993). Salmonid smolting: a pre-adaptation to the oceanic environment. In Rankin, J.C. and Jensen, F.B. (eds.) Fish Ecophysiology, 421 pp. Springer, ISBN: 978-0-412-45920-7.

Bonaiuti, D. and Zangeneh, M. (2009). On the Coupling of Inverse Design and Optimization Techniques for the Multiobjective, Multipoint Design of Turbomachinery Blades. Journal of Turbomachinery, vol. 131, no. 2. https://doi.org/10.1115/1.2950065.

Bonaiuti, D., Zangeneh, M., Aartojarvi, R. and Eriksson, J. (2010). Parametric Design of a Waterjet Pump by Means of Inverse Design, CFD Calculations and Experimental Analyses. Journal of Fluids Engineering. https://doi.org/10.1115/1.4001005.

Boubée, J.A.T. and Williams, E.K. (2006). Downstream passage of silver eels at a small hydroelectric facility. Fisheries Management and Ecology, 13(3), 165-176. https://doi.org/10.1111/j.1365-2400.2006.00489.x.

Boys, C., Baumgartner, L., Miller, B., Deng, Z., Brown, R., & Pflugrath, B. (2013). Protecting downstream migrating fish at mini hydropower and other river infrastructure. Fisheries Final Report Series No. 137. NSW Department of Primary Industries, Port Stephens Fisheries Institute. NSW Department of Primary Industries.

Boys, C., Navarro, A., Robinson, W., Fowler, A., Chilcott, S., Miller, B., Pflugrath, B., Baumgartner, L., McPherson, J., Brown, R., Deng, Z. (2014). Downstream fish passage criteria for hydropower and irrigation infrastructure in the Murray–Darling Basin. Fisheries Final Report Series No. 141. ISSN 1837-2112

Boys, C.A., Robinson, W., Miller, B., Pflugrath, B. D., Baumgartner, L., Navarro, A., Brown, R. S. & Deng, Z. D. (2016). How low can they go when going with the flow? Tolerance of egg and larval fishes to rapid decompression. Biology Open, bio. 017491. https://doi.org/10.1242/bio.017491.

Bozhinova, S., Hecht, V., Kisliakov, D., Müller, G., and Schneider, S. (2013). Hydropower Converters with Head Differences below 2·5M. Proc. Inst. Civil Eng. - Energ. 166 (3), 107–119. doi:10.1680/ener.11.00037.

Bracken, F.S.A., and Lucas, M. (2013). Potential impacts of small-scale hydroelectric generation on downstream moving Lampreys. River Research and Applications 29:1073–1081. https://doi.org/10.1002/rra.2596.

Brown, R.S., Carlson, T.J., Gingerich, A.J., Stephenson, J.R., Pflugrath, B.D., Welch, A.E., Langeslay, M.J., Ahmann, M.L., Johnson, R.L., Skalski, J.R. (2012a). Quantifying mortal injury of juvenile Chinook salmon exposed to simulated hydro-turbine passage. Trans Am Fish Soc 141: 147–157. https://doi.org/10.1080/00028487.2011.650274.

Brown, R.S., Carlson, T.J., Welch, A.E., Stephenson, J.R., Abernethy, C.S., McKinstry, C.A., and Theriault, M.H. (2007). Assessment of Barotrauma Resulting from Rapid Decompression of Depth Acclimated Juvenile Chinook Salmon Bearing Radio Telemetry Transmitters. United States. https://doi.org/10.2172/914683.

Brown, R.S., Colotelo, A.H., Pflugrath, B.D., Boys, C.A., Baumgartner, L.J., Deng, Z.D., Silva, L.G.M., Brauner, C.J., Mallen-Cooper, M., Phonekhampeng, O., Thorncraft, G., Singhanouvong, D. (2014). Understanding Barotrauma in Fish Passing Hydro Structures: A Global Strategy for Sustainable Development of Water Resources. Fisheries 39, 108–122. doi:10.1080/03632415.2014.883570.

Brown, R.S., Cook, K.V., Pflugrath, B.D., Rozeboom, L.L., Johnson, R.C., Mclellan, J.G., Linley, T.J., Gao, Y., Baumgartner, L.J., Dowell, F.E., Miller, E.A. and White, T.A. (2013). Vulnerability of larval and juvenile white sturgeon to barotrauma: can they handle the pressure? Conservation Physiology, 1, 1-9. DOI: 10.1093/conphys/cot019.

Brown, R.S., Pflugrath, B.D., Colotelo, A.H., Brauner, C.J., Carlson, T.J., Deng, Z.D. and Seaburg, A.G. (2012b). Pathways of barotrauma in juvenile salmonids exposed to simulated hydrotrubine passage: Boyle's law vs Henry's law. Fisheries Research, 121-122, 43-50. doi:10.1016/j.fishres.2012.01.006.

Brown, R.S., Walker, R.W. and Stephenson, J.R. (2015). A Preliminary Assessment of Barotrauma Injuries and Acclimation Studies for Three Fish Species. No. PNNL-24720. Pacific Northwest National Lab (PNNL), Richland, WA (United States).

Bruijs, M.C.M. and Durif, C.M.F. (2009). Silver Eel Migration and Behaviour. In: van den Thillart G., Dufour S., Rankin J.C. (eds) Spawning Migration of the European Eel. Fish & Fisheries Series, vol 30. Springer, Dordrecht. https://doi.org/10.1007/978-1-4020-9095-0_4.

Bunn, S.E., and Arthington, A.H. (2002). Basic principles and ecological consequences of altered flow regimes for aquatic biodiversity. Environmental Management 30:492–507. https://doi.org/10.1007/s00267-002-2737-0.

Čada, G., Loar, J., Garrison, L., Fisher, R., Neitzel, D. (2006). Efforts to reduce mortality to hydroelectric turbine-passed fish: Locating and quantifying damaging shear stresses. Environ. Manage. 37, 898–906. doi:10.1007/s00267-005-0061-1.

Čada, G.F. (2001). The Development of Advanced Hydroelectric Turbines to Improve Fish Passage Survival. Fisheries 26, 14–23. doi:10.1577/1548-8446(2001)026<0014:TDOAHT>2.0.CO,2

Cada, G.F., Amaral, S. (2011). Determining the Best Methods for Reducing Fish Mortality. https://www.hydroreview.com/world-regions/determining-the-best-methods-for-reducing/#gref.

Cada, G.F., Coutant, C.C., Whitney, R.R. (1997). Development of Biological Criteria for the Design of Advanced Hydropower Turbines. https://doi.org/10.2172/1218126.

Calles, O., Karlsson, S., Vezza, P., Comoglio, C. and Tielman, J. (2013). Success of a low-sloping rack for improving downstream passage of silver eels at a hydroelectric plant. Freshwater Biology, 58(10), 2168-2179. https://doi.org/10.1111/fwb.12199.

Calles, O., Olsson, I.C., Comoglio, C., Kemp, P.S., Blunden, L., Schmitz, M., Greenberg, L.A. (2010). Size-dependent mortality of migratory silver eels at a hydropower plant, and implications for escapement to the sea. Freshw. Biol. 55, 2167–2180. doi:10.1111/j.1365-2427.2010.02459.x.

Carlson, T.J., Duncan, J.P., Deng, Z. (2008). Data Overview for Sensor Fish Samples Acquired at Ice Harbor, John Day, and Bonneville II Dams in 2005, 2006, and 2007, PNNL-17398. Pacific Northwest National Laboratory, Richland, WA.

Chaput, G. (2012). Overview of the status of Atlantic salmon (*Salmo salar*) in the North Atlantic and trends in marine mortality. ICES J. Mar. Sci. 69, 1538–1548. doi:10.1093/icesjms/fss013.

CITES, 2021. https://cites.org/eng/app/appendices.php

CMS, 2020. https://www.cms.int/en/species/appendix-i-ii-cms

Coad, B.W. (1995). Freshwater fishes of Iran. Acta Sci. Nat. Acad. Sci. Brno. 29:1-64.

Colotelo, A.H., Pflugrath, B.D., Brown, R.S., Brauner, C.J., Mueller, R.P., Carlson, T.J., et al. (2012). The effect of rapid and sustained decompression on barotrauma in juvenile brook lamprey and Pacific lamprey: implications for passage at hydroelectric facilities. Fisheries Research, 129, 17-20. https://doi.org/10.1016/j.fishres.2012.06.001.

Cook, T.C., Hecker, G.E., Amaral, S.V., Stacy, P.S., Lin, F. and Taft, E.P. (2003). Pilot Scale Tests Alden/Concepts NREC Turbine. United States: N. p., 2003. Web. doi:10.2172/816298.

Costa, J.E. (1987). Hydraulics and basin morphometry of the largest flash floods in the conterminous United States. Journal of hydrology, 93, 313-338. https://doi.org/10.1016/0022-1694(87)90102-8.

Council of Europe, (1979). Convention on the Conservation of European Wildlife and Natural Habitats (ETS No. 104). https://www.coe.int/en/web/conventions/full-list?module=treaty-detail&treatynum=104.

Cresci A. (2020). A comprehensive hypothesis on the migration of European glass eels (*Anguilla anguilla*). Biol. Rev. 95:1273-1286. https://doi.org/10.1111/brv.12609.

Cresci, A., Durif, C.M., Paris, C.B., Shema, S.D., Skiftesvik, A.B., Browman, H.I. (2019). Glass eels (*Anguilla anguilla*) imprint the magnetic direction of tidal currents from their juvenile estuaries. Commun. Biol. 2, 366. doi:10.1038/s42003-019-0619-8.

Crozier, W.W., Potter, E.C.E., Prevost, E., Schon, P.J., and Maoiléidigh, N.Ó. (2003). A coordinated approach towards develop- ment of a scientific basis for management of wild Atlantic salmon in the North-East Atlantic (SALMODEL). An EU Concerted Action—Quality of Life and Management of Living Resources Key Action 5: sustainable agriculture, fisheries and forestry, and integrated development of rural areas including mountain areas. EU Contract No. QLK5-CT1999-01546. 431 pp.

Cutler, J.S., Olivos, J.A., Sidlauskas, B., Arismendi, I. (2020). Habitat loss due to dam development may affect the distribution of marine-associated fishes in Gabon, Africa. Ecosphere 11. doi:10.1002/ecs2.3024.

Debes, P.V. et al. (2019). Large single-locus effects for maturation timing are mediated via body condition in Atlantic salmon. bioRxiv. https://doi.org/10.1101/780437.

Dekker W (2016). Management of the eel is slipping through our hands! Distribute control and orchestrate national protection. ICES J. Mar. Sci. 73:2442-2452. https://doi.org/10.1093/icesjms/fsw094.

Dekker W., Casselman J.M. (2014). The 2003 Québec Declaration of concern about eel declines - 11 years later: are eels climbing back up the slippery slope? Fisheries 39:613-614. https://doi.org/10.1080/03632415.2014.979342.

Delpech C., Courrat A., Pasquaud S., Lobry J., Le Pape O., Nicolas D., Boët P., Girardin M., Lepage M. (2010). Development of a fish-based index to assess the ecological quality of transitional waters: the case of French estuaries. Mar. Pollut. Bull. 60:908-918. https://doi.org/10.1016/j.marpolbul.2010.01.001.

Deng, Z., Carlson, T.J., Ploskey, G.R., Richmond, M.C., and Dauble, D.D. (2007). Evaluation of blade-strike models for estimating the biological performance of Kaplan turbines. Ecological Modelling, 208(2-4), 165-176. https://doi.org/10.1016/j.ecolmodel.2007.05.019.

Deng, Z., Guensch, G.R., Mckinstry, C.A., Mueller, R.P., Dauble, D.D. and Richmond, M.C. 2005. Evaluation of fish-injury mechanisms during exposure to turbulent shear flow. Canadian Journal of Fisheries and Aquatic Sciences, 62, 1513-1522. https://doi.org/10.1139/f05-091.

Dixon, D., and Hogan, T. (2015). Session B3: Alden Fish-Friendly Hydropower Turbine: History and Development Status. In; International Conference on Engineering and Ecohydrology for Fish Passage, Groningen, Netherlands, 22–24 June

DOE (U.S. Department of Energy) (2009). Report to Congress on the Potential Environmental Effects of Marine and Hydrokinetic Energy Technologies. U.S. Department of Energy, Office of Energy Efficiency & Renewable Energy, Wind and Hydropower Technologies Program, DOE/GO-102009-2955.

Drouineau H., Durif C., Castonguay M., Mateo M., Rochard E., Verreault G., Yokouchi K., Lambert P., (2018a). Freshwater eels: a symbol of the effects of global change. Fish Fish. 19:903-930. https://doi.org/10.1111/faf.12300.

Drouineau, H., Carter, C., Rambonilaza, M., Beaufaron, G., Bouleau, G., Gassiat, A., Lambert, P., le Floch, S., Tétard, S., de Oliveira, E. (2018b). River continuity restoration and diadromous fishes: much more than an ecological issue. Environ. Man- age. 61:671-686. DOI: 10.1007/s00267-017-0992-3.

Duston, J., Saunders, R.L. (1999). Effect of winter food deprivation on growth and sexual maturity of Atlantic salmon (*Salmo salar*) in seawater. Canadian J FishAquat Sci 56:201–207. https://doi.org/10.1139/f98-165.

DWA (2005). Fish Protection Technologies and Downstream Fishways. Dimensioning, Design, Effectiveness Inspection. Available at http://www.dwa.de/dwa/shop/products_english.nsf/78C724A3CEDDD0D0C12575510033FB9B/$file/vorschau_DWA-Topics_Fish_Protection_Technologies.pdf.

Ebel, G. (2013). Fischschutz Und Fischabstieg an Wasserkraftanlagen. Handbuch Rechen-Und Bypasssysteme. Bd 4.

Eicher, G.J. (1987). Turbine-related fish mortality: review and evaluation of studies. Final report. [Contains glossary]. United States: N. p., 1987. https://www.osti.gov/biblio/5565651-turbine-related-fish-mortality-review-evaluation-studies-final-report-contains-glossary.

EIFAC/ICES (2006). Report of the 2006 Session of the Joint EIFAC/ICES Working Group on Eels, Rome, 23-27 January 2006. ICES CM 2006/ACFM:16. 352 p.

EPRI (2011). Fish Passage Through Turbines: Application of Conventional Hydropower Data to Hydrokinetic Technologies (Report No. 1024638). Report by Electric Power Research Institute (EPRI).

EPRI (1992). Fish entrainment and turbine mortality review and guidelines. Final Report TR-101231, Project 2694-01.

EPRI (2008). Evaluation of the effects of turbine blade leading edge design on fish survival. Electric Power Research Institute. Report No.: 1014937. Prepared by Alden Research Laboratory Inc, Palo Alto, CA, USA.

EPRI (2011b). EPRI. 2011. 2010 tests examining survival of fish struck by turbine blades. Electric Power Research Institute. Report No.: 1024684. Prepared by Alden Research Laboratory Inc., Palo Alto, CA, USA

European Commission (1992). Council Directive 92/43/EEC of 21 May 1992 on the conservation of natural habitats and of wild fauna and flora. https://eur-lex.europa.eu/legal-content/EN/TXT/?uri=CELEX:31992L0043.

European Commission (2008). Directive 2008/56/EC of the European Parliament and of the Council of 17 June 2008 establishing a framework for community action in the field of marine environmental policy (Marine Strategy Framework Directive) (Text with EEA

relevance). https://eur-lex.europa.eu/legal-content/EN/TXT/?uri=CELEX:32008L0056. General information: https://ec.europa.eu/environment/marine/good-environmental-status/index_en.htm.

FAO (2007). Report of the second FAO Ad Hoc Expert Advisory Panel for the Assessment of Proposals to Amend Appendices I and II of CITES Concerning Commercially exploited Aquatic Species. Rome, 26–30 March 2007. FAO Fisheries Report. No. 833. Rome: 133 pp.

Ferguson, J.W. (2005). The behavior and ecology of downstream migrating Atlantic Salmon (*Salmo salar* L.) and Brown Trout (*Salmo trutta* L.) in regulated rivers in northern Sweden. Vattenbruksinstitutionen, Sveriges lantbruksuniversitet.

Ferguson, J.W., Absolon, R.F., Carlson, T.J. and Sandford, B.P. (2006). Evidence of delayed mortality on juvenile Pacific salmon passing through turbines at Columbia River dams. Transactions of the American Fisheries Society 135(1), 139-150. https://doi.org/10.1577/T05-080.1.

Feunteun, E. (2002). Management and restoration of the European eel population (*Anguilla anguilla*): An impossible bargain? Ecol. Eng. 18:575-591. DOI: 10.1016/S0925-8574(02)00021-6.

Finstad, A.G., Jonsson, B. (2012). Effect of incubation temperature on growth performance in Atlantic salmon. Mar Ecol Progress Ser 454:75–82. https://doi.org/10.3354/meps09643.

Fishtek Consulting (2007). Fish monitoring and live fish trials. Ritz Atro Archimedes Screw Turbine, River Dart. Phase 1 report: live fish trials, smolts, leading edge assessment, disorientation study, outflow monitoring. Prepared for Mann Power Consulting Ltd., York, U.K.

Fishtek Consulting (2008). Archimedes screw turbine fisheries assessment. Phase II: eels and kelts. Prepared for Mann Power Consulting, York, U.K.

FIThydro DSS, 2022, website: https://www.dss.fithydro.wb.bgu.tum.de/home/ui.

Fjelldal, P.G., Hansen, T., Huang, T.-S. (2011). Continuous light and elevated temperature can trigger maturation both during and immediately after smoltification in male Atlantic salmon (*Salmo salar*). Aquaculture 321:93–100. https://doi. org/10.1016/j.aquaculture.2011.08.017.

Forseth, T., Barlaup, B.T., Finstad, B., Fiske, P., Gjøsæter, H., Falkegård, M., Hindar, A., Mo, T.A., Rikardsen, A.H., Thorstad, E.B., Vøllestad, L.A., Wennevik, V. (2017). The major threats to Atlantic salmon in Norway. ICES J. Mar. Sci. 74, 1496–1513. doi:10.1093/icesjms/fsx020.

Franke, G., Webb, D., Fisher, R., Mathur, D., Hopping, P., March, P., Hedrick, M., Laczo, I., Ventikos, Y. and Sotiropoulious, F. (1997). Development of environmentally advanced hydroturbine system concepts. Report prepared for the Department of Energy under Contract DE-AC07-96ID13382.

Fricke, H., Kaese, R. (1995). Tracking of artificially matured eels (*Anguilla anguilla*) in the Sargasso Sea and the problem of the eel's spawning site. Naturwissenschaften 82, 32–36. https://doi.org/10.1007/BF01167868.

Froese, R. and Pauly D. (2005). FishBase. World Wide Web electronic publication. www.fishbase.org

Fu, T., Deng, Z.D., Duncan, J.P., Zhou, D., Carlson, T.J., Johnson, G.E. and Hou, H. (2016). Assessing hydraulic conditions through Francis turbines using an autonomous sensor device. Renewable Energy Elsevier Ltd 99: 1244–1252. https://doi.org/10.1016/j.renene.2016.08.029.

Geiger, F. (2018). Fish Mortality Rate During Turbine Passage – Generalized Runner Blade Strike Probability Modelling. 12th International Symposium on Ecohydraulics. Tokyo, Japan, 2018.

Gowans, A.R.D., Armstrong, J.D., Priede, I.G., and Mckelvey, S. (2003). Movements of Atlantic salmon migrating upstream through a fish-pass complex in Scotland. Ecology of Freshwater Fish, 12(3), 177-189. https://doi.org/10.1034/j.1600-0633.2003.00018.x.

Hamor, T., and Garside, E.T. (1976). Developmental rates of embryos of Atlantic salmon, *Salmo salar* L., in response to various levels of temperature, dissolved oxygen, and water exchange. Canadian Journal of Zoology 54.11: 1912-1917. https://doi.org/10.1139/z76-221.

Haro, A. (2003). Downstream Migration of Silver-Phase Anguillid Eels. In Eel Biology, eds. Aida, K., Tsukamoto, K., Yamauchi, K. Springer Japan, Tokyo. doi:10.1007/978-4-431-65907-5.

Harvey, H.H. (1963). Pressure in the early life history of Sockeye Salmon. Doctoral Dissertation. PhD Doctoral Dissertation, University of British Columbia.

Hecker, G.E., and Allen, G.S. (2005). An Approach to Predicting Fish Survival for Advanced Technology Turbines. Hydro Review, November 2005, HCI Publications, Inc., St. Louis, Missouri.

Héland, M. and Dumas, J. (1994). Ecologie et comportement des juvéniles. In: Le saumon atlantique. Gueguen, J.C. and Prouzet, P., eds. IFREMER. https://hal.inrae.fr/hal-02846422.

Helfman, G.S., Collette, B.B., Facey, D.E., Bowen, B.W. (2009). The diversity of fishes: biology, evolution, and ecology, 2nd edition. ed. Wiley.

Hendry, A.P., Castric, V., Kinnison, M.T., Quinn, T.P. (2003). The evolution of philopatry and dispersal: homing versus straying in salmonids. In: Sterns SC (ed) Hendry AP. Salmon and Their Relatives. Oxford University Press, Evolution Illuminated, pp 53–91

Hindar, K. 2004. Wild Atlantic salmon in Europe: status and perspectives. In P. Gallaugher, and L. Wood, eds. The World Summit on Salmon, pp. 47–52. Simon Fraser University, Burnaby, BC (Canada).

Hoar, W.S. (1988). The physiology of smolting salmon. in Fish Physiology. Vol. lIB (eds W.S. Hoar and D.J. Randall). Academic Press. New York. pp. 275-343.

Hogan, T.W., Cada, G.F., Amaral, S. V. (2014). The Status of Environmentally Enhanced Hydropower Turbines. Fisheries 39, 164–172. doi:10.1080/03632415.2014.897195.

Hosfeld, C.D. et al. (2008). Long-term separate and combined effects of environmental hypercapnia and hyperoxia in Atlantic salmon (*Salmo salar* L.) smolts. Aquaculture 280:146–153. https://doi.org/10.1016/j.aquaculture.2008. 05.009.

Hou, H., Deng, Z., Martinez, J., Fu, T., Duncan, J., Johnson, G., Lu, J., Skalski, J., Townsend, R., & Tan, L. (2018). A Hydropower Biological Evaluation Toolset (HBET) for Characterizing Hydraulic Conditions and Impacts of Hydro-Structures on Fish. Energies, 11(4), 990. https://doi.org/10.3390/en11040990.

Hutchings, J.A. et al (2019). Life-history variability and conservation status of landlocked Atlantic salmon: an overview. Can J Fish Aquat Sci 76:1697–1708. https://doi.org/10.1139/cjfas-2018-0413.

ICES (2009). Report of the 2009 session of the Joint EIFAC/ICES Working Group on Eels. Göteborg, Sweden, from 7 to 12 September 2009. EIFAC Occasional Paper. No. 45. ICES CM 2009/ACOM:15. Rome, FAO/Copenhagen, ICES. 2010. 540p.

ICES (2011). Report of the Working Group on North Atlantic Salmon. ICES Document CM 2011/ACOM: 09. 286 pp.

ICES (2019). Joint EIFAAC/ICES Working Group on Eels (WGEEL). ICES Scientific Reports. 1:50. 177.

ICES (2019b). OSPAR request to advise on the current state of knowledge of studies into the deployment and environmental impacts of wet renewable technologies and marine energy storage systems. In Report of the ICES Advisory Committee, 2019, sr.2019.05.

ICES (2020). Report of the Joint EIFAAC/ICES/GFCM Working Group on Eels (WGEEL). ICES Scientific Reports. 2:85, 223 pp.

ICES (2021). North Atlantic salmon stocks In Report of the ICES Advisory Committee. ICES Advice 2021, sal.oth.nasco. https://doi.org/10.17895/ices.advice.8110.

Imsland, A.K., Handeland, S.O., Stefansson, S.O. (2014). Photoperiod and temperature effects on growth and maturation of pre- and post-smolt Atlantic salmon. Aquacult Int 22:1331–1345. https://doi.org/10.1007/s10499-014-9750- 1.

Jacobson, P., Amaral, S., Castro-Santos, T., Giza, D., Haro, A., Hecker, G., McMahon, B., Perkins, N., Pioppi, N. (2012). Environmental Effects of Hydrokinetic Turbines on Fish: Desktop and Laboratory Flume Studies. Report by Electric Power Research Institute (EPRI). https://doi.org/10.2172/1084623.

Jansen, H.M., Winter, H.V., Bruijs, M.C.M., Polman, H.J.G. (2007). Just go with the flow? Route selection and mortality during downstream migration of silver eels in relation to river discharge. ICES J. Mar. Sci. 64, 1437–1443. doi:10.1093/icesjms/fsm132.

Johnsen, B.O. and Jenser, A.J. (1991). The gyrodactylus story in Norway. Aquaculture, 98, 289– 302. https://doi.org/10.1016/0044-8486(91)90393-L.

Johnson, R. (1972). Fingerling fish research, high-velocity flow through four-inch nozzle.

Joint EIFAC/ICES Working Group on Eels (2001). Session, European Inland Fisheries Advisory Commission, & International Council for the Exploration of the Sea. Report of the Eleventh Session of the Joint EIFAC/ICES Working Group on Eels: Silkeborg, Denmark, 20-24 September 1999 (No. 34). Food and Agriculture Organization of the United Nations.

Jonsson, B., Jonsson, N. (2011). Ecology of Atlantic Salmon and Brown Trout: Habitat as a Template for Life Histories. Springer, London. https://doi.org/10.1007/978-94-007- 1189-1.

Jonsson, B., Jonsson, N. (2014). Early environment influences later performance in fishes. J Fish Biol 85:151–188. https://doi. org/10.1111/jfb.12432.

Jonsson, B., Jonsson, N. (2018). Egg incubation temperature affects the timing of the Atlantic salmon *Salmo salar* homing migration. J Fish Biol 93:1016–1020. https://doi.org/10. 1111/jfb.13817

Jonsson, B., Waples, R. S., and Friedland, K.D. (1999). Extinction considerations for diadromous fishes. ICES Journal of Marine Science, 56(4), 405-409. https://doi.org/10.1006/jmsc.1999.0483.

Julien, H.P., Bergeron, N.E. (2006). Effect of Fine Sediment Infiltration During the Incubation Period on Atlantic Salmon (*Salmo salar*) Embryo Survival. Hydrobiologia 563, 61. https://doi.org/10.1007/s10750-005-1035-2.

Kangur, M., T. Paaver and Drevs, T. (2003). Salmon, *Salmo salar* L. p. 91-97. In E. Ojaveer, E. Pihu and T. Saat (eds). Fishes of Estonia. Estonian Academy Publishers, Tallinn. 416 p.

Karlsson, S., Diserud, O.H., Fiske, P. and Hindar, K. (2016). Widespread genetic introgression of escaped farmed Atlantic salmon in wild salmon populations. ICES Journal of Marine Science, 73, 2488– 2498. https://doi.org/10.1093/icesj ms/fsw121.

Keenleyside, M.H.A., Yamamoto, F.T. (1962). Territorial behaviour of juvenile Atlantic salmon (*Salmo salar* L.) Behaviour 19:139–169. http://www.jstor.org/stable/4533008.

Kirkegaard, E., Aarestrup, K., Pedersen, M.I., Jepsen, N., Koed, A., Larsen, E., Lund, I., Tomkiewicz, J. (2010). European Eel and Aquaculture. DTU Aqua Rep. 19.

Knable, A.E. and Feathers, M.G. (1983). Device for examining the effects of pressure changes on fish. The Progressive Fish-Culturist, 45, 16-18.

Koskela, J., Pirhonen, J., Jobling, M. (1997). Effect of low temperature on feed intake, growth rate and body composition of juvenile Baltic salmon. Aquacult Int 5:479–488. https:// doi.org/10.1023/A:1018397014684.

Kottelat, M. and J. Freyhof (2007). Handbook of European freshwater fishes. Publications Kottelat, Cornol and Freyhof, Berlin. 646 pp.

Larinier, M. (2001). Environmental issues, dams and fish migration. FAO fisheries technical paper, 419, 45-89.

Larinier, M. (2008). Fish passage experience at small-scale hydro-electric power plants in France. Hydrobiologia, 609(1), 97-108.

Larinier, M. and Couret, D. (2008). Guide pour la conception de prises d'eau «ichtyocompatibles» pour les petites centrales hydroélectriques. RAPPORT GHAAPPE RA08, 4. Available at http://www.fleuve-charente.net/wp-content/uploads/2016/08/PM_Rapport-Prise-Eau-Ichtyocompatible-2008-11.pdf.

Larinier, M., and Travade, F. (1999). Downstream migration: problems and facilities. Bulletin Francais de la Peche et de la Pisciculture, 181-207. https://doi.org/10.1051/kmae/2002102.

Lin, F., Hecker, G.E. and Cook, T.C. (2004). Understanding Turbine Passage Survival Using CFD. Proceedings of Hydrovision 2004, HCI Publications, Inc., St. Louis, Missouri.

Lloret, J., Shulman, G., Love, R.M., (2014). Condition and Health Indicators of Exploited Marine Fishes. Wiley Blackwell. doi:10.1002/9781118752777.

Martinez, J.J., Deng, Z.D., Titzler, P.S., Duncan, J.P., Lu, J., Mueller, R.P., Tian, C., Trumbo, B.A., Ahmann, M.L., and Renholds, J.F. (2019). Hydraulic and biological characterization of a large Kaplan turbine. Renewable Energy 131: 240–249. https://doi.org/10.1016/j.renene.2018.07.034.

McCormick, S.D., Shrimpton, J.M., Moriyama, S., Björnsson, B.T. (2002). Effects of an advanced temperature cycle on smolt development and endocrinology indicate that temperature is not a zeitgeber for smolting in Atlantic salmon. J Exp Biol 205:3553–3560.

McCormick, S.D., Shrimpton, J.M., Moriyama, S., Björnsson, B.T. (2007). Differential hormonal responses of Atlantic salmon parr and smolt to increased daylength: A possible developmental basis for smolting. Aquaculture 273:337–344. https://doi.org/10.1016/j.aquaculture.2007.10.015.

McCosker, J.E. (1989). Freshwater eels (Family Anguillidae) in California: current conditions and future scenarios. Calif. Fish and Game. 75: 4-11.

Mcewen, D. and Scobie, G. (1992). Estimation of the hydraulic conditions relating to fish passage through turbines. NPC001. National Engineering Laboratory, East Kilbride, Glasgow.

Meng, L., Wang, W.P., Liao, C.L., Zhao, L. C., Li, T.Y., Zhang, H.P., and Ma, B.Q. (2019). Experimental evaluation of the effect of decompression on crucian carps injury during turbine passage. In IOP Conference Series: Earth and Environmental Science (Vol. 240, No. 4, p. 042008). IOP Publishing.

Metcalfe, N.B., Thorpe, J.E. (1992). Early predictors of life-history events: the link between first feeding date, dominance and seaward migration in Atlantic salmon *Salmo salar* L. J Fish Biol 41:93–99. https://doi.org/10.1111/j.1095-8649.1992. tb03871.x

Meusburger, H. (2002). Energieverluste an Einlaufrechen von Flusskraftwerken (Doctoral dissertation, ETH Zurich).

Miccoli, A., Manni, M., Picchietti, S., Scapigliati, G. (2021). State-of-the-Art Vaccine Research for Aquaculture Use : The Case of Three Economically Relevant Fish Species. Vaccines 9, 140. doi:10.3390/vaccines9020140.

Minkoff, D. (2019). Mechanisms and timing of olfactory and magnetic imprinting and homing in Atlantic salmon (*Salmo salar*). Boston University Theses & Dissertations, https://hdl.handle.net/2144/39568.

Mobley, K.B., Aykanat, T., Czorlich, Y. et al. (2021). Maturation in Atlantic salmon (*Salmo salar*, Salmonidae): a synthesis of ecological, genetic, and molecular processes. Rev Fish Biol Fisheries 31, 523–571. https://doi.org/10.1007/s11160-021-09656-w.

Montén, E. (1985). Fish and turbines: fish injuries during passage through power station turbines. Stockholm: Vattenfall.

Morgan, R.P., Ulanowicz, R.E., Rasin, V.J. Jr., Noe, L.A. and Gray, G.B. (1976). Effects of shear on eggs and larvae of striped bass, Morone saxatilis, and white perch, M. americana. Transactions of the American Fisheries Society. 105(1): 149-154. DOI: 10.1577/1548-8659(1976)105<149:EOSOEA>2.0.CO;2.

NASCO, 2019. State of North Atlantic Salmon. Available at: https://nasco.int/wp-content/uploads/2020/05/SoS-final-online.pdf.

Neitzel, D. a, Richmond, M.C., Dauble, D.D., Mueller, R.P., Moursund, R. a., Abernethy, C.S., Guensch, G.R., Cada, G.F. (2000). Laboratory Studies on the Effects of Shear on Fish - Final Report 2000 Prepared for the U.S. Department of Energy Idaho Operations Office under Contract DE-AC05-76RL01830.

Neitzel, D.A., Dauble, D.D., Čada, G.F., Richmond, M.C., Guensch, G.R., Mueller, R.P., Abernethy, C.S. and Amidan, B.G. (2004). Survival Estimates for Juvenile Fish Subjected to a Laboratory-Generated Shear Environment. Transactions of the American Fisheries Society, 133, 8. https://doi.org/10.1577/02-021.

Nielson, N.M., Brown, R.S., and Deng, Z.D. (2015). Review of Existing Knowledge of the Effectiveness and Economics of Fish-Friendly Turbines. Session II, Item 2: Fish Passage through Hydraulic Turbines. Vientiane, Laos PDR: Phnom Penh, Mekong River Commission. Technical Paper No. 57. Available at https://www.mrcmekong.org/assets/Publications/Events/Fish-n-Hydropower/062-Fish-Passage-through-Turbines.pdf.

Niemelä, E., et al. (2006). Temporal variation in abundance, return rate and life histories of previously spawned Atlantic salmon in a large subarctic river. Journal of Fish Biology 68.4: 1222-1240.

NOAA (2021). https://www.fisheries.noaa.gov/species/atlantic-salmon-protected#conservation-management

Normandeau Associates, Inc. (2009). An estimation of survival and injury of fish passed through the Hydro Green Energy hydrokinetic system, and a characterization of fish entrainment potential at the Mississippi lock and Dam no. 2 hydroelectric project (P-4306) Hastings, Minnesota.

Normandeau Associates, Inc., Skalski, J.R. and Mid Columbia Consulting, Inc. (1996). Fish survival investigation relative to turbine rehabilitation at Wanapum Dam, Columbia River, Washington. Report prepared for Grant County Public Utility District No. 2, Ephrata, Washington.

Odeh, M. (1999). A summary of environmentally friendly turbine design concepts, US Department of Energy, Idaho Operations Office. https://pubs.er.usgs.gov/publication/95318.

Odeh, M., Noreika, J.F., Haro, A., Maynard, A., Castro-Santos, T. and Cada, G.F. (2002). Evaluation of the effects of turbulence on the behavior of migratory fish. Prepared for: U.S. Department of Energy Bonneville Power Administration Division of Fish and Wildlife. Project Number 2000-057-00, Contract Number 00000022.

Oligny-Hébert, H., Senay, C., Enders, E.C., Boisclair, D. (2015). Effects of diel temperature fluctuation on the standard metabolic rate of juvenile Atlantic salmon (*Salmo salar*): influence of acclimation temperature and provenience. Canadian J Fish Aquat Sci, 72:1306–1315. https://doi.org/ 10.1139/cjfas-2014-0345.

Parrish, D.L., Behnke, R.J., Gephard, S.R., McCormick, S.D., and Reeves, G.H. (1998). Why aren't there more Atlantic salmon (*Salmo salar*)? Canadian Journal of Fisheries and Aquatic Sciences, 55(Suppl. 1): 281–287. https://doi.org/10.1139/d98-012.

Patrício, J., Teixeira, H., Borja, A., Elliott, M., Berg, T., Papadopoulou, N., Smith, C., Luisetti, T., Uusitalo, L., Wilson, C., Mazik, K., Niquil, N., Cochrane, S., Andersen, J.H., Boyes, S., Burdon, D., Carugati, L., Danovaro, R., Hoepffner, N. (2014). DEVOTES recommendations for the implementation of the Marine Strategy Framework Directive. Deliverable 1.5, 71 pp. DEVOTES project. JRC92131

Pedersen M.I., Rasmussen G.H. (2016). Yield per recruit from stocking two different sizes of eel (*Anguilla anguilla*) in the brackish Roskilde Fjord. ICES J. Mar. Sci. 73:158-164. https://doi.org/10.1093/icesjms/fsv167.

Peterson, R.H., Spinney, H.C.E., Sreedharan, A. (1977). Development of Atlantic salmon (*Salmo salar*) eggs and alevins under varied temperature regimes Journal of the Fisheries Research Board of Canada 34:31–43. https://doi.org/10. 1139/f77-004.

Pflugrath, B. (2017). Quantifying stressors and predicting injury and mortality in fish passing downstream through weirs and turbines, Ph.D Thesis, Civil & Environmental Engineering, Faculty of Engineering, UNSW

Pflugrath, B.D., Harnish, R., Rhode, B., Beirão, B., Engbrecht, K., Stephenson, J.R. and Colotelo, A.H. (2019). American eel state of buoyancy and barotrauma susceptibility associated with hydroturbine passage. Knowledge & Management of Aquatic Ecosystems, 20. https://doi.org/10.1051/kmae/2019012.

Pflugrath, B.D., Mueller, R.P., Engbrecht, K., Colotelo, A.H. (2021b). American eel resilience to simulated fluid shear associated with passage through hydroelectric turbines. Knowl. Manag. Aquat. Ecosyst. 2020-January. doi:10.1051/kmae/2021017.

Pflugrath, B.D., Saylor, R.K., Engbrecht, K., Mueller, R.P., Stephenson, J.R., Bevelhimer, M., Pracheli, B.M., Colotelo, A.H. (2021). Biological Response Models. Predicting Injury and Mortality of Fish During Downstream Passage through Hydropower Facilities. Hydropassage report prepared for the U.S. Department of Energy under Contract DE-AC05-76RL01830.

Pike, C., Crook, V. and Gollock, M. (2020). *Anguilla anguilla*. The IUCN Red List of Threatened Species 2020: e.T60344A152845178. https://dx.doi.org/10.2305/IUCN.UK.2020-2.RLTS.T60344A152845178.en.

Piper, A.T., Rosewarne, P.J., Wright, R.M., and Kemp, P.S. (2018). The Impact of an Archimedes Screw Hydropower Turbine on Fish Migration in a lowland River. Ecol. Eng. 118, 31–42. doi:10.1016/j.ecoleng.2018.04.009.

Piper, A.T., Wright, R.M., Walker, A.M., Kemp, P.S. (2013). Escapement, route choice, barrier passage and entrainment of seaward migrating European eel, *Anguilla anguilla*, within a highly regulated lowland river. Ecol. Eng. 57:88-96. DOI: 10.1016/j.ecoleng.2013.04.030.

Poff, N.L. and Schmidt, J.C. (2016). How dams can go with the flow. Science 353:1099–1100. DOI: 10.1126/science.aah4926.

Poppe, T.T., et al., "Swimbladder abnormality in farmed Atlantic salmon *Salmo salar*." Diseases of aquatic organisms 30.1 (1997): 73-76. doi:10.3354/dao030073.

Pracheil, B.M., Derolph, C.R., Schramm, M.P. and Bevelhimer, M.S. (2016a). A fish-eye view of riverine hydropower systems: the current understanding of the biological response to turbine passage. Reviews in Fish Biology and Fisheries, 26, 153-167. https://doi.org/10.1007/s11160-015-9416-8.

Quaranta, E., Pérez-Díaz, J.I., Romero–Gomez, P., Pistocchi, A. (2021). Environmentally Enhanced Turbines for Hydropower Plants: Current Technology and Future Perspective. Front. Energy Res. 9, 1–6. doi:10.3389/fenrg.2021.703106.

Rammler, A. (2017). Fish Friendly Designs by Andritz Hydro. Hydro Newsm, no 31/2017.

Raynal, S., Courret, D., Chatellier, L., Larinier, M., and David, L. (2013). An experimental study on fish-friendly trashracks–Part 1. Inclined trashracks. Journal of Hydraulic Research, 51(1), 56-66. https://hal.archives-ouvertes.fr/hal-00967468.

Reshetnikov, Y.S. (2003). Atlas of Russian Freshwater Fishes. Vols 1 & 2. Moscow, Nauka.

Richmond, M.C., Serkowski, J.A., Ebner, L.L., Sick, M., Brown, R.S., Carlson, T.J. (2014). Quantifying barotrauma risk to juvenile fish during hydro-turbine passage. Fish. Res. 154, 152–164. doi:10.1016/j.fishres.2014.01.007.

Rikardsen, A.H., Dempson, J.B. (2010). Dietary life-support: the food and feeding of Atlantic salmon at sea. In: Aas Ø, Einum S, Klemetsen A, Skurdal J (eds) Atlantic Salmon Ecology. Wiley-Blackwell, pp 115–143. https://doi.org/10. 1002/9781444327755.ch5.

Rochard, E. and Elie, P. (1994). La macrofaune aquatique de l'estuaire de la Gironde. Contribution au livre blanc de l'Agence de l'Eau Adour Garonne. p. 1-56. In J.-L. Mauvais and J.-F. Guillaud (eds.) État des connaissances sur l'estuaire de la Gironde. Agence de l'Eau Adour-Garonne, Éditions Bergeret, Bordeaux, France. 115 p.

Romero-Gomez, P. and Richmond, M.C. (2014). Simulating Blade-strike on Fish Passing Through Marine Hydrokinetic Turbines. Renewable Energy 71, 401-413. https://doi.org/10.1016/j.renene.2014.05.051.

Rowe, D.K., Thorpe, J.E. & Shanks, A.M. (1991). Role of fat stores in the maturation of male Atlantic salmon (*Salmo salar* L.) parr. Canadian Journal of Fisheries and Aquatic Sciences 48: 405–413. https://doi.org/10.1139/f91-052.

Sado, R.Y., de Souza, F.C., Behr, E.R., Mocha, P.R.E., Baldisserotto, B. (2020). Chapter 2 - Anatomy of Teleosts and elasmobranchs, in: Baldisserotto, B., Urbinati, E.C., Cyrino, J.E.P.B.T.-B. and P. of F.N.F. (Eds.), . Academic Press, pp. 21–47. doi:https://doi.org/10.1016/B978-0-12-815872-2.00002-6.

Sale, M.J., Cada, G.F., Rinehart, B.N., Sommers, G.L., Brookshier, P.A., Flynn, J.V. (2001). Status of the U.S. Department of Energy's Advanced Hydropower Turbine Systems Program.

Sandlund O.T., Diserud Poole, O.H., Bergesen, K., Dillane, M., Rogan, G., Durif, C., Thorstad, E.B., Vøllestad, L.A. (2017). Timing and pattern of annual silver eel migration in two European watersheds are determined by similar cues. Ecol. Evol. 7:5956-5966. https://doi.org/10.1002/ece3.3099.

Saylor, R., Fortner, A. and Bevelhimer, M. (2019). Quantifying mortality and injury susceptibility for two morphologically disparate fishes exposed to simulated turbine blade strike. Hydrobiologia, 842, 55-75. https://doi.org/10.1007/s10750-019-04026-x.

Saylor, R., Sterling, D., Bevelhimer, M. and Pracheil, B. (2020). Within and Among Fish Species Differences in Simulated Turbine Blade Strike Mortality : Limits on the Use of Surrogacy for Untested Species. Water, 12, 1-27. https://doi.org/10.3390/w12030701.

Scanu S., Carli F.M., Peviani M.A., Piermattei V., Bonamano S., Paladini de Mendoza F., Dampney K., Norris J., Marcelli M. (2015). Environmental monitoring techniques and equipment related to the installation and operation of Marine Energy Conversion Systems. EAI Speciale II Ocean energy: Ongoing research in Italy.

Schwebel, L.N., et al. (2018). Swim bladder inflation failure affects energy allocation, growth, and feed conversion of California yellowtail (*Seriola dorsalis*) in aquaculture. Aquaculture 497: 117-124. https://doi.org/10.1016/j.aquaculture.2018.07.050.

Shields, M.A., Woolf, D.K., Grist, E.P.M., Kerr, S.A., Jackson, A., Harris, R.E., Bell, M.C., Beharie, R.A., Want, A., Gibb, S.W., Osalusi, E. and Side, J. (2011). Marine renewable energy: The ecological implications of altering the hydrodynamics of the marine environment. Ocean and Coastal Management 54(1), pp. 2-9. https://doi.org/10.1016/j.ocecoaman.2010.10.036.

Smialek, N., Pander, J., Geist, J. (2021). Environmental threats and conservation implications for Atlantic salmon and brown trout during their critical freshwater phases of spawning, egg development and juvenile emergence. Fish. Manag. Ecol. 28, 437–467. doi:10.1111/fme.12507.

Smith K.M., Byron C.J., Sulikowski J.A. (2016). Modeling predator-prey linkages of diadromous fishes in an estuarine food web. Mar. Coast. Fish. 8:476-491. https://doi.org/10.1080/19425120.2016.1194920.

Spah, H. (2001). Fishery biological opinion of the fish compatibility of the patented hydraulic screw from Ritz Atro. Bielfield, Germany

Statzner, B. and Müller, R. (1989). Standard hemispheres as indicators of flow characteristics in lotic benthos research. Freshwater Biology, 21, 445-459. https://doi.org/10.1111/j.1365-2427.1989.tb01377.x.

Stephenson, J.R., Gingerich, A.J., Brown, R.S., Pflugrath, B.D., Deng, Z., Carlson, T.J., Langeslay, M.J., Ahmann, M.L., Johnson, R.L. and Seaburg, A.G. (2010). Assessing barotrauma in neutrally and negatively buoyant juvenile salmonids exposed to simulated hydro-turbine passage using a mobile aquatic barotrauma laboratory. Fisheries Research, 106, 271-278. https://doi.org/10.1016/j.fishres.2010.08.006.

Tabeta, O. and Mochioka, N. (2003). The Glass Eel. In Eel Biology, eds. Aida, K., Tsukamoto, K., Yamauchi, K. Springer Japan, Tokyo. doi:10.1007/978-4-431-65907-5.

Taggart, J.B., McLaren, I.S., Hay, D.W., Webb, J.H., Youngson, A.F. (2001). Spawning success in Atlantic salmon (*Salmo salar* L.): a long-term DNA profiling-based study conducted in a natural stream. Mol Ecol. Apr;10(4):1047-60. doi: 10.1046/j.1365-294x.2001.01254.x.

Thayer, L. (2017). Investigating Factors Contributing to Reduced Embryo Survival in Farm Raised Atlantic Salmon, *Salmo salar* L. Electronic Theses and Dissertations. 3476. https://digitalcommons.library.umaine.edu/etd/3476.

Thorpe, J.E., Metcalfe, N.B. (1998). Is smolting a positive or a negative developmental decision? Aquaculture 168:95–103. https://doi.org/10.1016/S0044- 8486(98)00342-1.

Thorstad, E. B., Økland, F., Aarestrup, K., and Heggberget, T. G. (2008). Factors affecting the within-river spawning migration of Atlantic salmon, with emphasis on human impacts. Reviews in Fish Biology and Fisheries 18(4), 345-371. https://doi.org/10.1007/s11160-007-9076-4.

Thorstad, E.B., Whoriskey, F., Uglem, I., Moore, A., Rikardsen, A.H., Finstad, B. (2012). A critical life stage of the Atlantic salmon *Salmo salar*: behaviour and survival during the smolt and initial post-smolt migration. J Fish Biol. 2012 Jul;81(2):500-42. doi: 10.1111/j.1095-8649.2012.03370.x. PMID: 22803722.

Todd, C., Hughes, S., Marshall, T., MacLean, J., Lonergan, M. & Martin Biuw, E. (2008). Detrimental effects of recent ocean surface warming on growth condition of Atlantic salmon. Global Change Biology 14: 958–970. DOI: 10.1111/j.1365-2486.2007.01522.x.

Tosi, L., Tongiorgi, P., Spampanato, A., Sola, C., and Sala, L. (1986). Influence of temperature and salinity on the orientation of the glass eels of *Anguilla anguilla* during migration from the sea to fresh waters. Nova Thalassia 8: 621-622.

Travade, F. and Larinier, M. (2006). French experience in downstream migration devices. https://hal.archives-ouvertes.fr/hal-02588294.

Travade, F., Larinier, M., Subra, S., Gomes, P. and De-Oliveira, E. (2010). Behaviour and passage of European silver eels (*Anguilla anguilla*) at a small hydropower plant during their downstream migration. Knowledge and Management of Aquatic Ecosystems, (398), 01. https://doi.org/10.1051/kmae/2010022.

Tsikata, J.M., Tachie, M.F., and Katopodis, C. (2014). Open-channel turbulent flow through bar racks. Journal of Hydraulic Research, 52(5), 630-643. https://doi.org/10.1080/00221686.2014.928805.

Tsvetkov, V.I., Pavlov, D.S. and Nezdoliy, V.K. (1972). Changes in hydrostatic pressure lethal to the young of some freshwater fish. Journal of Ichthyology, 307-318.

Turnpenny, A.W.H., Davis, M.H., Fleming, J.M., and Davies, J.K. (1992). Experimental studies relating to the passage of fish and shrimps through tidal power turbines. Marine and freshwater biology unit, National Power, Fawley, Southampton, Hampshire, England.

Turnpenny, A.W.H., Struthers, G., Hanson, K.P., Hanson, P. (1998). A UK Guide To Intake Fish-Screening Regulations, Policy and Best Practice With Particular Reference to Hydroelectric Power Schemes, Report No. ETSU H/O6/00052/REP.

Uria-Martinez, R., Johnson, M.M., O'Connor, P.W., Samu, N.M., Witt, A.M., Battey, H., Welch, T., Bonnet, M. and Wagoner, S. (2018). 2017 Hydropower Market Report. Oak Ridge, Tennessee

van Treeck, R., Van Wichelen, J., Coeck, J., Vandamme, L., Wolter, C. (2017). D1.1 Metadata overview on fish response to disturbance. EU H2020 Project FIThydro - Fishfriendly Innovative Technologies for Hydropower, ID 727830.

Verreault G., Mingelbier M., Dumont P. (2012). Spawning migration of American eel *Anguilla rostrata* from pristine (1843– 1872) to contemporary (1963–1990) periods in the St Lawrence Estuary, Canada. J. Fish. Biol. 81:387-407. DOI: 10.1111/j.1095-8649.2012.03366.x.

Vogel, S. (1981). Life in moving fluids: The physical biology of flow. Princeton University Press, Princeton, New Jersey. ISBN 0691026165.

Vogel, S. (1994). Life in velocity gradients. In “Life in moving fluids: The physical biology of flow”. 2nd ed. Princeton University Press, Princeton, New Jersey. ISBN 0691026165.

Vøllestad L.A. (1992) Geographic variation in age and length at metamorphosis of maturing European eel: environmental effects and phenotypic plasticity. J Fish Biol 61:41-48. https://doi.org/10.2307/5507.

Vøllestad, L.A., Jonsson, B., Hvidsten, N.A., Naesje, T.F., Haraldstad, O. and Ruud-Hansen, J. (1986). Environmental factors regulating the seaward migration of European silver eels (*Anguilla anguilla*). Canadian Journal of Fisheries and Aquatic Sciences 43: 1909-1916. https://doi.org/10.1139/f86-236.

von Raben, K. (1958). Zur Beurteilung der Schädlichkeit der Turbine für Fische. Wasserwirtschaft 48: 60-63.

Ward, J.V. (1989). The four- dimensional nature of lotic ecosystems. Journal of the North American Benthological Society, 8, 2– 8. https:// doi.org/10.2307/1467397.

Webb, J., Verspoor, E., Aubin-Horth, N., Romakkaniemi, A., and Amiro, P. (2007). The Atlantic salmon. In The Atlantic Salmon: Genetics, Conservation and Management, pp. 17–56. Ed. by E. Verspoor, L. Stradmeyer, and J. Nielsen. Blackwell Publishing Ltd, Oxford. 500 pp.

Weitkamp, D.E., Sullivan, R.D., Swant, T. and DosSantos, J. (2003). Gas Bubble Disease in Resident Fish of the Lower Clark Fork River. Transactions of the American Fisheries Society 132 (2003): 865-876. https://doi.org/10.1577/T02-026.

Williams, J.G., Armstrong, G., Katopodis, C., Larinier, M., and Travade, F. (2012). Thinking like a fish: a key ingredient for development of effective fish passage facilities at river obstructions. River Research and Applications, 28(4), 407-417. https://doi.org/10.1002/rra.1551.

Wirth T., Bernatchez, L. (2001). Genetic evidence against panmixia in the European eel. Nature, Feb 22;409(6823):1037-40. doi: 10.1038/35059079. PMID: 11234011.

Witten, P.E., Hall, B.K. (2003). Seasonal changes in the lower jaw skeleton in male Atlantic salmon (*Salmo salar* L.): remodelling and regression of the kype after spawning. J Anat.;203(5):435-450. doi:10.1046/j.1469-7580.2003.00239.x.

Wolter, C., Noble, R.A., van Treeck, R., Radinger, J. (2020). D1.3 Fish Population Hazard Index. EU H2020 Project FIThydro - Fishfriendly Innovative Technologies for Hydropower, ID 727830.

World Conservation Monitoring Centre. 1996. *Salmo salar*. The IUCN Red List of Threatened Species 1996: e.T19855A9026693. http://dx.doi.org/10.2305/IUCN.UK.1996.RLTS.T19855A9026693.en.

Yaragina, N.A. (2010). Biological parameters of immature, ripening, and nonreproductive, mature northeast Arctic cod in 1984–2006. ICES Journal of Marine Science 67: 2033–2041. https://doi.org/10.1093/icesjms/fsq059.

Zangeneh, M. (1991). A compressible three-dimensional design method for radial and mixed flow turbomachinery blades. International Journal for Numerical Methods in Fluids. https://doi.org/10.1002/fld.1650130505.

Zangeneh, M., Goto, A. and Takemura, T. (1996). Suppression of Secondary Flows in a Mixed-Flow Pump Impeller by Application of Three-Dimensional Inverse Design Method: Part 1—Design and Numerical Validation. Journal of Turbomachinery. https://doi.org/10.1115/1.2836700.